Role of leishmanial glyceraldehyde-3-phosphate dehydrogenase in host-parasite interaction

Thesis submitted to Jadavpur University for the degree of
Doctor of Philosophy (Science), 2021

By

PRIYA DAS

CSIR-Indian Institute of Chemical Biology

4, Raja S.C. Mullick Road, Jadavpur

Kolkata-700032, India

IICB
आइ. आइ. सी. बी.

भारतीय रासायनिक जीवविज्ञान संस्थान
INDIAN INSTITUTE OF CHEMICAL BIOLOGY

(सी. एस. आइ. आर. का एक अंग)
(A Unit of C.S.I.R.)
4, राजा एस. सी. मल्लिक रोड, यादवपुर, कोलकाता -700 032
4, RAJA S.C. MULLICK ROAD, JADAVPUR, KOLKATA -700 032, INDIA

तार/ TELEGRAM : LIVINGCELL
दूरभाष : कार्यालय
PHONE : 2473 3491/0492
2473 3493/6793
फैक्स / FAX : 91 3324730284
91 3324735197

From:
Subrata Adak, Ph.D.
Senior Principal Scientist
Structural Biology & Bio-informatics Division
e-mail : adaks@iicb.res.in

Dated: 17th Dec. 2021

Sub: Certificate from the supervisor(s)

This is to certify that the thesis entitled "**Role of leishmanial glyceraldehyde-3-phosphate dehydrogenase in host parasite interaction**" Submitted by **Smt. Priya Das** who got her name registered on 11.05.2017 for the award of Ph. D. (Science) degree of Jadavpur University, is absolutely based upon his own work under the supervision of Dr. Subrata Adak, and that neither this thesis nor any part of it has been submitted for either any degree / diploma or any other academic award anywhere before.

(Signature of the Supervisor(s) date with official seal)

“Dedicated to all those talents who don’t have the blessings to be discovered”

Acknowledgements

First and foremost, praise and appreciation to **God**, the Almighty, for giving me the opportunity, showering His blessings on me throughout my work and allowing me to successfully complete the research.

This thesis is a watershed moment which symbolizes not just my diligent writing work but also a turning point in my career at CSIR-IICB. We all know that difficult routes often lead to beautiful destinations, and I can attest to the fact that this is quite true for me. I would like to express my gratitude to a number of people who have helped me, supported me, and inspired me in various ways along this path.

I'd like to convey my heartfelt gratitude to **Dr. Subrata Adak**, my doctoral research adviser and mentor, for providing me with the opportunity to do research and for guiding me with vital assistance during this process. His dynamism, vision, genuineness, and motivation have all left an indelible impression on me. He showed me how to conduct research and present my findings in the clearest and concise manner possible. Working and studying under his direction was a wonderful honor and privilege and I appreciate everything he has done for me.

Next, I wish to thank **Dr. Arun Bandopadhay**, the present director of CSIR-IICB and **Dr. Samit Chattopadhyay**, the former director of CSIR-IICB for providing me with all of the resources I needed to complete my doctorate studies. I'd also like to express my gratitude to the Council for Scientific and Industrial Research (CSIR) for providing me with financial assistance throughout this course.

I gratefully recognize the help I received from former and present members of the IICB faculty **Dr. Krisnananda Chattapadhay, Dr. Siddhartha Roy, Dr. Suvendra Nath Bhattacharya, Dr. Subhas Biswas, Dr. Hemanta K. Majumder, Dr. Samit Adhya, Dr. Nahid Ali, Dr. Nakul C. Maity, Dr. Krisna Das Saha, Dr. Uday Bandopadhay, Dr. Saumen Datta, Dr. Jayati Sengupta, Dr. Chitra Mondol, Dr. Debabrata Biswas, Dr. Malini Sen** and **Dr. Shila Elizabeth.**

I am really grateful to my seniors Subhankar da **(Dr. Subhankar Dolai)**, Swati di **(Dr. Swati Pal)**, Moumita di **(Dr. Moumita Bose),** Rajesh da **(Dr. Rajesh Kumar Yadav) and** Sumit da **(Dr. Sumit Sen Santara).** They have been a constant source of inspiration and motivation for me. Rina di **(Dr. Rina Saha)** and Jayasree di **(Dr. Jayasree Roy)** were more like family members to me. Aditi di (**Dr. Aditi Mukherjee**), Ayan da (**Dr. Ayan Adhikari**) and **Saroj** have been extremely helpful to me during my bench works. I also had a bunch of most outstanding juniors **Sumit, Puja, Yuthika** and **Gaurav**, who were always there to encourage and support me.

I'd like to express my gratitude to Sushanta da (**Sushanta Ghosh**) for his tremendous indulgence in preparing media, autoclaving glass wares, animal handling and Khudiram da (**Khudiram Naskar)** for generously assisting me with the animal research.

In CSIR-IICB, I made a lot of friends with whom I shared so many thoughts both academic and non-academic throughout this journey. **Saikat, Diptankar, Sushanta da, Sambit, Anirban da, Dushyant da, Shinjini, Anoy, Gaurav, Jeet, Arkaprabha, Debraj, Sayantani, Satadeepa, Subarno, Deblina, Chinmoy da, Shiladitya, Milan da, Utpalendu**

da, Sayoni, Sayan da, Manideep da, Sandeep da, Bipro da, Bani da, are some of the mentionable names.
Recognizing those friends who have aided me during my PhD journey, primarily out of goodwill, has been a humbling experience. **Arnab, Sumangal, Rajeeb** and **Narattam** are those special friends.
I would like to express my gratitude to my college professors, **Dr. Chandana Barat** and **Dr. Uma Siddhanta**, for their tremendous guidance during my graduation and postgraduate studies. They have always been my idol.
I'd also like to express my gratitude to **Dr. Nayim Sepay**, a friend, philosopher and guide of mine for his invaluable assistance in determining the best path in this journey and finish it effectively. Away from work, I'd like to convey my gratefulness to Subhayu **(Dr. Subhayu Nayek**) my best friend, for whom friendship extends beyond writing.
I owe my parents, **Sankha Nath Das** and **Pratima Das,** a debt of gratitude for their love, prayers, care, and sacrifices in educating and preparing me for my future. I am grateful to them for their unwavering love and support, which keeps me determined and self-assured. They helped me achieve my goals and success because they believed in me. I would also like to thank my younger sister **Shriya Das** for her immense support and valuable prayers. She has always been an inspiration to me. I'm also grateful for the blessings of my grandparents, **Late Nandalal Adak** and **Late Malati Adak** in all I do.
I'd love to express my gratitude to my beloved husband, **Chiranjit Sinha**, who was not only my husband but also my best friend. It is always necessary to maintain a healthy balance with life outside the lab, and he has helped me overcome all of my tension and lunacy by creating a really friendly and relaxing atmosphere at home. It gives me a great pleasure to convey my gratitude to my daughter **Aradhya (Chini)**, because she is like an angel to me and it is through her good fortune that I am able to complete the research successfully. After a tiring day at work, when her heart-melting sweet gaze and cute little hands hugged me, it released all my stresses and anxiety.
I also extend my heartfelt thanks to my in-laws, my father-in-law **Jiten Sinha,** and mother-in-law **Malati Sinha,** for their endless support and love, which has always helped me. My sister-in-laws and brother-in-laws (**Beauty Sinha, Ramanuj Sinha, Lovely Singha** and **Archan Singha**) assisted me in overcoming various adversities. Their cumulative love and well wishes made my job a lot simpler. This acknowledgement will not be completed without recognizing the junior well-wishers of mine **Ahana**, **Avantika** and **Avnish**.
Finally, I'd like to express my gratitude to everyone who has provided me with inspiration and valuable advice throughout this research, both directly and indirectly. This thesis would not have been possible without encouragement and support from many people. Thank you everyone. Thank you God.

Dated: Priya Das

PREFACE

Glyceraldehyde-3-phosphate dehydrogenase (GAPDH) is a classic glycolytic enzyme and is involved in the reversible oxidative phosphorylation of glyceraldehyde-3-phosphate in the presence of inorganic phosphate and nicotinamide adenine dinucleotide (NAD). However, emerging evidence indicates that GAPDH is a multifunctional protein implicated in diverse functions independent of its role in energy metabolism; GAPDH participates in numerous cellular functions, in addition to glycolytic effects, contributes to nuclear tRNA export, DNA replication and repair, endocytosis, exocytosis, cytoskeletal organization, iron metabolism, carcinogenesis, and cell death. It also acts as an mRNA-binding protein, controlling posttranscriptional gene regulation.

In the case of *Leishmania*, apart from glycolysis, no other function of GAPDH is known. Specific post-translational modifications, protein-protein interactions, and subsequent changes in the intracellular distribution of GAPDH in leishmanial species remain unknown. Considering all these facts together, we tried to find out the role of GAPDH in *Leishmania* other than its role in glycolysis. To understand the non-glycolytic function of LmGAPDH, we have generated control (CT), overexpressed (OE), half-knockout (HKO) and complement (CM) cell lines. HKO cells exhibited reduced virulence compared to control cells when infected with macrophages and BALB/c mice, showing that LmGAPDH plays an important role in *Leishmania* infection and disease progression. We have demonstrated that LmGAPDH is localized within the extracellular vesicles (EVs) released by *Leishmania* during infection and, by different molecular biology techniques, established that EV mediated LmGAPDH suppresses the production of pro-inflammatory cytokines like Tumor Necrosis Factor α (TNF-α), which seems to have a primordial role in the process of controlling infection. *In vitro* protein translation and mRNA binding assays indicate that LmGAPDH binding to the AU-rich 3'-UTR region of TNF-α mRNA is the primary cause for the limitation of its production. Together, these findings confirm that the LmGAPDH found in EVs inhibits TNF-α expression in macrophages via post-transcriptional repression during infection. So, in this project, we attempted to uncover a novel mechanism by which the *Leishmania* parasite suppresses host immune response, which is critical for developing new drugs and therapeutic strategies against the disease. Here we have illustrated our research in three separate chapters; **Chapter1** elucidate mainly the cloning, expression and localization of LmGAPDH from *Leishmania major*. **Chapter2** deals with the functional characterization of LmGAPDH contained within the extracellular vesicles from *Leishmania major* and its essentiality in disease development and progression. **Chapter3** unravels a novel mechanism by which LmGAPDH contained in the extracellular vesicles modulate host immune response through post-transcriptional regulation of TNF-α expression.

ABBREVIATIONS

ADK	Adenosine kinase
ADP	Adenosine diphosphate
APS	Ammonium persulfate
APX	Ascorbate peroxidase
ARE	AU rich element
BSA	Bovine serum albumin
cDNA	Complementary DNA
CM	Complementary cells
CT	Control cells
DTT	Dithiothreitol
dNTP	Deoxynucleotide triphosphates
ECL	Enhanced chemiluminescence
EDTA	Ethyl diamine tetra acetic acid
FBS	Fetal bovine serum
GAPDH	Glyceraldehyde 3 phosphate dehydrogenase
HEPES	4-(2-hydroxyethyl)-1-piperazineethanesulfonic acid
hr	Hour
IFN- γ	Interferon-gamma
IPTG	Isopropyl β-D-thiogalactopyranoside
IRE	Iron responsive element
Kb	Kilo base
kDa	Kilo Dalton
Lm	*Leishmania major*
LmPAS-PGK	PAS domain containing phosphoglycerate kinase from *Leishmania major*
LPS	lipopolysaccharide
M	Molar
mg	miligram
ml	mililitre
mM	milimolar
mRNA	Messenger ribonucleic acid
NaCl	Sodium chloride
NAD^+	nicotinamide adenine dinucleotide
NADH	Reduced nicotinamide adenine dinucleotide
OD	Optical density
OE	Overexpressed cells
ORF	Open reading frame

PAGE	Polyacrylamide gel electrophoresis
PBS	Phosphate buffer saline
PCR	Polymerase chain reaction
PMSF	Phenyl methyl sulphonyl fluoride
PVDF	Polyvinylidene fluoride
RNA	Ribonucleic acid
RNaseA	Ribonuclease A
rNTP	ribonucleoside tri-phosphate
RNA-BP	Ribonucleic acid binding protein
RPMI	Roswell Park Memorial Institute Medium
RT-PCR	Reverse transcription-polymerase chain reaction
REMSA	RNA electrophoresis mobility shift assay
SDS	Sodium dodecyl sulphate
TEMED	Tetramethylethylenediamine
TBE	Tris borate EDTA
TNF-α	Tumor necrosis factor alpha
tRNA	transfer RNA
Tris	Tris (hydroxymethyl) aminomethane
UTR	Untranslated region
UV	Ultra Violet
µL	Microlitre
3 PGA	3- Phosphoglyceric acid

CONTENTS

"What we know is a drop, what we don't know is an ocean."

_ Isaac Newton

Introduction

INTRODUCTION

Parasitism is one of the most successful feeding strategies found in nature and parasitic lifeforms comprise more than 50% of all living organisms. Parasitic infection describes the infection of a host with a particular parasite. Parasites affect millions of people worldwide and parasitic infections cause a tremendous burden of disease in both the tropics and subtropics as well as in more temperate climates. Research into parasite biology and biochemistry is important because of these worldwide human health problems [1]. In addition, we may acquire important new insights into molecular pathology by studying such organisms, which have evolved to deceive and compromise the immune systems of infected animals with great success. Some of the major parasitic diseases infecting humans and animals are listed here in two categories: those caused by protozoans (single-celled organisms) and those caused by helminths (worms/metazoans) [2]. Medical science ensures us that the diseases caused by protozoan parasites have become a major target for the researchers to solve the problem. The major protozoan parasites include *Plasmodium* species (causing malaria), *Entamoeba histolytica* (causing amebiasis), *Leishmania* species (causing leishmaniasis), and *Trypanosoma* species (causing sleeping sickness and Chagas' disease). These parasites reside within the blood or internal organs of the host. They utilize a hematophagous (i.e., blood feeding) arthropod serving as an intermediary to infect the vertebrate hosts **(Fig.1).**

Fig. 1. Phlebotomine sandfly vector used by *Leishmania*. (Adapted from https://en.wikipedia.org/wiki/Pa

1.1. Biology of the Kinetoplastida

Kinetoplastida (or Kinetoplastea as a class) are flagellated protists that belong to the phylum Euglenozoa and are distinguished by the presence of a kinetoplast, a modified mitochondrion, with a huge massed DNA. Bronislaw M. Honigberg first described the kinetoplastids as members of the flagellated protozoans in 1963.

The kinetoplastids are mainly monophylic groups which is represented by the presence of a long, slender flexible body with one or two flagella at one stage in the life cycle of all the members of this group while the other stage is usually round devoid of any flagellum [3]. These flagellated protozoas are mainly divided into two suborders-(A) Prokinetoplastina (Ichthyobodo and Perkinsiella) and (B) Metakinetoplastina (otherbodonids and trypanosomatids). The order of the kinetoplastida in the group of the *Discicristates* covers a vast empire of unicellular eukaryotes many of whom have adopted a parasitic lifestyle. The kinetoplastids usually contain all the organelles that are typical of a eukaryotic organism **(Fig.2)**. However, some of the organelles are unique and specific to this group. One such unique organelle is the presence of a kinetoplast containing single mitochondrion [4].

Kinetoplast is a DNA-containing extra nuclear organelle found in kinetoplastid protozoans. It is normally found in an elongated mitochondrion next to the basal body. The size of the kinetoplast varies by species [5]. Despite its proximity to the basal body, it was previously recognized that kinetoplast aids in movement, hence it was given that name. However, it was later discovered

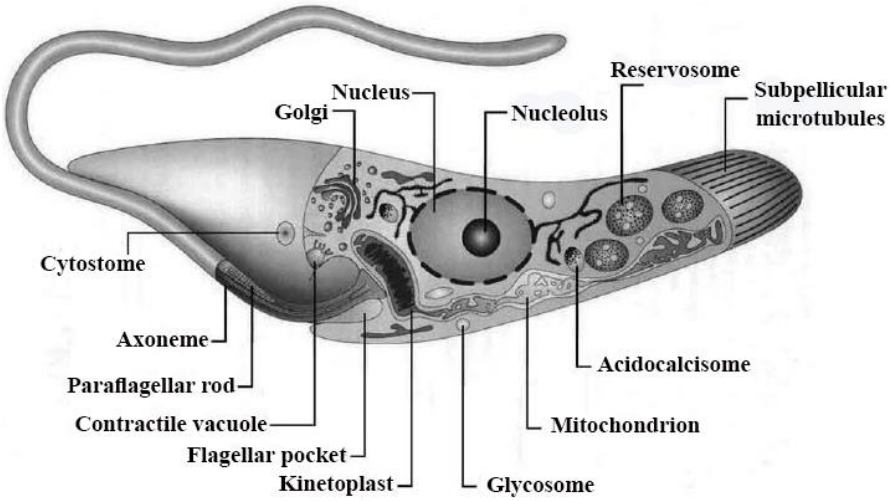

Fig. 2: Schematic representation of longitudinal section of an epimastigote showing the main structures and organelles found in *T. cruzi* (Adapted from Docampo et al, *Nat Rev Microbiol* 2005)

near the basal body, proving that it is not involved in kinetoplastid migration. It is primarily made up of kinetoplast DNA, which is the mitochondrial DNA of the cell (kDNA). kDNA has a structure that is unlike any other DNA [6].

It is made up of two types of circular DNA molecules, maxicircles (~20-40 kbp in size) and minicircles (~0.5-1 kbp in size) [7]. They topologically interlocked into a single, massive network **(Fig.3)**. The maxicircle DNA which is about 5-20% of the total cellular DNA, encodes ribosomal RNAs and a few mitochondrial proteins. On the other hand, the minicircles are responsible for encoding for small guide RNAs (gRNAs) that are required to ensure the specificity of editing [8].

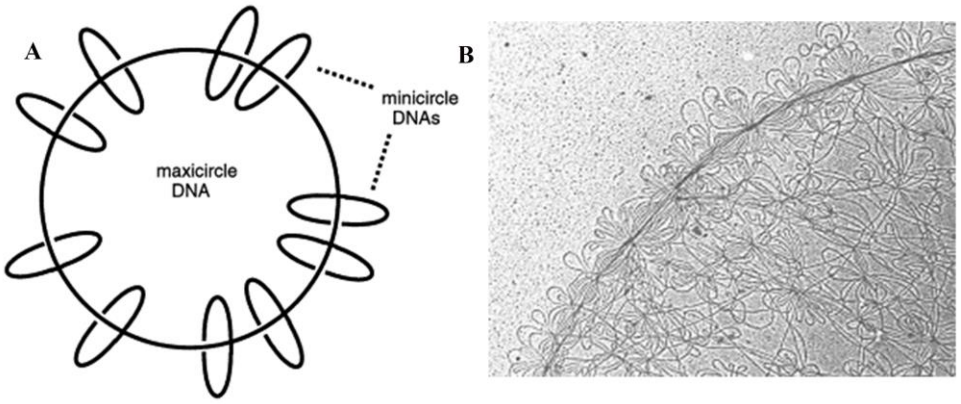

Fig. 3. (A) Schematic representation and B) Electron microscope showing maxicircles and minicirles of kinetoplast DNA (kDNA) (Adapted from: Michele M. Klingbeil Laboratory's web page.)

Other peculiar characteristics of kinetoplastid protozoa that distinguish them from higher eukaryotes include the presence of GPI-anchored glycoproteins [9] and GPI-related glycolipids, antigenic variation accompanied by gene rearrangements, nuclear RNA trans-splicing, and polycistronic expression of functionally unrelated proteins [7, 10]. The metabolism and regulation of metabolism in kinetoplastids are also quite distinct from other eukaryotes' conceptions. The majority of glycolytic enzymes are compartmentalized in trypanosomatid-specific glycosomes, which are peroxisome-like organelles. The absence of catalase and the presence of trypanothione (a glutathione-spermidine conjugate) instead of glutathione are two other metabolic features of this group [11]. Trypanothione is a key component of these parasites' antioxidant defense system. They don't have a *de novo* purine synthesis route, either. Kinetoplastid protozoa are a fascinating model for studying molecular biology, biochemistry,

and cell biology because of their quirks and distinctiveness [12]. Kinetoplastid parasites have a biology that is related to many of the most interesting areas of contemporary interest and research in the biological realm [13]. These evolutionarily organisms have fascinating strategies for controlling gene expression and maintaining a complicated pattern of cell morphogenesis by changing cell shapes throughout their lives. These distinctions only apply to interactions with mammalian hosts or insect vectors. Finally, differentiations result in parasite transmission from vector to host and vice versa [3, 14]. The overabundance of mitochondrial DNA in trypanosomes, which belong to the kinetoplastida category, distinguishes them [15]. Kinetoplasts' distinct cellular characteristics have piqued the interest of other protozoa. A thorough investigation of the kinetoplast could provide fresh insights not only for medicine development but also for other fields of biological system.

1.2. *Leishmania* and leishmaniasis- an introduction

Protozoan parasite of the genus *Leishmania* are responsible for a spectrum of infectious human disease termed leishmaniasis. The parasite is spread to people mostly by the bites of two species of sand flies, *Phlebotomus* and *Lutzomyia* [16]. During their life cycle, these parasites alternate between intracellular macrophage parasitism and external life in the gut of their sandfly vector, demonstrating a remarkable ability to resist destruction in the adverse settings they face [17]. According to the World Health Organization (WHO), leishmaniasis is a serious tropical illness that, if not treated effectively, can have serious consequences. Around 12 million individuals are infected with 30 distinct varieties of *Leishmania*, which results in 60,000 fatalities each year. The symptoms of leishmaniasis are usually determined by the *Leishmania* species that infects the host and the type of the host immune response. For hundreds of years, leishmaniasis has been widespread [18]. Alexander Russell initially described the condition in 1756, referring to it as an "Aleppo boil". Many distinct names have been given to this group of diseases, including Kala-azar, Dum-dum fever, white leprosy, and espundia. W.B. Leishman and Captain Charles Donovan were the first to detect one of the first *Leishmania* stains and named it as *Leishmania donovani* in 1901 [19]. In Latin America, Africa, the Indian subcontinent, the Middle East, and the Mediterranean regions, roughly two million new cases of human leishmaniasis (maximum visceral) are discovered each year. In recent years, *Leishmania* infected patients have been at a higher risk of developing immunosuppressive conditions, as evidenced by the significant rise in fatality rates in cases of *Leishmania*/HIV co-infection [20].

1.2.1. Taxonomy of *Leishmania*:

Systemic position of *Leishmania* as described by Levine et al 1980 [21].

Kingdom:	Protista
Subkingdom:	Protozoa
Phylum:	Sarcomastigophora
Class:	Zoomastigophora
Order:	Kinetoplastida
Sub order:	Trypanosomatina
Family:	Trypanosomatidae
Genus:	*Leishmania*.

1.2.2. Types of leishmaniasis

Depending on the clinical symptoms of leishmaniasis, There are 3 main forms of the disease:1) visceral leishmaniasis (VL) or kala-azar 2) cutaneous leishmaniasis (CL), 3) muco cutaneous leishmaniasis and 4) Post Kala Azar Dermal Leishmaniais (PKDL) **(Fig.4)** [22].

Fig. 4. Types of Leishmaniasis. Top left panel: Cutaneous leishmaniasis; top right panel: Viceral leishmaniasis; lower left panel: Mucocutaneous; and lower right panel: PKDL. (www.wikipedia.com)

1) **Visceral leishmaniasis** (VL): In almost 95 percent of cases, visceral leishmaniasis (VL), often known as kala-azar, is fatal if left untreated. It is characterized by fevers that come and go, weight loss, spleen and liver enlargement, and anemia. The majority of cases are found in Brazil, East Africa, and India[23]. Every year, an estimated 50 000 to 90 000 new cases of VL are reported to the World Health Organization (WHO), with approximately 25 to 45 percent of these cases being reported to WHO. It is still one of the most dangerous parasitic infections in terms of outbreaks and death [22, 24]. In 2019, ten countries accounted for more than 90% of new cases reported to WHO: Brazil, Ethiopia, Eritrea, India, Iraq, Kenya, Nepal, Somalia, South Sudan, and Sudan.

2) **Cutaneous leishmaniasis** (CL): Cutaneous leishmaniasis (CL) is the most prevalent type of leishmaniasis. It causes skin lesions, primarily ulcers, on exposed regions of the body, leaving life-long scars as well as major impairment or stigma. The Americas, the Mediterranean basin, the Middle East, and Central Asia account for nearly all CL cases. Afghanistan, Algeria, Brazil, Colombia, Iran (Islamic Republic of), Iraq, Libya, Pakistan, Syria Arab Republic, and Tunisia accounted for nearly 87 percent of new CL cases in 2019. Every year, between 600,000 and 1 million new cases are anticipated to occur over the world [25, 26].

3) **Mucocutaneous leishmaniasis:** Mucous membranes in the nose, mouth, and throat are destroyed partially or completely in mucocutaneous leishmaniasis. In Bolivia (the Plurinational State of), Brazil, Ethiopia, and Peru, almost 90% of mucocutaneous leishmaniasis cases are diagnosed [27].

4) **Post kala-azar dermal leishmaniasis (PKDL):** The aftereffect complication of visceral leishmaniasis is post-kala-azar dermal leishmaniasis (PKDL). In most cases, the disease begins with a minor rash on the face that spreads across the body depending on severity,

generating larger lesions, and is followed by growth of facial features such as the nose and lips, similar to leprosy [28].

1.2.3. Life cycle of *Leishmania*

Leishmania's life cycle is complicated, involving both vertebrate and invertebrate hosts. It has two developmental stages: promastigotes, which proliferate in the female sandfly's lumen, and amastigotes, which proliferate inside a variety of mammalian host cells **(Fig.5)** [29]. They use rodents, edentates, and marsupials as reservoir hosts in addition to humans. One nucleus and a kinetoplast are situated near the anterior end of this slightly elongated, motile organism with a single anterior flagellum containing promastigotes. This promastigotes change to slightly round to oval single nuclei and kinetoplast bearing amastigotes after entering a vertebrate host[30]. In different hosts, both of these stages are engaged in binary fission replication. During a blood meal, an infected female sandfly bites an uninfected human (vertebrate) host, injecting the infective metacyclic promastigotes. The macrophages quickly engulf these metacyclic promastigotes, resulting in infection [31]. As an intracellular parasite, *Leishmania* persists in the phagolysosome of the host and transforms into amastigotes. Binary fission multiplies these amastigotes. The macrophages are finally lysed, and the amastigotes are discharged into the bloodstream. Blood monocytes, lymph node macrophages, bone marrow, spleen, liver, and other tissues of reticuloendothelial (RE) cells are all invaded by these amastigotes. When an uninfected female sandfly bites this infected human, these amastigotes are picked up. These amastigotes are transformed to flagellar promastigotes by numerous flagellated intermediates within a few hours in the midgut of a sandfly (invertebrate). These promastigotes eventually move to the sandfly's pharynx and buccal cavity after a period of time. In the end, the sandfly bite spreads the sickness to others who aren't infected. As a result, *Leishmania's* life cycle differs between invertebrate and vertebrate hosts **(Fig.6)** [32, 33].

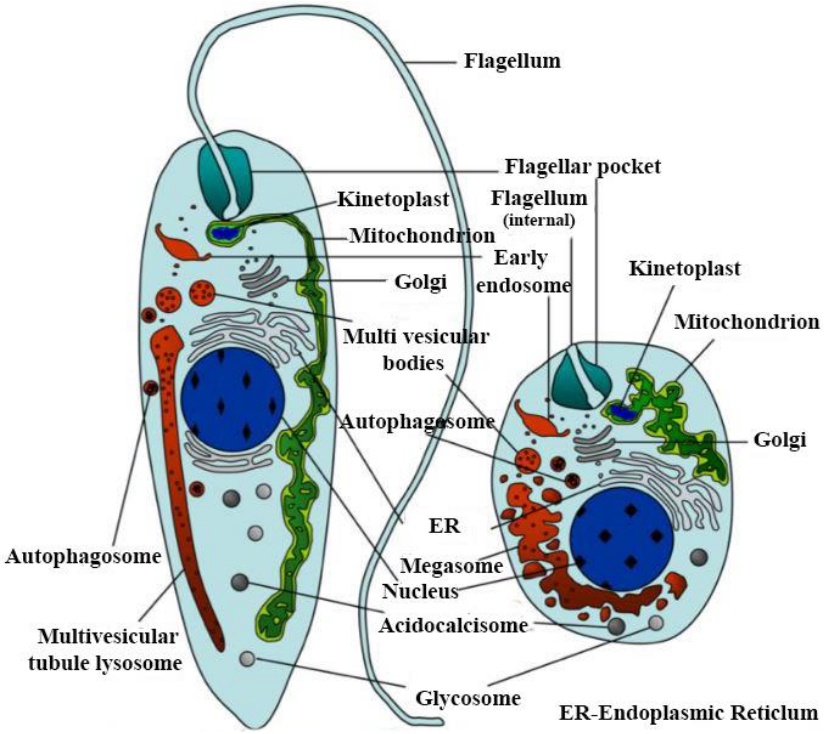

Fig. 5. Schematic representation of Cell structure of *Leishmania* promastigote (right) and amastigote (left) (Adapted from Beistero et al, Int *J Parasitol*, 2007)

A) Parasite-vector interaction: Development in sandflies

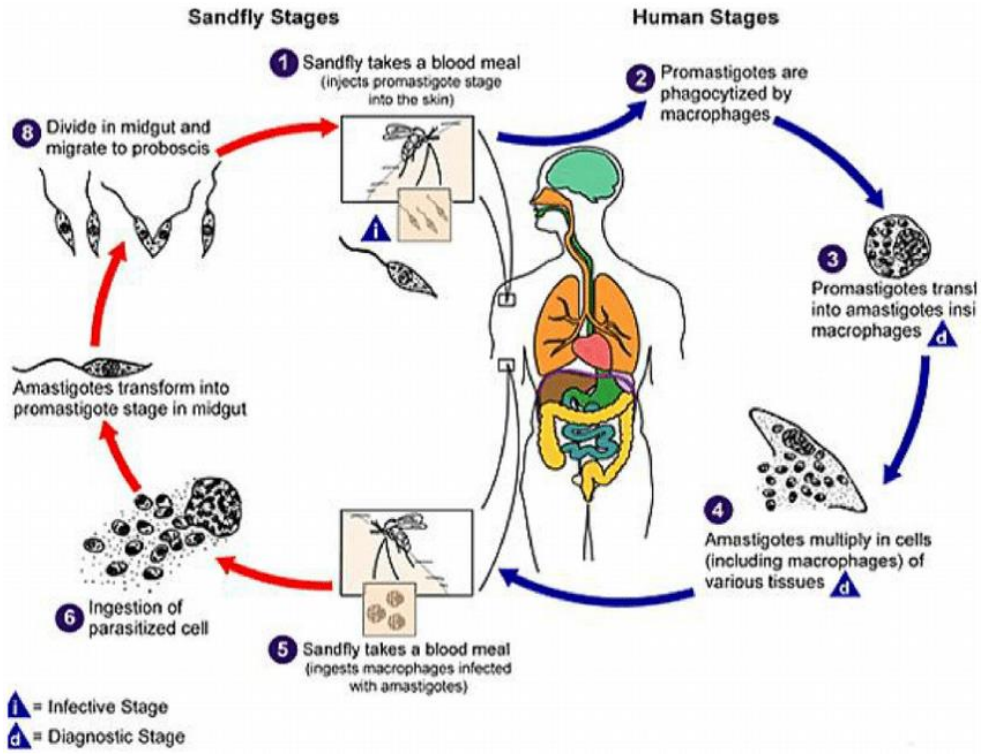

Fig. 6. **Life cycle of *Leishmania* spp**. (Adapted from www.cdc.gov)

Insect vectors, phlebotomine sandflies of the Phlebotominae family, transfer *Leishmania* to mammalian hosts. There are over 500 phlebotomine species belonging to six genera, however the old world Phlebotomous and the new world Lutzomyia are the only *Leishmania* species infectious to humans [34]. These are mainly little (1.5–2 mm in length) insects that live in tropical and subtropical areas. The *Leishmania* life cycle takes place in the digestive system of sand flies, but the exact position of parasites within the sand fly vector varies between subgenera *Leishmania* and Viannia [35]. The New World subgenus Viannia, commonly known as *Leishmania braziliensis*, is also known as peripylarian parasites because it enters the hindgut before migrating forward into the midgut. Despite this, most *Leishmania* species are suprapylarian parasites because their development is limited to the midgut [36]. Female sand flies ingest blood containing macrophages that have previously been infected by the amastigote stage of the parasite, which is a tiny (3–5 m), immotile, and circular form of the parasite [37]. The morphological alterations and development of the parasite within the vector are triggered by changes in circumstances during the transition from the mammalian host to the sand fly midgut (temperature and pH). Amastigotes are further transformed into procyclic promastigates, which are weakly motile forms with a short flagellum beating at the anterior end. They multiply in the early blood and are retrieved from the midgut using a type I peritrophic matrix. By reducing their reproduction, parasites begin to convert into strongly motile long nectomonad promastigotes [38] after 48 to 72 hours. They evolve into short nectomonad promastigotes, also known as leptomonads, as they go into the anterior midgut, where they commence a new proliferative cycle [16, 38, 39]. Detachment, forward migration, and colonization of the stomodeal valve are all required for successful transmission, and once these steps are completed, *Leishmania* transforms into infective metacyclic stages [39]. During the following blood feeding, they are transferred to the skin of the vertebrate host. *Leishmania's* life cycle in the sandfly vector spans between 6 and 9 days, depending on the species. *Leishmania* metacyclics have been found in salivary glands and pee droplets discharged by infected female sandflies after blood feeding on numerous occasions [40]. There are two widely acknowledged routes for metacyclic parasite

transmission: a limited number of metacyclics discovered in the proboscis are deposited into the skin during feeding, or parasites remaining in the back of the stomodeal valve are regurgated by ingested blood backflow [41]. Regurgitation was formerly thought to be caused by a mechanical barrier in the foregut or the stomodeal valve, but now damage to the chitin layer of the stomodeal valve [42] and the role of parasite proteophosphoglycan [43] are also being considered.

B) *Leishmania*-host cell interaction: Living within a phagolysosome

Leishmania spp. are renowned for their ability to survive and multiply within the phagolysosomal compartment of mononuclear phagocytes. Macrophage phagocytosis of promastigotes occurs either before or after sand fly bite infection of neutrophils [44]. Within the vacuolar compartments of macrophages, promastigotes differentiate into amastigotes, which have the characteristics of adult phagolysosomes. Amastigotes divide via binary fission within the vacuole and can elude other macrophages, dendritic cells, and fibroblast cells. *Leishmania* promastigote stages include a thick glycocalyx layer consisting of glycosylphosphatidylinositol (GPI)-anchored proteins containing GPI-anchored phosphoglycan, lipophosphoglycan (LPG), and glycoinositolphospholipids (GIPLs) [43]. *Leishmania* mutant studies that lack individual or multiple surface components suggest that LPG plays a crucial role in macrophage infection, while the deletion of other components has little impact on promastigote pathogenicity in the host [45]. Macrophages are the most well-known cell types that can be infected by a large number of amastigotes that can circumvent isolated vacuoles holding one parasite per vacuole or big communal vacuoles containing many parasites (determined according to the species involved) [46]. *Leishmania spp.* amastigotes, for example, elude individual vacuoles, whereas the *L. mexicana* complex (*L. mexicana, L. amazonensis, and L. pifanoi*) remains in vast communal vacuoles. These vacuoles, which have a pH of roughly 5.4, have all of the luminal and membrane indicators of a mature phagolysosome, including hydrolases and membrane NADH oxidases, which generate anti-microbial oxidative burst [47]. Because it perceives a wide variety of host macromolecules, the phagolysosome compartment harbouring *Leishmania* is very dynamic, and the mechanism comprises fusion of the phagolysosome compartment with the phagocytic, endocytic, and autophagic vesicles, as well as the endoplasmic reticulum [48, 49]. Hydrolases, such as proteases, lipases, and glycosidases, breakdown diverse host macromolecules after absorption, generating free sugar moieties, lipids, and amino acids [50]. Amastigote plasma membrane transporters then take up these products. The phagolysosome contains numerous carbon sources and necessary nutrients since the parasite's amastigote stage can directly internalise and breakdown host macromolecules using their own lysosome (purines, vitamins, heme, and a range of amino acids) [51]. Other compartments of the endo-lysosomal network, on the other hand, may be detached from the lysosome. In animal models carrying mutations resulting to deficiencies in de novo synthesis pathways of metabolites (glycine, amino sugars) or nutrient salvage pathways (nucleotide/nucleoside/purine base), significant sacking in nutrient uptake /de novo biosynthesis pathways has been suggested [51-53].

1.2.4. *Leishmania* pathogenicity

The co-infection of visceral leishmaniasis with HIV is one of the biggest threats to its control. According to statistics, an estimated 39.5 million people are infected with HIV, with 95 percent of the population living in underdeveloped nations [54]. When VL is co-infected with HIV, the

probability of acquiring active VL increases by 100 to 2320 times, demonstrating that VL is an opportunistic infection associated with HIV. HIV-positive patients are particularly sensitive to VL, because VL hastens HIV infection and progression to AIDS [55]. Treatment failure is common, and individuals who do not get antiretroviral therapy eventually (ART) die from recurrence.

1.2.5. Treatment of leishmaniasis

The World Health Organization (WHO) classifies leishmaniasis as a Neglected Tropical Disease, affecting around 12 million people worldwide each year. It is endemic in 98 countries, 72 of which are developing countries and 13 of which are among the least developed. However, no such vaccines or medications against leishmaniasis have been developed to far [56]. Avoiding being bitten by a sand fly is the only way to avoid contracting leishmaniasis. The medications routinely used to treat leishmaniasis have a variety of negative effects, are expensive, and are sometimes useless owing to drug resistance [57]. As a result, new medications are really necessary. Several novel medications and vaccines are now being studied, with some showing promising therapeutic applications.

1.2.5.1. Following are some of the drugs commonly used in treating leishmaniasis [58] (Table 1)

Drugs	Route of Administration	Dosage	Effectivity	Toxicity
Pentavalent antimonials	Intramuscular (IM), Intravenous (IV) or Intralymphatic (IL) administration	20mg/kg/day(28-30 days)	35-95% (drug resistance in some parts of India, low cost treatment with sodium stibogluconate, irregular response in CL.)	From pain, oedema, abdominal pain, nausea to Severe cardiotoxicity, pancreatitis, nephrotoxicity and hepatotoxicity.
Amphotericin B	Intravenous (IV)	1mg/kg/day (15-20 days, daily or alternatively)	>90% (primary drug for VL in India, in case of Sb resistance .Used for VL, CL and complex forms of CL.)	Infusion related anemia or hypokalemia, azotemia,
Miltefosine	oral	100-150mg/day (28 days)	94% (India) 60-90% (Africa) (Topical formulation with gentamycin and surfactants in Phase III trial)	Vomiting and diarrhoea, nephrotoxicity, hepatotoxicity
Paromomycin	Intramuscular (IM) for VL	15mg/day (21 days) 20mg/kg(17 days)	94% (India) 45-85% (Africa) (used for VL in India, under clinical trials for VL in East Africa.)	pain, blisters, erythema along with severe nephrotoxicity and ototoxicity
Pentamidine	Intramuscular (IM)	3mg/kg/day	35-96%(Depending) (for specific CL in South America only)	High rate of hyperglycaemia, hypotension and cardiotoxicity

1.2.5.2. Vaccines against *Leishmania*

The development of *Leishmania* vaccines could be a long-term solution to leishmaniasis. However, there is currently no *Leishmania* vaccine in use anywhere in the globe [59]. Antigenic variety, genomic plasticity, and *Leishmania's* digenetic life cycle make developing an effective vaccination difficult. Over the last two decades, scientists have devised novel methods for producing leishmanial vaccines and several of them are in advanced stages of clinical trials [60, 61]. *Leishmania* vaccines are classified into several categories based on their development: Live *Leishmania* vaccine (Leishmanization, LZ); First generation vaccines (whole killed *Leishmania*); second generation vaccines (recombinant proteins); third generation vaccines (Naked DNA vaccines).

Live vaccines: Extrudes from active lesions were inoculated into the covered part of the body of healthy people in ancient times to produce a self-healing lesion and provide protection against multiple lesions on exposed areas of their bodies. Later, this method was termed 'leishmanization' (LZ). During the 1970s and 1980s, for example, live virulent *L. major* promastigotes were extracted from free cultures and utilised in large-scale vaccination trials in Israel, Iran, and the former Soviet Union. LZ had a high rate of effective lesion creation and subsequent immunity to *L. major* infection, but it was neither repeatable nor safe.

First generation vaccines (whole killed *Leishmania*): By evaluating the *Leishmania* skin test (LST) reactivity, a vaccine containing promastigotes of five dead *Leishmania* strains was demonstrated to be safe and immunogenic in the 1930s in Brazil, but it only provided a minor degree of protection (50 %) [62]. Mayrink and his colleagues later created a vaccine in 1970 that contained 5 *Leishmania* isolates from four different species [63]. With varied parameters such as adjuvant dosages and vaccine administration route, these killed parasites exhibit inconsistent efficacy. Repeated injections of deceased parasites, on the other hand, help to expand effector-like memory T-cells, resulting in protection against virulent challenge [64].

Second generation vaccines (recombinant proteins): Recombinant proteins or polypeptides of bacteria, viruses, or parasites carrying the *Leishmania* gene are created through DNA cloning in these vaccines. These recombinant proteins work best when combined with an adjuvant for a large-scale application. Surface expressed glycoprotein (gp63)[65] or leishmanolysin, *Leishmania* homologue for receptors of activated C kinase (LACK) [66], Hydrophilic acylated surface proteins (HASP) [67], *Leishmania*-derived recombinant poly-protein (Leish-111f) or LEISH-F1 are some of the best adjuvants [68].

Third generation vaccines (Naked DNA vaccines): The naked DNA vaccine is a novel method for preventing infectious diseases. The target genes are cloned into a mammalian expression vector, and the DNA is directly administered as a single or multiple antigenic DNA molecule as an intradermal or intramuscular injection of DNA vaccine. This immunization is exceedingly safe because it does not contain any pathogens to demonstrate their pathogenicity [59]. A cocktail DNA vaccine encoding cysteine proteinases types I, II, and III was successfully protected against *L. major* infection using solid lipid nanoparticles as an example [69].

1.3. Introduction to GAPDH- a multifunctional "housekeeping" gene.

Biochemists, molecular biologists, and other scientists of many fields and ages are familiar with glyceraldehyde-3-phosphate dehydrogenase (GAPDH, EC 1.2.1.12). It's been researched not only for its role in glycolysis **(Fig.7)**, but also as a model protein for enzyme kinetic studies, crystallographic modelling, and gene isolation and characterization [70]. As a result, GAPDH

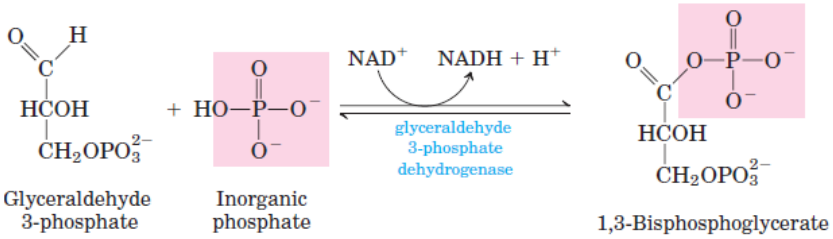

Fig. 7. Role of glyceraldehyde-3-phosphate dehydrogenase (GAPDH) in glycolysis. (Adapted from www.wikipedia.com)

was seen as a "cellular heirloom," a protein, enzyme, or gene from another epoch. Recent investigations, however, show that mammalian GAPDH is not just a remnant used solely for mere laboratory exercises or as the mandatory loading control in gene or protein analyses, as is the case with conventional wisdom in so many other domains of life. Instead, it is a multifunctional protein with a wide range of functions and a specific subcellular localization, as indicated in [71].

1.3.1. Structural and functional analysis of Glyceraldehyde-3-phosphate dehydrogenase (GAPDH)

GAPDH is a homo tetramer made up of four 37 kDa subunits that are all similar **(Fig.8)**. The

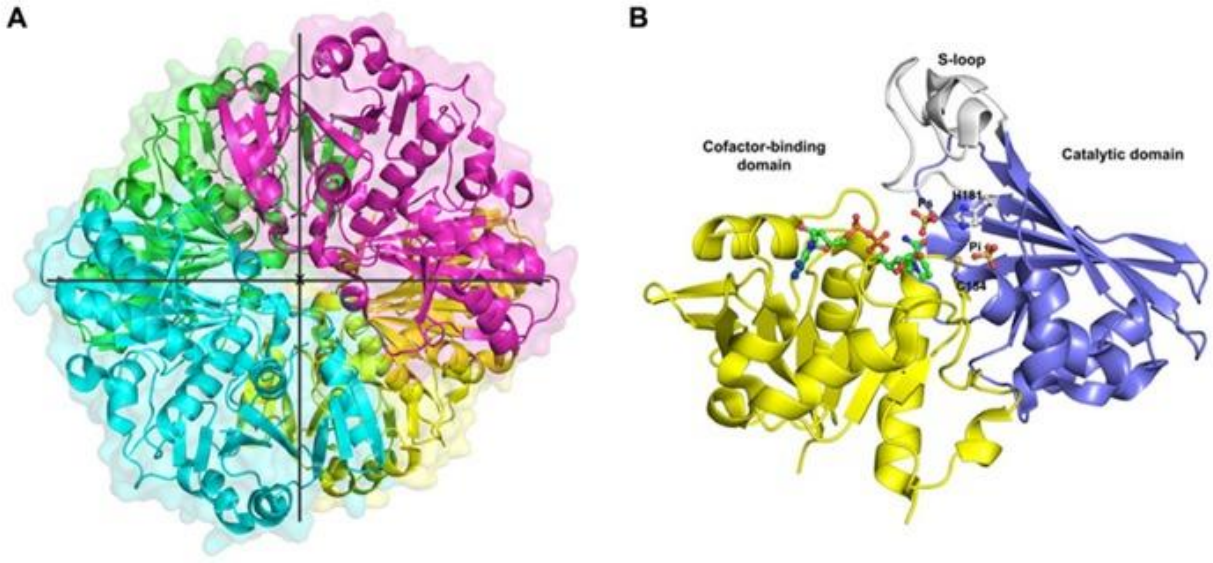

Fig. 8. Crystal structure of cytoplasmic GAPDH from rice. (A) Ribbon representation of the homotetramer of Oryzasativa (Os) GAPDH (PDB code 3E5R), each subunit is differently colored. The three symmetry molecular axes are represented (the x-axis is perpendicular to the plane). (B) Ribbon representation of the crystal structure of a single OsGAPDH subunit. The cofactor-binding domain is yellow, the catalytic domain blue and the S-loop gray. The NAD+, the sulfate ions occupying the Ps and Pi sites and the catalytic residues (Cys-154 and His-181) are represented as ball-and-sticks. (Adapted from Zaffagnini et al, *Frontiers in Plant Science*, 2013)

human GAPDH gene, which is found on chromosome 12, transcribes a single mRNA species, resulting in the production of a 335-amino-acid polypeptide chain. The NAD^+ binding domain (amino acids 1→ 150) and the catalytic or glyceraldehyde-3-phosphate domain (amino acids 151→ 335) with an active site cysteine are the two primary domains [72]. Recent research has identified the GAPDH amino acid sequences that are used for its new roles. Its NAD^+ binding site, in particular, is the locus for its role in controlling mRNA stability and translation [73-76]; its membrane functions based on a phosphatidyl serine binding site [77] and also its binding to glutathione [78]. Interactions with the active site cysteine are critical for its role in heme metabolism, cellular response to oxidative stress [79, 80], and apoptosis **(Fig.9)** [81]. Finally, its distinct CREM nuclear export signal is found in the molecule's distal region, within the catalytic site [82].

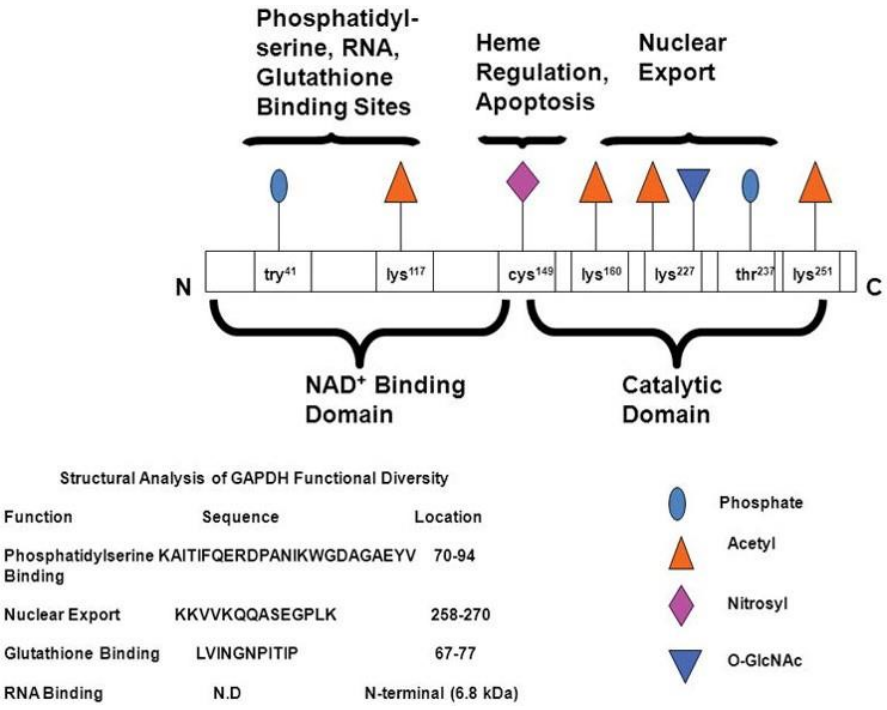

Fig. 9. Structural Basis of GAPDH Functional Diversity: The position of GAPDH functional domains, post-translational modifications, and binding sequences are localized as indicated within the GAPDH protein. (Adapted from Sirover, M. A., *Int J Biochem Cell Biol,* 2014)

GAPDH's canonical enzymatic function is to catalyze the oxidation and phosphorylation of glyceraldehyde-3-phosphate (G3P) to 1, 3-bisphosphoglycerate (1, 3- BPG) in the presence of NAD^+ as a co-substrate. This is the sixth step in the glycolytic breakdown of glucose, which occurs in the cytoplasm of eukaryotic cells and is an important mechanism for energy and carbon molecule supply. Simultaneous oxidation and phosphorylation of G3P produces 1,3-bisphosphoglycerate (1,3-BPG) and NADH. Inorganic phosphate, rather than ATP, is used in this phosphorylation step. The conversion is split into two parts. The first is favorable, allowing the second unfavorable step to take place [83]. Traditionally, the GAPDH gene has been employed as a conserved gene for species identification [84]. Its promoter is terribly effective in microorganisms for heterologous protein production [85, 86].

In recent years, GAPDH has been considered to be a moonlighting protein [71, 87]. New and novel studies show that it is directly engaged in transcriptional [88, 89] and posttranscriptional gene regulation [73-76], vesicular transport [90-95], receptor mediated cell signaling [96, 97], chromatin structure [98, 99], and DNA integrity maintenance [100], according to new and original studies [87]. Furthermore, such studies have provided important information about the cellular response to oxidative stress [79, 81, 101, 102] and apoptosis [80, 103-107]. Surprisingly,

additional research suggests that GAPDH plays a function in autophagic gene regulation [108, 109], as well as a critical involvement in diabetes [110-113], age-related neurodegenerative illnesses [114, 115], malaria [116], and even cattle brucellosis [117]. Each evidence suggesting GAPDH's role in human disease is consistent with now-classic studies linking GAPDH expression to cancer [118, 119].

1.3.2. GAPDH as a Moonlighting protein

"Moonlighting" proteins participate in cell pathways that are separate and distinct from those with which they have long been associated and accepted; and, perhaps most surprisingly, exhibit distinct changes in their subcellular localization that are a priori requirements for these alternative functions [120, 121]. In the past two decades, the glycolytic enzyme glyceraldehyde-3-phosphate dehydrogenase (GAPDH) that was once considered a simple "housekeeping" protein has been shown to be involved in many cellular processes **(Fig.10)** in addition to glycolysis [122].GAPDH, for example, acts as a cellular kinase through phosphotransferase/kinase activity [123], auto phosphorylation, and phosphorylation of other proteins. It interacts with tubulin and catalyzes tubulin polymerization into microtubules [124], as well as plasmenylethanolamine and cholesterol-specific membrane fusion [125] and Ca^{2+}-dependent fusogen activity [126]. It has been discovered to be a nitric oxide target protein [127] as well as a binding protein for nucleic acids, DNA [128], and nuclear tRNA [129]. It's also a uracil DNA glycosylase [130] and an Ap4A-binding protein [131], suggesting it's involvement in DNA replication and repair. GAPDH also functions as a specialized mRNA-binding protein, engaging with 5'-UTR or 3'-UTR mRNA regions that are critical for translational regulation of gene expression [132]. GAPDH's other known functions include regulating heme inclusion in hemoproteins and nitrosylation of nuclear proteins [107, 133, 134]. Furthermore, recent and novel research suggests that GAPDH is involved in a range of diseases, including diabetes, age-related neurodegenerative illnesses, and cancer [135, 136].

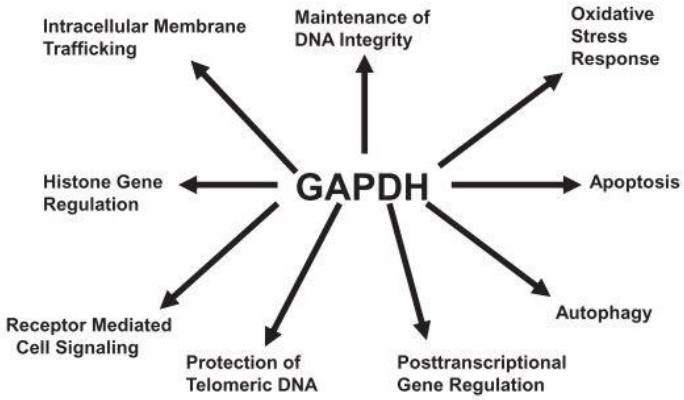

Fig.10 Functional Diversity of Glyceraldehyde-3-phosphate dehydrogenase (GAPDH) (Adapted from Sirover et al, *Biochim Biophys Acta* 2011)

1.3.2.1. GAPDH and intracellular membrane trafficking regulation

The development of multiprotein complexes capable of moving from one subcellular location to another is required for intracellular membrane trafficking [137]. GAPDH appears to play a key role in the development, control, and function of Rab2-mediated ER-to-Golgi cargo shuttling, according to new findings. This is due to its physical connection with the Rab2 protein complex, which is membrane bound [92]. Rab2 forms vesicular tubular complexes (VTC), which are involved in ER to Golgi trafficking, by recruiting a series of cytosolic proteins in a certain

temporal sequence. Immunoreactive GAPDH found in vesicular tubular complexes defined the role of GAPDH in VTC formation and intracellular membrane trafficking. According to kinetic studies Rab2 attracted cytosolic GAPDH in a dose-dependent manner, which was prevented by anti-GAPDH antibody neutralization of its membrane attachment. The ability of an anti-GAPDH antibody to block ER to Golgi transport indicates the physiological importance of GAPDH in membrane trafficking [92, 94, 95].

GAPDH: tubulin interactions were one of the first to show the former's functional variety. The physiological relevance of these observations, however, remained unknown. As with many aspects of biomedical science, further investigation and analysis were required to identify the significance of these protein-protein interactions for normal cell function. GAPDH promoted cytosolic-to-membrane tubulin connection and bundled microtubules, transforming tubulin structure from perinuclear to cross-linked subcellular network [91]. Again, immunological investigation revealed that an anti-GAPDH antibody inhibited cytosolic tubulin translocation, microtubule bundling, and intracellular tubulin structural alterations. Pre-incubation with an anti-GAPDH antibody prevented dynein membrane attachment and subsequent function, indicating that GAPDH was essential for the specific recruitment and activity of this motor protein in membrane trafficking [95].

Intracellular membrane trafficking is a complex process, as demonstrated. It necessitates not only the involvement of multiple proteins, but also the change of intracellular cytoskeletal structure followed by cargo transit from one subcellular location to another. It goes without saying that such a complex metabolic route would necessitate some kind of regulatory mechanism to ensure not only appropriate complex formation but also the temporal sequence in which each protein is recruited to become a component of this subcellular structure. According to new data, GAPDH is not only a critical component of the complex, but also a focal point for the regulatory mechanisms that exist to manage this complex metabolic system **(Fig.11).**This includes two independent post-translational phosphorylation stages, each catalyzed by a different protein kinase: the first at GADPH^{tyr41} by src [94], and the second at a yet-to-be-defined serine residue by PKC [91, 95]. It is plausible to assume that each phosphorylation affects GAPDH conformation sequentially, resulting in specified changes in the structure of the membrane bound protein complex. The latter would speed up the sequence of processes required for intracellular membrane trafficking.

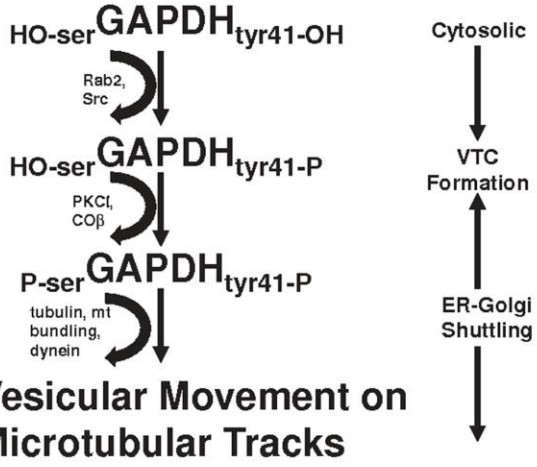

Fig. 11. Role of GAPDH in vesicular movement (Adapted from Sirover et al, *Biochim Biophys Acta* 2011)

1.3.2.2. GAPDH and the prevention of telomere shortening

Telomeres play an important role in protecting the integrity of DNA as well as chromosomal shape. Recent research has shown not just GAPDH's functional role as a telomere shape

determinant, but also the mechanisms involved in GAPDH: telomere DNA binding [98, 99]. GAPDH binds to telomeric DNA specifically, and the resulting GAPDH: DNA complex protects telomeres from shortening during replication and due to DNA damage from ceramide or cancer drug induced shortening. GAPDH was shown to be the most abundant protein attached to single-strand telomeric DNA. Ceramide, a telomere shortening inducer, prevented the formation of the GAPDH: telomere complex. The dynamics of GAPDH: telomeric DNA binding were discovered by cell cycle analysis [98, 138]. In S phase nuclei, GAPDH and telomeric DNA co-localize. GAPDH levels in the nucleus decreased as the cell cycle progressed, indicating that GAPDH is actively moving from one subcellular location to another. Reduced endogenous GAPDH expression, as measured by siRNA knockdown, enhanced telomeric DNA shortening, whereas overexpression of GAPDH reversed telomeric DNA shortening generated by the cancer chemotherapy drugs gemcitabine and doxorubicin. NAD^+ inhibited complex formation competitively, demonstrating the role of that binding site in this new GAPDH function. GAPDH-telomeric DNA binding was found by mutational research in numerous ways [139]. DNA binding was inhibited by replacing Asp32 in the NAD^+ binding site with alanine and cys149 in the catalytic site with alanine. GADPH Ala32 and GAPDH Ala149 bind to telomeric DNA but do not relocate to the nucleus [140]. As a result, not only does this mutational study clarify GAPDH's new, nuclear job, but it also demonstrates two distinct features of GAPDH function, namely, changes in GAPDH's subcellular location as a precondition for this new role and its dissociation from its classical glycolytic activity.

1.3.2.3. GAPDH in maintaining DNA integrity with APE-1

Apurinic/Apyrimidinic Endonuclease (APE-1) is a transcriptional regulator as well as a necessary enzyme for DNA damage repair. APE-1o is formed at a physiologically relevant rate in vivo, putting DNA integrity and gene transcription regulation in jeopardy. According to new data, nuclear GAPDH is a key method through which cells ensure that APE-1 remains in its catalytically active form [100]. During these investigations, one significant protein was discovered to bind to APE-1. GAPDH was discovered to be the protein in question. Further research revealed that GAPDH could catalyze the conversion of APE-1o to APE-1r [141]. The restoration of APE-1 endonuclease activity after inactivation by hydrogen peroxide chemical oxidation demonstrated the functional importance of this GAPDH activity. The sensitivity of GAPDH knock down cells to methylmethane sulfonate and bleomycin indicated the physiological importance of this activity. Each chemical causes DNA damages that lead to the development of AP sites [100, 142]. APE-1 is in charge of repairing the latter. Furthermore, when cells were treated with GAPDH siRNA to diminish endogenous GAPDH levels, the rate of spontaneous AP sites increased while APE-1 activity decreased [143, 144]. These findings show that modifying the endogenous level of GAPDH interferes with APE-1's ability to maintain DNA integrity, and they may be the first to show the significance of GAPDH function to rates of spontaneous mutation in vivo. As a result of its ability to reactivate APE-1o to APE-1r, GAPDH may operate as a "guardian protein" for APE-1 activity.

1.3.2.4. Posttranscriptional gene expression regulation and GAPDH

Proteins that bind to the 5′ and/or 3′ untranslated regions (UTR) of mRNA may affect its function post transcriptionally. GAPDH had previously been classified as a 3′UTR binding

protein that interacts with AU rich elements (ARE) in the corresponding mRNA and the GAPDH NAD^+ binding site, as well as a 5′ UTR binding protein [74]. Not only did these investigations show GAPDH-mRNA binding *in vitro* but also their co-localization *in vivo*.
Recent research suggests that GAPDH may act as an mRNA destabilizing protein, speeding up mRNA degradation and reducing the production of the corresponding protein [76]. Other fresh discoveries, however, suggest that GAPDH may act as an mRNA stabilizing protein, preventing mRNA decay and guaranteeing that the related protein's biosynthesis continues. In the case of the former, the findings suggest that GAPDH is useful in maintaining homeostasis, whereas the latter may not represent a useful new function. In **Fig.12**, it would imply that GAPDH may regulate posttranscriptional gene regulation via three different mechanisms, namely, its binding may increase mRNA stability (CSF-1) [145], relax mRNA structure, allowing the latter to be degraded (ET-1) [146, 147], or competitively inhibit its translation (AT1R). These findings could point to a fascinating intracellular quandary. GAPDH binds to the corresponding 3-UTR decay elements in each case. According to structural research, the binding site in each mRNA is likely identical. However, the functional outcome of that binding is separate. This would imply that the binding sites are indeed distinct, that a control mechanism is required such that GAPDH binding to a single site yields three such divergent effects, or that other sequences in the individual mRNA may be downstream regulatory factors [147, 148].

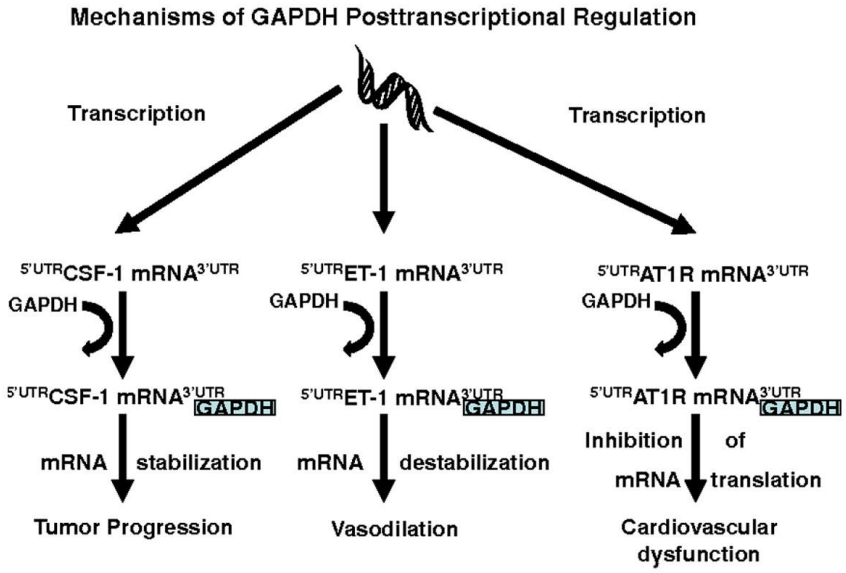

Fig. 12. Mechanisms of GAPDH post transcriptional regulation (Adapted from Sirover et al, *Biochim Biophys Acta* 2011)

1.3.2.5. GAPDH and oxidative stress

GAPDH's vulnerability to oxidative stress has been linked to S-nitrosylation of its active site cysteine in previous investigations. GAPDH, on the other hand, isn't just a bystander whose inactivation causes cell death. Rather, it is a key component of the cell's reaction to reactive oxygen species [79, 87]. Surprisingly, this could be due to the development of two competing GAPDH protein complexes: GAPDH and Siah1: oxidative stress-induced protein interactions as a mechanism for cell toxicity Protein interactions as a regulatory mechanism for decreasing GAPDH-induced cell toxicity, according to GOSPEL, GAPDH, and oxidative stress **(Fig.13).**

Siah1 is an E3 ubiquitin ligase that catalyzes protein degradation, which is a key process in apoptotic cell death [149]. Siah1 is, on the other hand, fundamentally unstable. As a result, its constitutive levels are negligible under normal physiological settings [150, 151]. According to new research, GAPDH and Siah1 have a one-of-a-kind association. A yeast two-hybrid screen employing C-terminal GAPDH sequences as bait identified GAPDH as an in vivo Siah1 binding partner. The formation of the GADPH: Siah1 complex boosted Siah1 stability, as evidenced by a decrease in *in vivo* turnover. Siah1 half-life was shortened when GAPDH Lys225 in the Siah1 binding region was mutated [152]. Significantly, S-nitrosylation of GAPDH caused by oxidative stress increased Siah1 binding, which was both time-dependent and reliant on SNO-GAPDH production. Binding was disrupted when its active site cysteine, which is needed for SNO modification, was mutated. S-nitrosylation of GAPDH boosted the SNO-GAPDH: Siah1 protein complex's nuclear translocation.

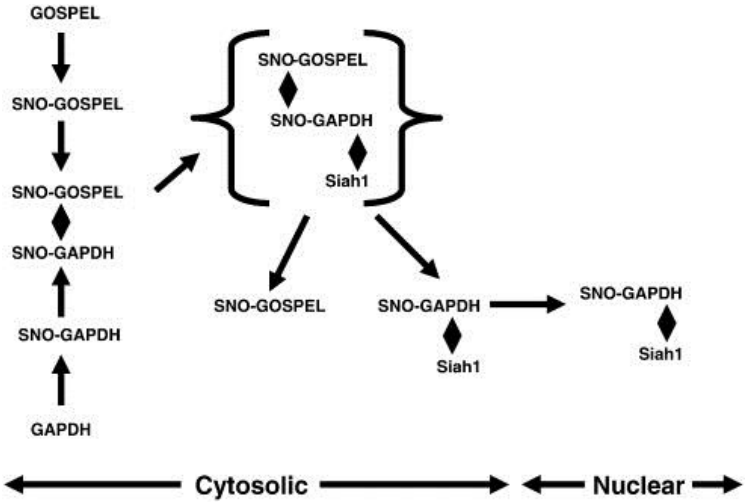

Fig. 13. Role of GAPDH in oxidative stress (Adapted from Sirover et al, *Biochim Biophys Acta* 2011)

Recent research reveals that GAPDH is not only a key target for oxidative stress, but it may also serve as a focal point for protective mechanisms aimed at mitigating the harmful consequences of reactive oxygen species. These findings suggest that cells possess a distinct protein known as GOSPEL (GADPH's competitor of Siah Protein Enhances Life). A yeast two-hybrid screen employing N-terminal GAPDH sequences as bait yielded GOSPEL [153]. The binding of GOSPEL-GAPDH is important because it hinders the development of the SNO-GAPDH-Siah1 complex. *In vitro* competitive binding analyses show that GOSPEL competes with Siah1 for GAPDH binding [154]. GOSPEL may be critical to the cell's ability to defend itself against oxidative stress. Overexpression of GOSPEL prevented oxidative stress-induced cell viability reductions. According to genetic studies, N-terminal GOSPEL sequences were necessary, which is the portion of the protein that can be S-nitrosylated. Furthermore, siRNA-mediated inhibition of endogenous GOSPEL enhanced cell toxicity in response to oxidative stress.

1.3.2.6. GAPDH in apoptosis

Apoptosis, a defined program of gene expression that leads in orderly cell death, is triggered by nitric oxide-induced cell damage. GAPDH's role in programmed cell death was unknown despite many research indicating its nucleus localization and contribution to apoptosis [103]. Recent research has not only characterized that contribution, but also shown that it may consist of two unique and independent roles, each of which may be critical in apoptosis. As mentioned in the preceding section, oxidative stress causes the development of a SNO-GAPDH: Siah1 complex as well as its subcellular nuclear translocation [79, 155]. The induction of apoptosis was used to define the physiological importance of complex formation and translocation. Ubiquitination and degradation of nuclear proteins are two mechanisms that underpin GAPDH Siah1's function

[156]. Apoptosis is prevented by mutations that reduce Siah1 function, erase its nuclear localization signal, or prevent the formation of the GAPDH-Siah1 complex [157]. Studies that suggest that GAPDH-Siah1-induced apoptosis is independent of GAPDH glycolytic activity are also intriguing. GAPDH is a crucial target for oxidative stress-induced apoptosis, according to new research, not only because it stimulates the latter's E3 ubiquitin ligase activity, but also because it initiates an apoptotic gene expression program [134]. According to new research, the latter is predicated on S-nitrosylated GAPDH-Siah1 binding to P300/CBP, generating a second nuclear protein complex that is disrupted in iNOS mutant mice [107, 158]. The significance of this second protein: protein interaction is that it triggers a sequence of protein processes, including SNO-GAPDH acetylation at Lys160, after the complex is established [159]. GAPDH acetylation was eliminated by mutations in GAPDH Lys160 (K160R) or RNAi depletion of P300/CBP. In LPS-treated macrophages, this causes autoacetylation of P300. P300 modification was eliminated by inhibiting iNOS activity, RNAi-induced GAPDH depletion [160], or production of GAPDH K160R (a dominant negative mutant) and alteration triggers an apoptotic pleiotropic cascade involving p53, PUMA, Bax, and other downstream regulators [134]. These findings also point to a complex biochemical process in which cells regulate oxidative stress-induced apoptosis via changes in GAPDH structure and function, as seen in **Fig.14**. The assumption is that each mutation alters GAPDH conformation and the structure of the GAPDH protein complex in a sequential manner, enhancing the chain of reactions required for downstream apoptotic gene regulation [161].

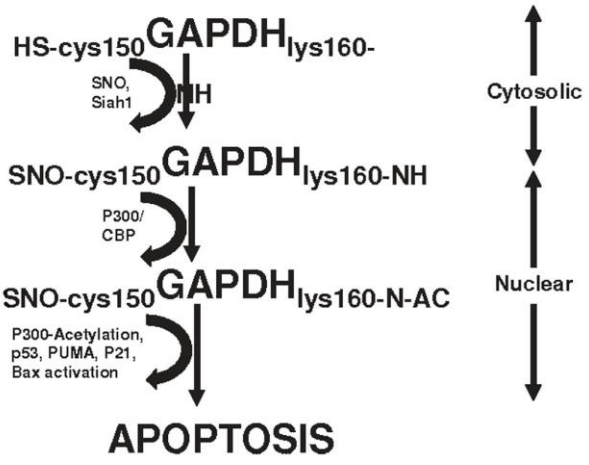

Fig. 14. Role of GAPDH in Apoptosis (Adapted from Sirover et al, *Biochim Biophys Acta* 2011)

1.3.2.7. GAPDH and autophagy

Autophagy is a restorative pathway that allows injured cells to undergo intracellular repair, allowing them to regain viability and normal cell function [162, 163]. This, like apoptosis and caspase independent cell death (CICD), necessitates a well-defined program of gene expression selection. GAPDH may be intimately involved in the autophagic process, according to recent evidence [108]. Studies identified two mechanisms through which GAPDH functioned to increase cell survival: cytoplasmic production of ATP via glycolysis to provide an energy source in the absence of mitochondrial function, and nuclear regulation of autophagic gene expression [118]. In the case of the former, GAPDH boosted ATP levels by a factor of two above what was reported in controls. In the case of the latter, GAPDH promoted the transcription of agt12, an autophagy-related gene [164]. The use of GAPDH mutant constructs indicates that both functions are required for protection against CICD, as GAPDH mutants that reduce glycolysis or prevent autophagic gene expression by themselves failed to protect against CICD, whereas co-transfection of both mutants provided protection similar to that seen for wild type GAPDH [165]. It may be claimed that while overexpression of GAPDH was required for protection against CICD, this is essentially a laboratory discovery that has nothing to do with GAPDH's functional diversity *in vivo* [108]. Although this may be true in normal cells, the role of GAPDH in cell

protection may give a cell survival strategy associated to human disease pathology [166]. GAPDH expression is upregulated in age-related neurodegenerative illnesses and is raised in most, if not all, malignancies [167, 168]. As a result, this additional GAPDH function could be significant in terms of etiology.

1.4. Introduction to leishmanial GAPDH

Unlike higher eukaryotic cells, where the glycolytic metabolic process occurs in the cytoplasm, the glycolytic pathway is mostly found in specialized organelles called glycosomes [169] in protozoan Kinetoplastida such as *Trypanosoma* and *Leishmania* [170-173]. Glyceraldehyde-3-phosphate dehydrogenase (GAPDH) is an enzyme that catalyses the conversion of glyceraldehyde 3-phosphate (GAP) to D-glycerate 1, 3-bisphosphate in the sixth step of glycolysis (1,3BPGA) **(Fig.15).** GAPDH and phosphoglycerate kinase (PGK) are enzymes that could partially govern glycolytic flux in the circulation of *Trypanosoma brucei*, according to computer modelling [174-176]. *T. brucei*, *Trypanosoma cruzi*, and *Leishmania mexicana* glycosomal GAPDHs have all had their crystal structures determined. *T. brucei* and *T. cruzi* have been found to be killed by inhibitors that selectively disrupt *Trypanosome* glycosomal GAPDH activity but not human GAPDH activity. GAPDH activity has been identified in the cytoplasm of *T. brucei* and *L. mexicana*, despite the fact that the Kinetoplastida glycolytic pathway occurs primarily within glycosomes. *T. brucei* and *L. mexicana* both carry two copies of the glycosomal GAPDH (gGAPDH) gene in tandem array and one copy of the cytosolic GAPDH (cGAPDH)-encoding gene [177, 178]. Genes encoding gGAPDH and cGAPDH have also been identified in *Leishmania infantum* and *Leishmania donovani*. In *Leishmania major*, the cGAPDH gene has developed into a pseudogene, while in *Leishmania braziliensis*, it is completely gone [179-181]. Sequences with glycosomal targeting signals are found in the gGAPDH enzymes. The amino acid sequences of the gGAPDH and cGAPDH isoenzymes are only around 55% identical, and phylogenetic analyses suggested that the genes encoding the gGAPDH and cGAPDH isoenzymes are related [182, 183]. One gene comes from the trypanosome lineage, while the other may have entered the cell 108 years ago through horizontal gene transfer that happened before *Trypanosoma* and *Leishmani*a diverged [184].

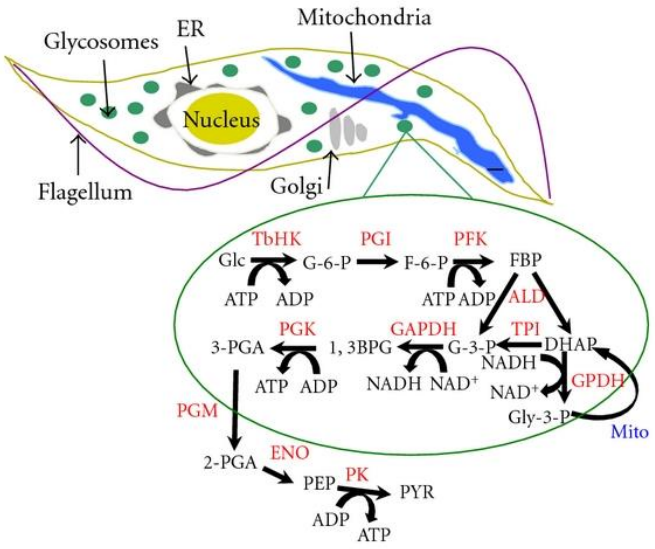

Fig. 15. Glycolysis occurring in the glycosomes of the African Trypanosomes (Adapted from Coley et al, *Mol. Biol. Int*, 2011**)**

1.5 Objective of the present work

Leishmaniasis is one of the most severe and highly disabling disease of tropical and subtropical countries. Despite of its severity, only a first line drugs such as antimonials are in use but are highly unsatisfactory. Chemotherapeutic drugs like amphotericin, paromomycin, pentamidines are used but again all these drugs are extremely expensive with numerous side effects. As a result, there is an urgent need to create new medications that are both cost-effective and specialised for the parasite, i.e., they will not harm the host. To develop new medications, researchers must identify new potential drug targets that are particular to the parasite and not present in the host. Glycolysis is perceived as a promising target for new drugs because this pathway plays an important role in the supply of ATP and at the same time this process is compartmentalized within a specialized organelle called glycosome protozoan Kinetoplastida such as *Trypanosoma* and *Leishmania*.

Glyceraldehyde-3-phosphate dehydrogenase (GAPDH) is a classic glycolytic enzyme and is involved in the reversible oxidative phosphorylation of glyceraldehyde-3-phosphate in the presence of inorganic phosphate and nicotinamide adenine dinucleotide (NAD). Besides being a glycolytic enzyme it has got several other functions independent of its role in energy metabolism and is considered as a moonlighting protein.

But in the case of *Leishmania*, apart from glycolysis, till now, no other function of GAPDH is known. In *Leishmania* species, specific post-translational modifications, protein-protein interactions, and subsequent alterations in the intracellular distribution of GAPDH are still unknown. So, considering all these facts together, in this project, our main objective is to find out the possible role of GAPDH in *Leishmania* other than its role in glycolysis that could be critically important for designing new drugs or therapeutic strategies against the disease.

“In Sciences, thousands of opinions is not worth as much as one tiny spark of reason in an individual man.”

_ Galileo Galilei

Materials and Methods

MATERIALS & METHODS

2.1 Materials

2.1.1 Reagents

L. major (strain 5ASKH) was procured from the *Leishmania* strain bank of our Institute. Kits for plasmid DNA isolation, genomic DNA isolation, DNA extraction from agarose gel, PCR product purification and Ni-NTA Agarose from Qiagen. Protein estimation reagent was purchased from Bio-Rad. Restriction enzymes, T4 DNA ligase, Pfu DNA polymerase, Taq DNA polymerase, Rapid DNA ligation kit, DNA molecular weight marker purchased from Thermo Scientific. Antibiotics, agarose, acrylamide, N, N'-bisacrylamide, TEMED, β-mercaptoethanol, bromophenol blue, coomassie brilliant blue R-250, SDS, Tris, glycine, BSA, sodium acetate, ethidium bromide, IPTG and all other chemicals, unless mentioned, were purchased from Sigma. Alpha-tubulin antibody (1:5000) was from Millipore. Rabbit polyclonal antibody for TNF-alpha (1:1000) was from Abcam and also from Merck. Anti-rabbit (1:80000) and anti-mouse (1:80000) IgG antibodies conjugated to alkaline phosphatase were from sigma. NBT/BCIP reagents were purchased from Roche and Puregene. DEPC water was purchased from Merck. RPMI was bought from GIBCO, Invitrogen. Any other reagents, used in any experiment not mentioned here, is described otherwise or reported previously [185-187].

2.1.2. Strains used

A. *Leishmania*

Leishmania major (5 ASKH).

B. Macrophage

Mouse macrophage cell line RAW264.7.

C. Bacterial strain used

The following strains of *Escherichia coli* were used: DH5α, JM109 and BL21 (DE3)

2.1.3. Plasmid vectors used

- For cloning of open reading frame: pET15B.
- For overexpression: pXGNeo.
- For knockout construct formation: pXGNeo and pXGHgo plasmids were used.
- For complementation: pXGPhleo plasmid was used.

2.1.4. *Leishmania* culture media

M199 powder	11.0 gm
HEPES	5.1 gm
Adenine	200 μM
Folic acid	150 μg/ml
Haemin	10 μg/ml

Volume was made up to 1000 ml and pH adjusted to 7.4 with HCl. Penicillin streptomycin was added at 1.5% and gentamycin added to 50μg/ml. Finally, the media was filtered through 0.22 μM sterilized filter unit and stored at 4° C.

2.1.5 Bacterial culture media

A. Luria Bertani (LB) medium (pH 7.5)

Composition	*concentration*
Luria broth	20g/L

B. Terrific Broth (TB) (pH 7.5)

Composition	*concentration*
Bacto- tryptone	12g/L
Yeast extracts	24g/L
Glycerol	4ml/L

Volume was made up to 900 ml by de-ionized water and was sterilized by autoclaving. Potassium Phosphate Solution (0.17M KH_2PO4 and 0.72M K_2HPO4) was made by dissolving 2.31g of the former and 12.54g of the latter in a final volume of 100 ml de-ionized water and sterilized by autoclaving.

2.1.6. Buffers and solutions

A. Potassium phosphate buffer

KH_2PO_4	170 mM
K_2HPO_4	720 mM

B. Phosphate buffered saline (pH– 7.4)

Na_2HPO_4	14.4 g/L
KH_2PO_4	2.4 g/L
NaCl	80 g/L
KCl	2.0 g/L

C. 50X TAE buffer

Tris base	242 g/L
Glacial acetic acid	57.1 ml/L

EDTA (0.5 M, pH – 8)	100 ml/L

D. Electroporation buffer for *Leishmania major*

HEPES (pH- 7.4)	21 mM
NaCl	137 mM
NaH_2PO_4	0.7 mM
D-glucose	6 mM

E. SDS-PAGE running buffer

Glycine	14.4 g/L
Tris	3.0 g/L
SDS	1.0 g/L

F. Bacterial cell lysis buffer

Tris-HCl, pH-7.5	50 mM
NaCl	150 mM
PMSF	1 mM
B-mercaptoethanol	0.05%
Lysozyme	1 mg /ml

Protease inhibitor (without EDTA) 0.5 tablet

G. Equilibration buffer for protein purification

Tris-HCl, pH-7.5	50 mM
NaCl	250 mM
PMSF	1 mM
Imidazole, pH-7.5	20 mM
Glycerol	10%

H. Buffer for protein elution

Tris-HCl, pH-7.5	50 mM
NaCl	250 mM
PMSF	1 mM
Imidazole, pH-7.5	20 mM
Glycerol	10%

Protease inhibitor (without EDTA) 0.5 tablet

2.2. Methods

2.2.1. Methods for cloning LmGAPDH

2.2.1.1. Isolation of genomic DNA from *Leishmania major*

The genomic DNA from *Leishmania major* was isolated by using the 'Genomic DNA isolation kit' (Qiagen). 2×108 *Leishmania major* promastigote cells were washed twice with 1X cold PBS and pelleted down at 4000 rpm for 6 mins in a 1.5 ml micro-centrifuge tube. 200 µl Buffer ATL (lysis buffer), containing 20 µl proteinase K and 10 mg/ml RNaseA was added and pulse vortexed for 30 secs. It was then incubated at 56°C until the cells were completely lysed (15 mins approximately). After complete cell lysis, 200 µl of ethanol was added and again pulse vortexed followed by a pulse spin. Then the mixture was transferred on to a spin column provided by the manufacturer. It was centrifuged at 8000 rpm for 1 min. The solution deposited at the bottom tube was discarded. 500 µl of AW1 buffer was then added to the column and centrifuged at 8000 rpm for 1 min. The solution deposited at the bottom tube was again discarded. Then, 500µl of AW2 buffer was added to the column and centrifuged at 14000 rpm for 3 mins. The supernatant deposited at the bottom of the tube was discarded. Finally, DNA was collected in a fresh centrifuge tube by eluting the column with 75 µl of nuclease free water by centrifuging at 14000 rpm for 1 min. For long-term storage of DNA was stored at –20°C. The DNA purity was checked with an A260/A280 ratio of 1.7–1.9.

2.2.1.2. Polymerase Chain Reaction (PCR)

PCR amplification was done by using purified leishmanial genomic DNA as template. Each 50 µl reaction having 30 ng of template genomic DNA, 20 Pico moles of forward and reverse primers, 200 µM of each dNTP, 1.5 mM $MgCl_2$ and 2.0 U of High fidelity DNA polymerase. PCR was done in a Veriti Thermal Cycle (Applied Biosystems) for 30 cycles. Each cycle consisted of: i) denaturation at 95°C for 1.0 minutes; ii) annealing at 52°C for 30 seconds; iii) extension at 68°C for 2.5 minutes and iv) a final cycle of extension at 68°C for 10 minutes. The amplified product was purified by PCR purification kit (Qiagen).

2.2.1.3. Cloning of LmGAPDH

Forward primer 5'- AAAACATATGATGGCTCCTATCAAGGTCGG-3' and reverse primer 5'-AAAAGGATCCCTACATCTTGGCGCTCGCAG-3, were used to amplify the entire ORF of the GAPDH (accession no: Lmjf.30.2970) to get a 1083bp fragment that was digested and cloned within pET15B vector in NdeI/BamHI restriction sites. To confirm the ORF DNA sequencing was performed.

2.2.1.4. Agarose gel electrophoresis

1% agarose gel was run depending upon the size of DNA fragments to be separated. DNA samples were mixed with 1X DNA loading buffer (Thermo Scientific) and then loaded onto the wells of the submerged gel. The gel was run in 1X TAE at a constant voltage of 12 V/cm. DNA was visualized by staining with ethidium bromide solution (0.5 µg / ml) by UV irradiation.

2.2.1.5 Isolation of plasmid DNA using miniprep kit

10 ml of bacterial cell culture containing the plasmid of interest, was grown overnight in LB medium and then harvested in a 2.0 ml micro centrifuge tube. 300 µl of resuspension buffer P1

containing RNaseA was added to the bacterial cell pellet and the cells were vortexed mildly. 300 µl of lysis buffer P2 was added to that solution and mixed by gentle shaking. 400 µl of neutralizing buffer N3 was finally added and was mixed gently. The resultant solution was centrifuged at 14000 rpm for 30 minutes to eliminate the cell debris, genomic DNA and proteins. The supernatant was then loaded on to the column provided by the manufacturer and centrifuged at 14000 rpm for 1 minute. Solution deposited at the bottom tube was discarded. Column was then washed with 500 µl of binding buffer PB followed by a wash with 750 µl of wash buffer PE containing ethanol. Then the empty column was re-centrifuged to get rid of any trace of PE buffer. Finally, 70 µl of autoclaved double distilled water was added to the column and it was placed on the top of a fresh 1.5 ml micro centrifuge tube. After centrifugation DNA pellet (70 µl) was deposited in the micro centrifuge tube. Concentration of DNA was checked spectrophotometrically or by running agarose gel with suitable standards.

2.2.1.6. Restriction digestion of the amplified DNA and the cloning vector:

Restriction digestion of the PCR amplified DNA and the cloning vector was carried out at 37°C for 4 hrs according to the following

Sterile, deionized water	9.5 µl
Restriction Enzyme 10X Buffer	4.0 µl
Acetylated BSA, (10 µg/µl)	0.5 µl
DNA, (1 µg/µl)	25.0 µl
Restriction Enzyme, (10 u/µl)	1.0 µl
Final volume	40.0 µl

2.2.1.7. Purification of DNA by gel extraction kit

The digested products were run on a 1% agarose gel from where the DNA band of interest, as visualized, was cut out by using a sterile scalpel blade. The gel piece obtained was taken in a micro centrifuge tube. The DNA was eluted out of the gel piece by using gel extraction kit (Qiagen): Briefly, QG buffer (300 µl/100 mg gel piece) was added to the gel piece and was incubated for 10 minutes at 56°C and vortexed at every 2 minutes intervals. After complete solubilization of the gel, the suspension was loaded onto a spin column provided by the manufacturer. It was centrifuged at 14000 rpm for 60 seconds and the solution at the bottom tube was discarded. 500 µl of QG buffer was added to silica column and again centrifuged at 14000 rpm for 60 seconds. Like before, the supernatant deposited at the bottom tube was discarded. Pellet was re-suspended in nucleic acid binding buffer, PB (500 µl) and again centrifuged. Then the pellet was washed twice with wash buffer PE containing ethanol and centrifuged at 14000 rpm for 60 seconds. The column was re-centrifuged to eliminate any traces of PB buffer. 35 µl of autoclaved double distilled water was then added to the pellet, incubated at room temperature for 2 mins. Finally, it was centrifuged at 14000 rpm for 1 minute to obtain purified DNA.

2.2.1.8. Ligation of insert and vector DNA

Ligation reactions were performed at 22ºC for 1 hour in the following way using 'rapid DNA ligation kit' from 'Thermo Scientific':

Vector DNA (1 µg/µl)	0.1 µl
Insert DNA (0.4 µg/µl)	1.0 µl
5X buffer	3.0 µl
T4 Ligase (10U/µl)	1.0 µl
Ionised water	5.9 µl
Final volume	10 µl

2.2.1.9. Transformation

The transformation of *E. coli* cells with purified plasmid DNA or ligation mix was carried out by the conventional $CaCl_2$ heat shock method. Desired amount of DNA was mixed with 100 µl of *E. coli* competent cells (previously prepared). It was then kept in ice for 30 mins. Next, heat shock was given for 90 secs at 42ºC and then immediately put in ice for 5 mins. 1 ml of LB media (without antibiotic) was added to the tube and incubated for 1 hour at 37ºC. After 1 hour, it was centrifuged at 14000 rpm for 2 mins and the pellet was dissolved in the remaining media. The re-suspended pellet was then spread plated on a 90 mm bacterial culture petriplate having the concerned antibiotic selection.

2.2.1.10. DNA sequencing

Automated DNA sequencing was done according to the chain termination method. Briefly, a 10 µl reaction was prepared containing 1 µl BD mix (provided with the sequencing kit), 1.5 µl of 5X buffer, 150-200 ng of template DNA and 6 pmol of sequencing primer. PCR was carried out in a Perkin Elmer automated thermal cycler for 30 cycles. Each cycle consisted of: i) denaturation at 96°C for 10 sec; ii) annealing at 53°C for 10 sec; iii) extension at 60°C for 4 minutes. After the PCR, 20 µl of water was added to the reaction mixture. The DNA was purified using ethanol precipitation method. 19 µl high dye (provided with the kit) was added to the DNA pellet and kept in dark for 15 mins. The mixture was then heat-chilled and finally 10 µl of the mix was loaded on to a well of 96-well plate of Perkin Elmer ABI Prism™ DNA sequencer.

2.2.2. Methods for expression & purification of LmGAPDH

2.2.2.1. Expression and purification

Recombinant pET15B/LmGAPDH were transformed into *Escherichia coli* BL21 (DE3) and were grown overnight in 100 ml of Luria-Bertani broth containing 100 µg/ml ampicillin at 37 °C shaker. The overnight grown culture was then inoculated in 1L of terrific broth. When the culture reached an absorbance of around 0.8-1.0 at 600 nm, 0.25 mM isopropyl β-D-1-thiogalactopyranoside was added and bacteria was further grown at 28 °C for around 18 hours. Cells were then harvested by centrifugation at 6000 x g for 10 min and washed 2 times with 1X PBS and resuspended in 50 mM Tris-HCl buffer pH 7.5 containing 0.5 mM EDTA, 10% glycerol, 150 mM NaCl, protease inhibitor cocktail (Roche), 0.5 mM PMSF and 1.0 mg/ml lysozyme. The resuspended solution was kept for 45 mins at 4ºC and then the cells were lysed

by sonication. The lysate was centrifuged at 14000 rpm for 1 hr. The supernatant was loaded on to a Ni^{2+}-nitrilotriacetate column. After loading the crude extract, the column was washed with 10 column volumes of washing buffer (50 mM Tris-HCl pH 7.5, 150 mM NaCl, 10% glycerol and 1 mM PMSF). The enzyme was eluted with the washing buffer supplemented with 250 mM imidazole. The enzyme thus obtained was dialysed three times against 50 mM Tris-HCl buffer pH 7.5, 150 mM NaCl, and 10% glycerol. Molecular weight and purity of the proteins were confirmed by 13% SDS PAGE. As expected, purification yielded a single protein band of approximately 39 kDa. No other protein band could be detected in the gel stained with coomassie brilliant blue.

2.2.2.2. SDS-Polyacrylamide gel electrophoresis (SDS-PAGE)

SDS-PAGE was performed using the method of Laemmli [188]. Briefly, induced cells or enzyme preparations were boiled for 10 minutes with Laemmli buffer and loaded onto either 10% or 13% cross-linked SDS-polyacrylamide gel.

2.2.2.3. SDS-gel staining by Coomassie Brilliant Blue

The SDS-PAGE gel was immersed in a solution of acetic acid (10%) and methanol (45%) containing 0.25% Coomassie brilliant blue R-250 for the purpose of staining. Staining was usually done by keeping the gels for 1-2 hrs as per requirement. De-staining was carried out with the de-staining solution containing acetic acid (10%) and methanol (45%).

2.2.3. Methods for physical characterization of LmGAPDH

2.2.3.1. Protein Concentration Determination

Protein concentrations of LmGAPDH was measured using Bio-Rad reagent. BSA was used as the standard [189].

2.2.3.2. Enzyme assay using UV-visible spectroscopy

The activity of LmGAPDH was measured spectrophotometrically at 25°C using Shimadzu UV-2550 spectrophotometer by monitoring NADH generation at 340 nm wavelength. The assay mixture consisted of 40 mM Tris-HCl buffer (pH 7.5), 50 mM K_2PO_4, 0.15 mM NAD^+, 2.5 mM glyceraldehyde 3-phosphate. After incubating in 1.0 ml cuvette at 25°C for 5 min to achieve temperature equilibrium and establish blank values, the reaction was initiated with the addition of enzyme. Absorbance from 0 to 5 min was recorded.

2.2.3.3. Production of polyclonal antibodies against LmGAPDH

Polyclonal antibodies against the purified recombinant LmGAPDH (20µg) was raised by subcutaneous injection in 6-month old rabbit using Freunds complete adjuvant. This was followed by three booster doses of recombinant LmGAPDH (15µg) with incomplete adjuvant at two-week intervals. The rabbit was bled 2 weeks after the last booster and sera was collected and used for Western blot analysis.

2.2.4. Methods for functional characterization of LmGAPDH

2.2.4.1. Parasite culture

Leishmania major (strain 5ASKH) promastigotes obtained from CSIR-IICB repository, were routinely cultured at 22 °C in M199 medium (Invitrogen) supplemented with 40 mM HEPES (pH 7.4, Amresco), 200 µM adenine (sigma), 1% penicillin-streptomycin (v/v), 50 µg/ml gentamycin (Abott), and 10% heat-inactivated fetal bovine serum (Invitrogen).

2.2.4.2. Construction of different cell lines of *Leishmania* promastigotes

A) Transfection in *Leishmania major*

Transfection of all the constructs in *L. major* was done by electroporation [190]. Late log phase promastigotes (1.0×10^7 cells/ml) were pelleted down at 4000 rpm (4ºC) for 10 minutes and washed twice in electroporation buffer. Finally, the cell suspension was made up to a density of 1×108/ml and 360µl from this was taken in a 0.2 mm ice chilled electroporation cuvette (Biorad Laboratories). 30-50 µg of circular DNA or 15-20 µg of linear DNA dissolved in 40 µl of electroporatic buffer was then added to the cuvette and incubated in ice for 10 minutes. Then electroporation was done with a Biorad Gene Pulser apparatus using 450 volts and 500 µF capacitance. The cells after electroporation were then added to 5 ml of drug free Schneider *Drosophila* media (GIBCO) and kept for 24 hours at 22 ºC in shaking for revival. Depending on the drug-resistant gene present in the plasmid or construct, proper concentration of antibiotic was added and kept at 22ºC for another 10 days. Presence of transfected cells was monitored visually by microscope and the drug concentration was increased gradually with each passage.

B) Construction of over-expression system for GAPDH in *Leishmania*

To amplify the ORF of *L. major* GAPDH gene by PCR, primers 5'-AAAACCCGGGATGGCTCCTATCAAGGTCGG-3' (forward) and 5'-AAAAGGATCCCTACATCTTGGCGCTCGCAG-3' (reverse) were used. The amplified portion was then cloned into the SmaI/BamHI site of pXG-B2863 vector, which was then transfected into *L. major* by electroporation [191]. Over expressed cells were maintained at 200 µg/ml neomycin.

C) Generation of half knock out strain for LmGAPDH alleles

To generate the half knock out constructs of LmGAPDH gene, modified pXG-neo and pXG-hyg vectors were used. Primers 5'-AAAAAAGCTTAGCTGACCGGCATGTCC-3' and 5'-AAAAGTCGACCGACCTTGATAGGAGCC-3' used for amplifying 5' flank and primers 5'-AAAACCCGGGTATGATAGCAGCGCAGCTG-3' and 5'-AAAAGGATCCCTGCCTCATTGTGCATGTGC-3' used for amplifying 3' flank of the gene. The 5'F and 3'F DNA fragments were cloned on either side (at HindIII/ SalI and SmaI/BamHI site) of neomycin and hygromycin gene of pXG-neo and pXG-hyg vectors, respectively. Both

constructs were then digested with HindIII and BamHI to get linear fragments of gene deletion constructs LmGAPDH::NEO and LmGAPDH::HYG, were transfected into *L. major* sequentially as described [192]. Knock out strain was cultured in presence of 50 µg/ml neomycin and 100 µg/ml hygromycin drug.

D) Complementation of LmGAPDH in null mutants

To recover LmGAPDH in the half knock out parasites, LmGAPDH ORF was PCR-amplified using a LmGAPDH containing plasmid as template and the following forward primer 5'-AAAAGGATCCATGGCTCCTATCAAGGTCGG-3' and reverse primer 5'-AAAAGGATCCCTACATCTTGGCGCTCGCAG-3. The amplified product was cloned at the BamHI site of pXG-PHLEO vector. 10 µg of the pXG-PHLEO- LmGAPDH was then transfected into the half knockout promastigotes. Transfected promastigotes were selected with minimal doses of phleomycin (5 µg/ml) and finally was maintained in the presence of 60 µg/ml neomycin, 100 µg/ml hygromycin and 10 µg/ml phleomycin drug.

2.2.4.3. Isolation of different subcellular organelles:

A) Isolation of mitochondrial and cytosolic and nuclear fractions

Mitochondrial, nuclear and cytosolic fractions were isolated from *L. major* promastigotes using the mitochondria isolation kit (Qiagen). The purity of the fractions was confirmed by immunoblotting using specific markers for the organelle i.e., rabbit anti- (*L. major*) ascorbate peroxidase (1:50) antibody for the mitochondria, rabbit anti- (*L. donovani*) adenosine kinase (1:50) for the cytosol and rabbit anti-goat histone 2B antibody (1:2000) for nuclear fraction. The alkaline phosphatase-conjugated anti rabbit secondary antibody (Sigma) were used at a dilution 1:15,000.

B) Isolation of extracellular vesicles (EVs)

For all extracellular vesicles (EVs) related experiments, EVs- depleted FBS was used and it was prepared by ultracentrifugation of the FBS at 110,000×g for 5 h. For isolation of EVs, cells were grown in media made from EVs-depleted FBS. The cell culture, having 2×10^8 cells were taken and then centrifuged first at 300×g for 10 min, then at 2000×g for 15 min followed by centrifugation at 10,000×g for 30 min. All centrifugations were done at 4°C. The supernatant was then filtered through a 0.22 µm filter unit. This supernatant was overlaid on a 30% sucrose cushion and then centrifuged at 100,000×g for 90 min at 4°C. After centrifugation, the supernatant just above the sucrose cushion was discarded leaving behind a narrow layer of medium with EVs at the interface. EVs were then re-suspended with 1X PBS (filtered) and again centrifuged at 100,000×g for 90 min at 4°C. The pellet used as the EVs.

C) Isolation of glycosomal fractions

Glycosomes from *L. major* promastigotes were isolated using Colasante et al's [193] technique with a little modifications. *L. major* promastigotes were harvested by centrifugation for 10 min at 2,000× g, and were washed once in 10 ml of wash buffer (25 mM Tris, 1 mM EDTA, 1 mM

DTT, 250 mM sucrose, pH 7.8). After centrifugation, the cell pellet was resuspended in 2 ml homogenization medium (250 mM sucrose, 1 mM EDTA, 0.1% (v/v) ethanol, 5mM MOPS, pH 7.2) containing protease inhibitor (complete EDTA-free, Roche Applied Science) and was lysed using syringe (needle gauge-0.30 x 12.5mm). Cell lysis was confirmed by light microscopy. The cell lysate was centrifuged sequentially for 5 minutes each at 100× g and 3000 x g to remove cell debri and cell nuclei. The resulting supernatant was centrifuged at 17,000 x g for 15 minutes to obtain glycosomal enriched pellet. This pellet was resuspended in 1.0 ml homogenizing buffer and was loaded on top of a 24 ml linear 20-40% (v/v) optiprep gradient (sigma), mounted on 50% 2.5 ml optiprep cushion and centrifuged at 1,70000 x g for 1 hr. 9 fractions (1.0 ml each) were collected from the bottom of the tube. They were centrifuged at 30,000 x g to obtain the pellet. The pellet was resuspended in homogenizing buffer and again centrifuged at 30,000 x g to obtain the purified glycosomal pellet. The purity of the fraction was checked by western blotting using the glycosome specific rabbit LmPAS-PGK antibody (1:50).

2.2.4.4. Approaches for verification of size and nature of the Extracellular vesicles (EVs)

A) AFM for visualizing EVs structure

Purified EV preparations were diluted with filtered PBS (1:100) for AFM imaging, and a 5µl aliquot of the diluted sample solution was put on a newly cleaved mica sheet and incubated for 10 minutes at room temperature. To remove salt and weakly attached moieties, the dried sample was gently washed with 200 µl of Milli-Q water. AFM experiments were performed in intermittent contact mode (called "tapping" or AAC mode) to minimize tip-induced damage. AAC mode AFM was performed using a Pico plus 5500 inverted light microscope AFM (Agilent Technologies) with a Piezo scanner (maximum range 9 µm). Micro fabricated silicon cantilevers 225 µm in length with a nominal spring force constant of 21–98 N/m were used (Nano Sensors). Cantilever oscillation frequency was tuned into resonance frequency. The cantilever resonance frequency was 150–300 kHz. The images (512 × 512 pixels) were captured with a scan size between 0.5 and 0.8 µm at a scan speed rate of 0.5 lines/s. Images were processed by flatten using Pico view1.1 version software (Agilent Technologies). Image manipulation was done using Pico Image Advanced version software (Agilent Technologies).

B) Dynamic Light Scattering (DLS) Zeta (ζ) Potential Measurements

The extracted EVs (100µl) were diluted 10 times using 1XPBS and then transferred into a disposable cuvette (40 µl), and then the EVs-containing cuvette was put into the DLS device to start measuring. All size distribution and ζ-potential experiments were conducted using the Nano-ZS instrument (Malvern Instruments, Worcestershire, U.K.) at 25 °C (5 mW, He–Ne laser, λ = 632 nm, scattering angle = 173°). For determining size distributions by DLS, the operation procedure was programmed using the DTS software supplied with the instrument to record the average of an automated number of runs. Every run was collected for 10 s, and an equilibration time of 5 min was used, prior to starting the measurement. For all ζ-potential measurements, samples were loaded into a folded capillary cell and average ζ-potential values obtained from an automated number of runs (maximum 100) were noted. The instrument

measured ζ-potential from the electrophoretic mobility (μ), using a model described by the Smoluchowski equation.

2.2.4.5. Methods for determining the physiological role of LmGAPDH

A. *In vitro* promastigote growth profile analysis

10^6 mid-log phase CT (control cells), OE (overexpressed cells), HKO (half knockout cells) and CM (complement cells) promastigotes were inoculated in 10 ml of M199 media containing 10% heat inactivated foetal bovine serum. Growth rates for each type of cell were determined by counting the number of cells in an improved Neubauer chamber (haemocytometer) at a 24-h interval. Experiments were carried out in triplicate for each type of cell.

B. Infection assays

a) In-vitro macrophage infection

CT, OE, CM and KO promastigotes at their stationary phase were used to infect the cultures of adherent murine macrophage cell line (RAW264.7) on glass cover slips (22 mm; $5X10^5$ macrophages/cover slip) in 0.5 ml of RPMI 1640/10% FBS mixture at a parasite to cell ratio of 10:1. Following the incubation, unphagocytosed parasites were removed by washing with medium, and cells were resuspended in RPMI 1640/10% FCS mixture at 37 °C. 2 hrs incubation period was used for the determination of parasite entry. Cultures were transferred to a CO_2 incubator at 37°C for an infection period of 24 hrs, 48 hrs and 72 hrs. Cells were then fixed in methanol and stained with propidium iodide. Cells were visualized and quantified using Olympus IX81 microscope.

b) Infection in mice

6–7 weeks old female BALB/c mice were infected subcutaneously with $5X10^6$ stationary-phase promastigotes in their left hind footpads (8 mice per group). Disease progression was monitored by daily caliper measurement of footpad swelling. Parasite loads in footpad of mice containing WT, OE, CM and HKO parasites were determined by limiting dilution assay with a little modification. Before homogenization of weighed tissue in M199 medium supplemented with gentamycin and penicillin-streptomycin containing 10% heat inactivated FBS, footpads were sequentially submerged in 70% ethanol and sterile water. In a 96 well flat bottomed tissue culture plate, each tissue homogenate was serially diluted in the same media. The highest dilution at which promastigotes could be grown out after up to 10-15 days of incubation at 22°C was used to calculate the number of viable parasites per milligrams of tissue.

C. Cytokine measurement

i. Macrophage cell culture

The murine macrophage cell line RAW 264.7 was maintained in RPMI-1640 medium containing 10% heat-inactivated foetal bovine serum (FBS), 100U/ml penicillin, and 100 µg/µl streptomycin at 37ºC in a humidified atmosphere containing 5% CO_2. Cells between passages 5–10 were used for the experiments.

ii. Isolation of mRNA

RAW264.7 cells were cultured in tissue culture flasks to 70-80% confluency and then cells ($1x10^6$ cells/ ml) were plated in 6 well plates for around 24h. After 24h incubation, the 6 well plates were washed twice with RPMI-1640 medium and then incubated again for 8 h with either LPS (1 µg/ml) for the positive control or different type of *Leishmania* cell lines (at a promastigote to macrophage ratio of 10:1). Total RNA was isolated from the RAW264.7 cells infected with *L. major* using Trizol reagent (Invitrogen Life Technologies) according to the manufacture's protocol. Briefly, plates were washed twice with ice cold PBS after infection and then cells were scrapped with trizol reagent (0.5ml of trizol for 5-10x 106 cells) in a 1.5 ml micro centrifuge tube. Then chloroform was added to it (0.2ml chloroform per 1ml of trizol) and agitated for few second followed by incubation for 2-3 min. The sample was then centrifuged at 12000g for 15min at 4°C. The aqueous phase was transferred to a fresh tube which contained the RNA. Isopropanol was added to the RNA (0.5ml of isopropanol per 1ml of trizol), incubated for 3 min and centrifuged for 10 min at 12000g at 4°C. The resultant pellet was washed with 75% ethanol and air dried. The pellet was then resuspended in RNase free water and concentration of RNA was measured by Nanodrop.

iii. cDNA synthesis and Real time PCR

Real time PCR was then performed using High Capacity cDNA Reverse Transcription Kit (Applied Biosystems, ABI) and real-time quantitative PCR was set up on the StepOne Real-Time PCR system (Applied Biosystems, ABI) using Power SYBR Green PCR Master Mix (ABI) and primers to investigate the relative quantities of cytokines TNF α, IL 10 and TGFβ1 mRNA with the following PCR amplification conditions: initial denaturation at 95ºC for 10 min and amplification for 40 cycles (10 sec for 95ºC denaturation, 30 sec for the 56ºC annealing and 45 sec for 72ºC extension). Relative mRNA expression was measured using the Comparative ΔΔCt method by using uninduced macrophage cells as reference sample and beta-actin as the endogenous control as described in the manufacturer's protocol.
Primers 5'-GGATTATGGCTCAGGGTCCA-3' (Forward) and 5'-ACATTCGAGGTCCAGTGAA-3' (Reverse) for TNF- α and primers 5'-TTGTGATGGACTCCGGAGAC-3' (Forward) and 5'-TGATGTCACGCACGATTTCC-3' (Reverse) for beta-actin were used.

iv. Cytokine measurement by ELISA

The supernatant from the *L. major*/macrophage co-culture media and extracellular vesicles treated macrophage were collected and centrifuged to remove non-internalized parasites and debris. The production of pro-inflammatory cytokine TNF-α was quantified using TNF-α Quantikine ELISA kits (R&D systems) according to the manufacturer's instructions.

v. Cytokine measurement by Western blotting

Following 24 hrs of infection cells were collected and lysed in mammalian cell lysis buffer (Cell Signaling Technology). The protein concentrations in the cleared supernatants were estimated using a protein assay mixture (Bio-Rad). 50 µg of protein was subjected to 10% SDS-polyacrylamide gel electrophoresis and proteins were transferred to a nitrocellulose membrane (Millipore), and blocked for 2 hours at 37 °C in TBS-T (20 mM Tris-HCl, 137 mM NaCl, 0.05% (v/v) Tween 20, pH 7.6) containing 5% BSA to prevent nonspecific binding of antibodies. Immunoblotting was performed by incubating in TNF-α monoclonal primary antibody (Abcam) at 1:1000 dilution overnight at 4 ºC. Membranes were washed three times in TBS-T, followed by incubation with anti -rabbit IgG coupled to alkaline phosphatase (1:15000). Again after three washes with TBS-T, membranes were developed by NBT-BCIP (Roche) method.

D. In vitro GAPDH protein transfection

Adherent RAW 264.7 cells were grown on 6 well plates in RPMI 1640 supplemented with 10% FBS. Recombinant LmGAPDH protein was purified according to the protocol mentioned above. Purified protein in a suitable buffer (10 mM Tris, 150 mM NaCl, pH 7.0) was then transfected to the adherent RAW cells through Pierce Protein Transfection Reagent kit (Thermo Scientific) following manufacture's instruction.

E. Immunofluorescence and Confocal microscopy

The transfected cells grown on glass cover slips were washed in 1X PBS and then cell fixation was done by 4% paraformaldehyde. Cells are then permeabilized with 1.0% TritonX 100 in 1X PBS with 50 µg /ml RNaseA (Calbiochem). The cover slips were air dried and blocked with 1.5% BSA for 2 hours. The cover slips were then incubated with anti-rabbit LmGAPDH antibody (1:200) overnight at 4°C. Next day the cover slips were washed with 1X PBS and incubated with Alexa fluor 488 conjugated anti rabbit secondary antibody (Life Technologies) at a dilution of 1:600 for 2 hours. Finally, the cells were mounted on a slide with DAPI containing antifade mounting media (Invitrogen) and observed under confocal microscope (Leica). The wavelength used were DAPI (Ex_λ = 350nm, Em_λ = 470nm), Alexa Flour 488 secondary antibody (Ex_λ = 488 nm and Em_λ = 522 nm).

F. *In vitro* protein translation of TNF-α mRNA in presence or absence of purified leishmanial GAPDH

Total RNA was isolated from the parasite infected RAW264.7 cells using Trizol reagent (Invitrogen Life Technologies) according to the manufacture's protocol. 20 µg of LPS induced mRNA expression in Raw 264.7 cells were subjected to *in vitro* translation by addition of 35 µl rabbit reticulocyte lysate (Promega), 20 mM methionine free amino acid mixture, 40 U of RNase inhibitor (Roche) and 20 µCi of ^{35}S methionine with or without LmGAPDH in a 50 µl reaction for 90 min at 30ºC. A 45 µl aliquot were subjected to immunoprecipitation with TNF-α monoclonal antibody (Abcam) and protein A/G plus agarose (Santa cruz biotechnology) in a buffer containing 50 mM Tris-Cl (pH 7.6), 50 mM NaCl, 1mM PMSF, 1mM DTT, 0.5%

NP40, 1X protease inhibitor cocktail (Roche). Immunoprecipitated proteins were resolved on 10% SDS-PAGE. To analyse the general translation pattern, a 5µl aliquot of the reaction mixture that was not be subjected to immunoprecipitation was resolved by 10% SDS-PAGE. The gels were analyzed auto radiographically by fixing, drying and exposing the gel on X-ray film.

G. RNA Electrophoretic mobility shift assay (REMSA)

For our experiment, we used AU-rich RNA derived from TNF-α 3' UTR (ARE38 5'-GUGAUUAUUUAUUAUUUAUUUAUUAUUUAUUUAUUUAG- 3') and an arbitrary region derived from TNF-α 5' UTR (5'-AGAACAUCUUGGAAAUAGCUCCCAGAAAAGCAAGCAGC-3') synthesized and biotin end-labelled by using biotin at 3' end by Biotech Desk Pvt. Ltd. The Light Shift chemiluminescent RNA EMSA kit (Thermo Scientific) was then used to perform RNA-EMSA according to the manufacturer's instructions. Purified LmGAPDH protein and 2 nM biotin-labeled probe were incubated in a volume of 20 µl for 30 minutes at room temperature with 2 µg tRNA, 5% glycerol in 1X REMSA binding buffer to perform RNA binding assays. Before adding the labelled probes, unlabeled TNF-α 3' UTR RNA oligonucleotides were added to the reaction mixture (200-fold excess) to monitor cold competition experiments. The REMSA super shift is carried out using another lane loaded with labelled probe, LmGAPDH purified protein and LmGAPDH antibody (raised) specific for the protein. Samples were separated on native polyacrylamide gels (6%) in 0.5X Tris-borate-EDTA (TBE) buffer at 100V at 4˚C that were pre-run for 30 mins. Then the gel was transferred into positively charged nylon membranes (Sigma) in Trans-Blot Semi dry apparatus (Biorad). A UV-light cross linker (UVP HL-2000 HybriLinkerTM) was used to cross-link biotin-labeled RNA on the membrane, which was subsequently detected using horseradish peroxidase-conjugated streptavidin. Exposure to the Bio-Rad ChemiDocTM MP imaging system revealed band shifts.

2.2.5. Statistical analysis

All data were expressed as the mean ± SD from at least three independent experiments. Student's t test or analysis of variance (ANOVA) were used to calculate statistical analysis for parametric wherever applicable data using Origin 7.0 software (Microcal software, Inc. Northampton, MA, USA). Statistical significance was defined as a p value of less than 0.05.

“Imagination is more important than knowledge.”

_ Albert Einstein

Results

CHAPTER 1

"Cloning, expression and localization of LmGAPDH from Leishmania major"

RESULTS (Chapter 1)

"Cloning, expression and localization of LmGAPDH from Leishmania major"

3.1.1. Background

Glyceraldehyde-3-phosphate dehydrogenase (GAPDH), initially identified as a glycolytic enzyme is now considered as a housekeeping gene. GAPDH involves in the reversible oxidative phosphorylation of glyceraldehydes-3-phosphate to 1, 3-bisphosphoglycerate in the presence of inorganic phosphate and nicotinamide adenine dinucleotide (NAD). In mammalian system, GAPDH has been revealed as a multifunctional protein with diverse activities and a distinct subcellular distribution. In protozoan kinetoplastida, the glycolytic pathway is localized mainly in unique membrane bound organelles called glycosomes. In *T. brucei* and *L. Mexicana* two copies of glycosomal GAPDH (gGAPDH) in tandem array and one copy of cytosolic GAPDH (cGAPDH) gene have been identified. In *L. braziliensis* the cGAPDH is absent and in *L. major* it has become a pseudogene.
Several secretory virulence proteins have been identified in extracellular vesicles (EVs) over the past two decades, including GP63 [194, 195], heat shock protein 100 [196], proteophosphoglycan pPPG2 [197], acid phosphatase [198], heat shock protein 70 [199], EF1 alpha [200], fructose 1,6-bisphosphatealdolase [201], etc. Researchers have shown that exosomes of *Leishmania* from the extracellular environment, acquired by host cells, selectively secrete IL8. These data suggest that *Leishmania* uses exomes to deliver effector molecules to host cells as well as to communicate with the host's cellular environment. Recently several studies demonstrated that GAPDH is translocated to different subcellular organelles for exhibiting non glycolytic function. So, in this chapter, localization of LmGAPDH is our main focus as knowing where LmGAPDH is found can help us forecast its possible involvement and correlate its functions.

3.1.2. Purification of LmGAPDH

A sequence (LmjF.30.2970) in the *L. major* genome database was identified as containing an ORF related to conserved protein in human (http/www.genedb.org/genedb/leish/). Based on this we amplified a 1083 bps fragment with the potential to encode a 39 kDa protein (designated as LmGAPDH). Sequence comparison showed the presence of conserved cysteine residues in the active site of the enzyme **(Fig.16)**. Comparison of leishmanial genome revealed that it contains two copies of GAPDH genes in tandem array. Interestingly, *L. major* glycosomal GAPDH show only 55% sequence similarity with its cytosolic GAPDH (which has turned into a pseudo gene in *Leishmania major*).
Isolation and purification of the recombinant LmGAPDH was achieved by chromatographic step which used nickel-nitrilotriacetic acid-agarose and resulted in the separation of GAPDH from the soluble *E. coli* proteins. The protein compositions of samples obtained from the various purification steps are shown in **(Fig.17A)**. As expected, purification yielded a single protein band of approximately 39 kDa. No other protein band could be detected in the gel stained with coomassie brilliant blue.

```
LmGAPDH  MAPIKVGINGFGRIGRMVLQAICDQGLIGNEIDVVAVVDMSTNAEYFAYQMKYDTVHGRPKYTVEAVKST 70
yGAPDH   --MVRVAINGFGRIGRLVMRIALSR----PNVEVVALNDPFITNDYAAYMFKYDSTHGRYAGEVSHD--- 64
hGAPDH   MGKVKVGVNGFGRIGRLVTRAAFNS----GKVDIVAINDPFIDLNYMVYMFQYDSTHGKFHGTVKAE--- 66
mGAPDH   --MVKVGVNGFGRIGRLVTRAAICS----GKVEIVAINDPFIDLNYMVYMFQYDSTHGKFNGTVKAE--- 64
             ::*.:********:* :          ::::**: *     :* .* ::**:.**:   *.

LmGAPDH  PSVKTPDVLVVNGHRIKCVKAQRNPADLPWGKLGVDYVIESTGLFTDKLQAEGHIKGGAKKVVISAPASG 140
yGAPDH   -----DKHIIVDGKKIA-TYQERDPANLPWGSSNVDIAIDSTGVFKELDTAQKHIDAGAKKVVITAPSST 125
hGAPDH   -----NGKLVINGNPIT-IFQERDPSKIKWGDAGAEYVVESTGVFTTMEKAGAHLQGGAKRVIISAPSAD 127
mGAPDH   -----NGKLVINGKPIT-IFQERDPTNIKWGEAGAEYVVESTGVFTTMEKAGAHLKGGAKRVIISAPSAD 125
                   ::::*: *     :*:*:.: **. ..: .::***:*.    *  *:..***:*:*:**::

LmGAPDH  GAKTIVMGVNQHEYSPTSHHVVSNASCTTNCLAPIVHVLTKENFGIETGLMTTIHSYTATQKTVDGVSLK 210
yGAPDH   -APMFVMGVNEEKYTS-DLKIVSNASCTTNCLAPLAKVI-NDAFGIEEGLMTTVHSLTATQKTVDGPSHK 192
hGAPDH   -APMFVMGVNHEKYDN-SLKIISNASCTTNCLAPLAKVI-HDNFGIVEGLMTTVHAITATQKTVDGPSGK 194
mGAPDH   -APMFVMGVNHEKYDN-SLKIVSNASCTTNCLAPLAKVI-HDNFGIVEGLMTTVHAITATQKTVDGPSGK 192
           *  :*****..:*   . :::************:.:*::: ***  *****:*: ********* * *

LmGAPDH  DWRGGRAAAINIIPSTTGAAKAVGMVIPSTKGKLTGMSFRVPTPDVSVVDLTFRSTRETSIQEIDKAIKK 280
yGAPDH   DWRGGRTASGNIIPSSTGAAKAVGKVLPELQGKLTGMAFRVPTVDVSVVDLTVKLNKETTYDEIKKVVKA 262
hGAPDH   LWRDGRGALQNIIPASTGAAKAVGKVIPELNGKLTGMAFRVPTANVSVVDLTCRLEKPAKYDDIKKVVKQ 264
mGAPDH   LWRDGRGAAQNIIPASTGAAKAVGKVIPELNGKLTGMAFRVPTPNVSVVDLTCRLEKPAKYDDIKKVVKQ 262
          **.** *  ****::******** *:*. :******:***** :******* :  : :. ::*.*.:*

LmGAPDH  AAQTYMKDILGFTNDELVSSDFINDNRSSVYDSKATLQNNLPGEKRFFKIVSWYDNEWGYSHRVVDLVRY 350
yGAPDH   AAEGKLKGVLGYTEDAVVSSDFLGDSHSSIFDASAGIQL----SPKFVKLVSWYDNEYGYSTRVVDLVEH 332
hGAPDH   ASEGPLKGILGYTEHQVVSSDFNSDTHSSTFDAGAGIAL----NDHFVKLISWYDNEFGYSNRVVDLMAH 334
mGAPDH   ASEGPLKGILGYTEDQVVSCDFNSNSHSSTFDAGAGIAL----NDNFVKLISWYDNEYGYSNRVVDLMAY 332
         *::  :*.:**:*:. :**. ** .:.:** :*:* :      . .*.*::******:*** *****: :

LmGAPDH  MAATDAASAKM      361
yGAPDH   VAKA-------      332
hGAPDH   MASKE------      335
mGAPDH   MASKE------      333
         :*
```

Fig. 16. Sequence alignment of LmGAPDH (*l. major*), yGAPDH (yeast), hGAPDH (human) and mGAPDH (mouse). The residues that are identical with LmGAPDH are denoted by asterix. (Sequences adapted from https://www.uniprot.org/ and alignment done with the help of clustal omega multiple sequence alignment program, https://www.ebi.ac.uk/Tools/msa/clustalo/)

3.1.3. Measurement of specificity of rabbit anti LmGAPDH polyclonal antibody against LmGAPDH

Polyclonal antibodies against the purified recombinant LmGAPDH (20µg) was raised by subcutaneous injection in 6-month old rabbit using Freunds complete adjuvant and sera were collected and used for Western blot analysis. To check the specificity of the antibody, lysates from *Leishmania major* and macrophage and purified recombinant LmGAPDH were used as samples. Western blot analysis shown in **(Fig.17B)** confirmed that the anti-LmGAPDH antibody is specific for *Leishmania spp.*

3.1.4. Western blot for subcellular localization

The fact that cytosolic human GAPDH enzymes are directed to the plasma membrane and nucleus for moonlighting action is well known. Despite the fact that both copies of LmGAPDH include the anticipated C-terminal glycosomal tri-peptide (PKL) signal sequence, the enzyme may be present in other organelles for non-glycolytic activities. To see if the mature LmGAPDH protein was found in any organelles other than the glycosome as a native protein,

L. major cell homogenates were fractionated by differential centrifugation, glycosomes were isolated from *L. major* promastigotes using Colasante et al's technique, and *Leishmania*-secreted microvesicles were harvested using the traditional exosome isolation method from conditioned medium subjecting to ultracentrifugation with prior incubation of the promastigotes at 37˚C for ~2 hours. The LmGAPDH protein band was recovered from both glycosomal and EVs fractions, where the glycosomal PAS domain containing phosphoglycerate kinase and the EVs GP63 protein (as a marker protein) were concentrated, indicating that the enzyme is found in both the glycosome and the exosome of *Leishmania*. The LmGAPDH protein band, on the other hand, was missing from the cytosol, mitochondria, and nucleus fractions, which contained cytosolic adenosine kinase, mitochondrial ascorbate peroxidase, and nuclear histone H2B (as a marker protein) **(Fig.18).**

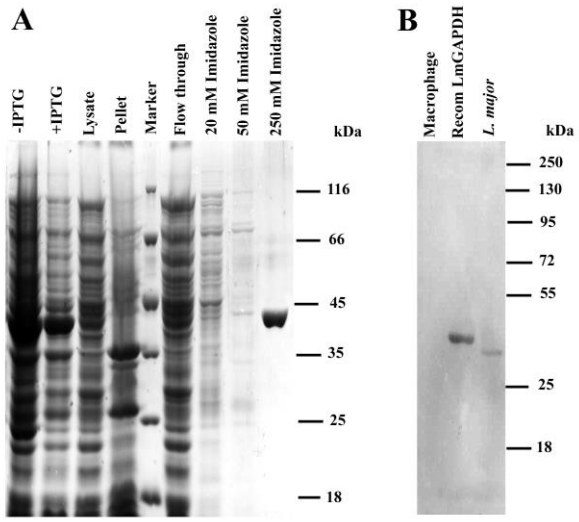

Fig. 17. Purification of LmGAPDH and measurement of specificity of polyclonal anti-LmGAPDH antibodies against LmGAPDH. (A) SDS–PAGE during recombinant LmGAPDH purification. (B) Western-blot for macrophage cell lysate and L. major cell lysate by using polyclonal anti-LmGAPDH antibodies. (Adapted from Das et al, *J Biol Chem*, 2021)

3.1.5. GAPDH enzyme assay of the subcellular fractions using UV-visible spectroscopy

To confirm above observation, the enzymatic activity of LmGAPDH was measured with 0.5% Triton X-treated purified glycosome and extracellular vesicles by using UV-visible

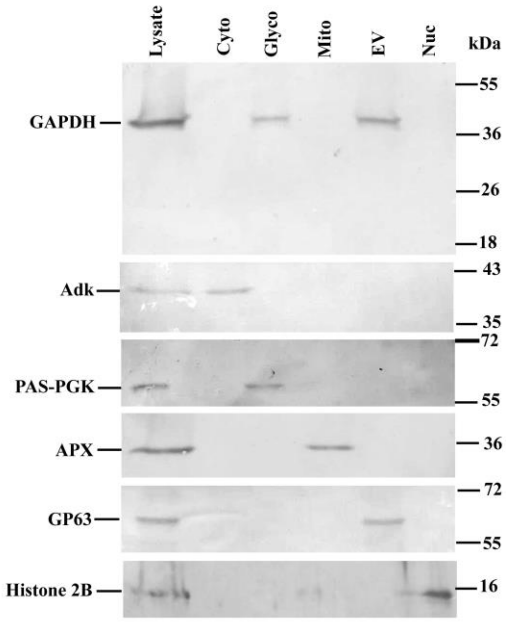

Fig. 18. Subcellular localization of LmGAPDH by Western blotting was performed using promastigotes cells. Lanes: 1, cell lysate; 2, cytosolic; 3, glycosomal; 4, mitochondrial; 5, extracellular vesicle and 6, nuclear fraction. Adenosine kinase, PAS domain containing phosphoglycerate kinase, ascorbate peroxidase, GP63 and histone 2B were used in the subcellular fractions as cytosolic, glycosomal, mitochondrial, extracellular vesicle and nuclear markers, respectively. (Adapted from Das et al, J *Biol Chem*, 2021)

spectroscopy. Essentially, the GAPDH activity within the crude extract was recuperated from both the glycosomal and the EVs fraction shown in **Fig. 19**, suggesting that the enzyme is almost entirely localized in the glycosome and the EV of *Leishmania.*

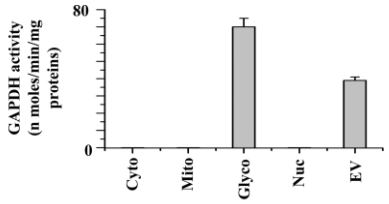

Fig. 19. The enzymatic activity of LmGAPDH in different subcellular fractions. Cyto, glyco, mito, ev and nuc denoted as cytosolic, glycosomal, mitochondrial, EVs and nuclear fraction, respectively. (Adapted from Das et al, *J Biol Chem*, 2021)

3.1.6. Verification of size and morphology of the isolated extracellular vesicles (EVs)

Using atomic force microscopy, we confirmed the form and size of extracellular vesicles (AFM). The vesicles' spherical morphology and size of roughly 65.5 nm in diameter were validated by two-dimensional (tapping mode topographic and phase AFM) and three-dimensional views, which were identical to extracellular vesicles' previously recognized form **(Fig.20A and 20B)**. Dynamic light scattering (DLS) analysis was used to further confirm this information. The DLS results showed that the extracellular vesicles derived from *Leishmania* had a mean diameter of 65 nm and were highly homogeneous (96%) **(Fig.20C).**

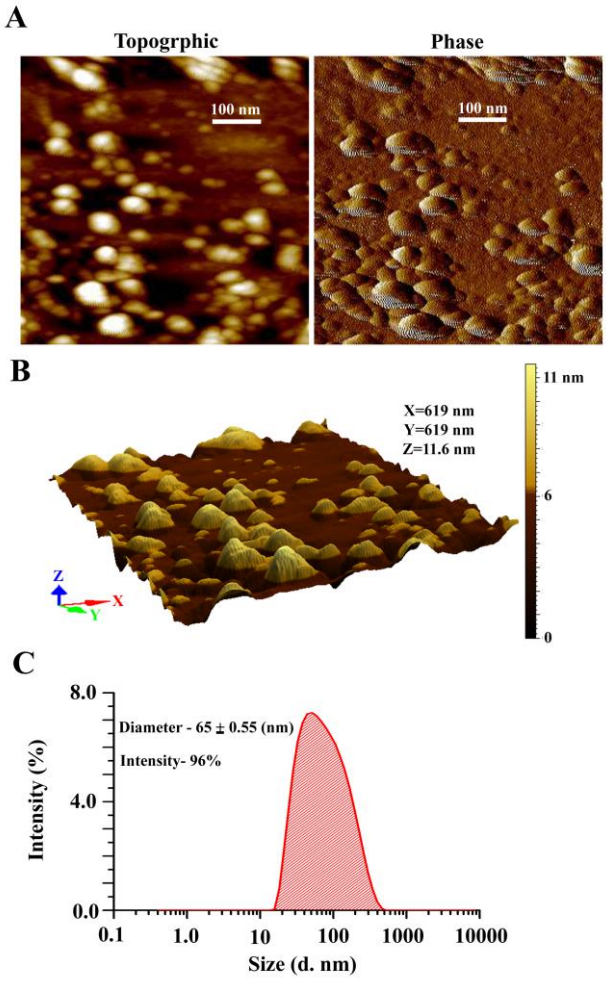

Fig. 20. Atomic force microscopy (AFM) and Dynamic Light Scattering (DLS) to identify the shape and size of extracellular vesicles (EVs) extracted from L major. (Adapted from Das et al, *J Biol Chem*, 2021)

3.1.7 Discussion

Several recent investigations have shown that GAPDH is translocated to several subcellular organelles for non-glycolytic functions. As a result, accurate knowledge of LmGAPDH's localization will aid in predicting the protein's possible involvement and allow us to correlate its actions with those of other proteins. GAPDH, both glycosomal and cytosolic, is well established to play a key role in trypanosomatid glycolytic activity.

In this chapter, we have established for the first time that LmGAPDH is located in both the glycosomal and the EVs fractions, similar to where the leishmanial GP63 protein is found, utilizing a variety of molecular techniques (including Western blot analysis and protein activity measurement). As a result, LmGAPDH present in extracellular vesicles (EVs) is expected to have a direct impact on the host defense system. The identification of an EV-mediated LmGAPDH begs the question of how this protein gets to extracellular vesicles. Because LmGAPDH lacks an N-terminal secretion signal peptide, it is thought to be secreted by non-traditional pathways.

Several secretory pathogenic proteins previously mentioned, have been found in *Leishmania* extracellular vesicles over the last two decades and it was already reported that *Leishmania* extracellular vesicles are an integral part of the parasite’s infectious life cycle and it strongly affects macrophage signaling and function. In our data since we have shown the presence of LmGAPDH in EVs isolated from infectious *L. major* promastigotes in-vitro, so we may suggest that LmGAPDH might have a role in *L. major* infection.

CHAPTER 2

"Functional characterization of LmGAPDH contained within the extracellular vesicles from Leishmania major; its essentiality in disease development and progression"

RESULTS (Chapter 2)

"Functional characterization of LmGAPDH contained within the extracellular vesicles from Leishmania major; its essentiality in disease development and progression"

3.2.1. Background

The main function of GAPDH is to catalyze the sixth stage of glycolysis to produce energy and carbon molecules. Moreover, GAPDH has recently been implicated in several non-metabolic processes in higher eukaryotic cells, DNA replication [131], initiation of apoptosis [134], tubulin polymerization [124], nitrosylation of nuclear proteins [107, 133], post-transcriptional gene regulation [202], tumorigenesis [135] and many others. So far, the non-glycolytic function of GAPDH in trypanosomal parasites is still missing in the literature. Recently, in *L. donovani* cGAPDH null mutant has shown reduced infectivity in visceral organs of experimentally infected mice demonstrating the role of cGAPDH in the survival of *L. donovani* in visceral organs [177].

In the previous chapter we have shown the presence of LmGAPDH in Extracellular vesicles (EVs) isolated from infectious *L. major* promastigotes *in-vitro*. However, the exact function of this parasite-derived EV mediated LmGAPDH is not known. So, in this chapter, to elucidate the physiological importance of the protein, half knockout (HKO), overexpressed (OE) and complement cells (CM) were generated. The growth profile and the infection profile of all these cell types were compared with the control wild type (CT) *L. major* cell. Furthermore, in this chapter by doing both in vitro and in vivo experiments in macrophage and mice respectively, we have given attention to the role of LmGAPDH gene in *Leishmania* infection, disease development and progression.

3.2.2. Targeted gene replacement of LmGAPDH alleles

L. major Gene data base revealed that the LmGAPDH gene has two identical copies in a parallel array. To investigate the non-glycolytic role of the LmGAPDH gene in *L. major*, a gene replacement technique was performed **(Fig.21 A).** Since LmGAPDH is a gene essential for the survival of the *Leishmania* parasite, only one of the two copies of the gene can be

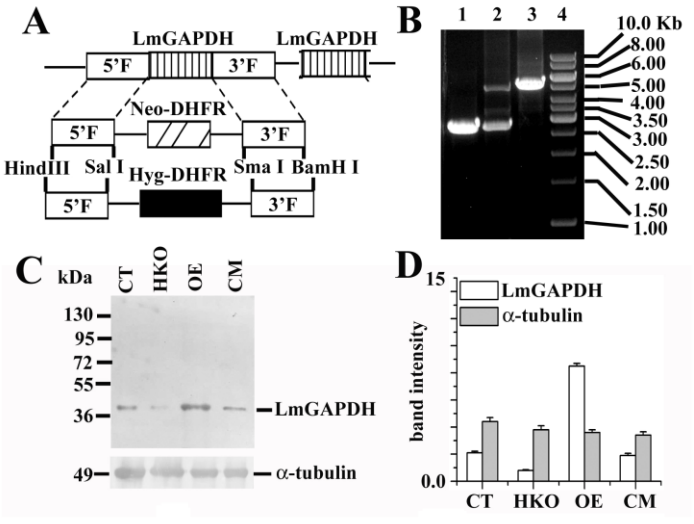

Fig. 21. Targeted gene replacement of single copy of LmGAPDH gene: (A) Schematic representation of the LmGAPDH locus and the plasmid constructs used for gene replacement. DHFR denotes dihydrofolate reductase. (B) Agarose gel analysis of PCR-amplified products of LmGAPDH gene. Lane 4 shows the molecular mass marker, lanes 1, 2 and 3 correspond to PCR with genomic DNA from CT, +/− allele, and HKO mutants, respectively, with external (5' and 3' flanking region) primers to the LmGAPDH gene. The expected size of the LmGAPDH, NEO, and HYG gene PCR product are 2.75, 5.3 and 5.7 kb, respectively. (C) L. major lysate was used for Western blotting. Western blot results using rabbit anti-LmGAPDH and mouse anti-tubulin antibody are shown. (D) Bar diagram depicted as the percentage of band intensities in the Panel C. (Adapted from Das et al, J *Biol Chem*, 2021)

deleted. We generate half of the LmGAPDH deletion construct by replacing the selectable marker genes for hygromycin and neomycin. After two rounds of transformation and selection with neomycin and hygromycin, both LmGAPDH alleles of the intracellular single-copy gene were replaced. To screen for medium knockout mutations, we first performed PCR analysis of genomic DNA with primers derived from the 5' and 3' regions **(Fig.21B).** Western blotting with anti-LmGAPDH antibody further confirmed the presence of ~ 50% LmGAPDH in the half-knockout cell line. These results suggest that both LmGAPDH alleles of one copy of the gene were eliminated in the resistant primary *L. major* cell line. On the other hand, Western-blotting results showed that the overexpressed cell line (OE) expressed nearly 4.5-fold more LmGAPDH than the control cell line (CT), although the complementary cell (CM) cell line expressed comparable amounts of LmGAPDH compared to control cells **(Fig.21C).**

3.2.3. Analysis of EV mediated LmGAPDH in overexpressed (OE), control (CT), half knockout (HKO), and complement (CM) cells

We then investigated whether the level of LmGAPDH in extracellular vesicles of HKO and OE cells was changed compared to CT and CM cells. Western blotting confirmed that extracellular vesicles from HKO cells contain negligible amounts of LmGAPDH protein, while extracellular vesicles from OE cell lines express 2.3 times more LmGAPDH compared to CT or CM cell lines **(Fig.22).**

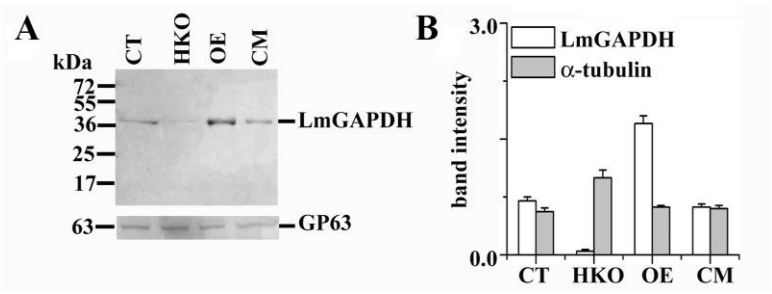

Fig.22 Extracellular vesicles isolated from L. major were used for Western blotting. (A) Western blot results using rabbit anti-LmGAPDH and mouse anti-GP63 antibody are shown. (B) Bar diagram denoted as the percentage of band intensities in the Panel A. Band intensity was quantified by ImageJ software (NIH). OE, CT, CM and HKO denote overexpressed, control, complement and half knock out cell lines. (Adapted from Das et al, J *Biol Chem*, 2021)

3.2.4. Growth profile and morphology analysis

To investigate whether the growth rate of overexpressed and double-knockout cells is similar

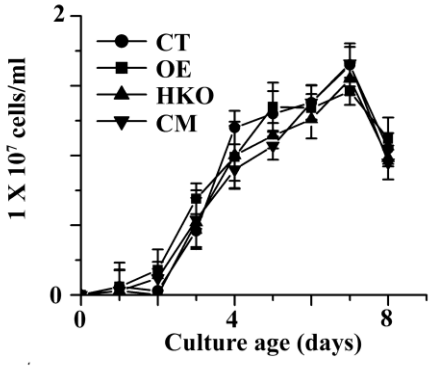

Fig. 23. The growth curves of CT, OE, CM and HKO cells measured using improved Neubauer chamber for a span of 8 days showing deletion of single isoform of LmGAPDH gene does not affect growth of *Leishmania* promastigotes in culture. (Adapted from Das et al, J BiolChem, 2021)

to the growth rate of wild-type or complement cells, viable cell count analysis was performed under glass microscopy. The growth curve shows that the HKO and OE populations have more or less equal growth rates as that of CT in culture **(Fig.23).** We compared the properties of single isoform LmGAPDH knocked out (HKO) parasites with wild type (CT), overexpressed (OE) and complement (CM) parasites in culture. LmGAPDH KO promastigotes showed no gross morphological abnormalities compared with CT, OE and CM promastigotes **(Fig.24).**

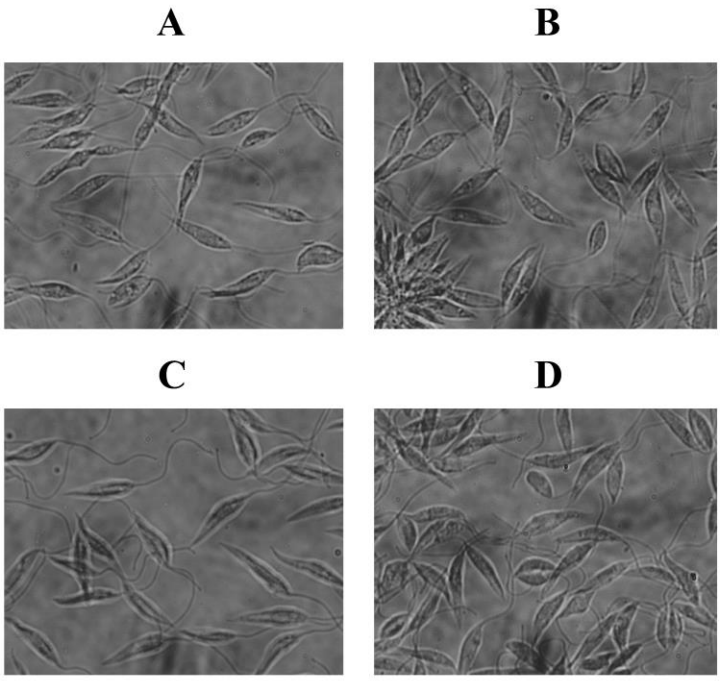

Fig. 24. The morphology of all the log phase *Leishmania* promastigote mutants A) CT, B) OE, C) HKO, D) CM seen under 1X81 Olympus microscope were similar.

3.2.5. In vitro infection assay

As an obligate intracellular pathogen, *Leishmania* primarily prefers phagocytic cells as a host cell. Among phagocytic cells, macrophages are the major host cells of *L. major* promastigotes. We examined the extent to which HKO, CT, CM and OE cells are colonized by intracellular macrophages. The adhering rates of all promastigotes were almost same after 2 hours of incubation period. Moreover, HKO promastigotes were internalised insignificantly at a lower rate than WT, OE, or CM cells after 24 and 48 hours of incubation. Most of the infected macrophages still contained the parasites for 72 hours after phagocytosis of the WT and CM promastigotes, while the percentage of parasites in HKO-infected macrophages was significantly reduced **(Fig.25A).** These results indicate that HKO parasites die more easily in macrophages. In addition, the proportion of macrophages infected with OE was significantly increased compared to the proportion of CT infection **(Fig.25B).**

3.2.6. In vivo infection assay

To check whether *Leishmania major* LmGAPDH half knock out parasites are able to develop infections in mice, we performed *in-vivo* infection studies. For those studies, promastigotes were inoculated into the footpads of BALB/c mice, and we found that the CT and OE cell line

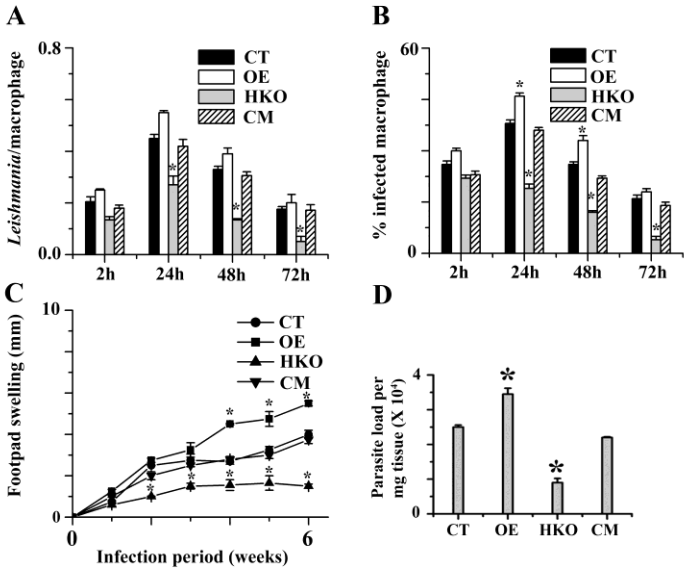

Fig. 25. Role of LmGAPDH in infection A) The percentage of macrophages infected with CT, OE, CM and HKO parasites. For each time point, 200 macrophages were counted. (B) The number of *Leishmania* within each infected macrophage was counted. For each time point and cell type, 200 infected macrophages were analysed. (C) Infection in BALB/c mice. Footpad swelling of CT, OE, CM and HKO were observed for the three groups (15 mice/group). (D) Parasite burden in the footpad after 6 weeks of post-infection in CT, OE, CM and HKO cells. (Adapted from Das et al, *J Biol Chem*, 2021)

induced a more severe disease progression compared to HKO cells although the complementation (CM) cell lines rescued more than 90% of the phenotypes compared to wild type cells **(Fig.25C).** These data were further confirmed by counting parasite burden up to 6 weeks post infection. The result of parasite burden indicated that HKO parasites, compared to CT or CM, had about 2.6-fold less parasite burden (Fig. 3D inset) in 1 mg of footpad tissue **(Fig.25D).** These findings indicated that the GAPDH gene in parasites plays an important role in macrophage infection and disease development in mice.

3.2.7. Discussion

Consistent with previous studies using other *Leishmania* species, we were able to generate LmGAPDH null mutant of *L. major* parasite by standard gene targeting approaches based on replacement of the LmGAPDH coding region with a drug resistance gene by homologous recombination. But here we have completely deleted only one isoform of LmGAPDH as deletion of both hampers the viability of the cells. Nevertheless, we evaluated the consequence of disrupting a single isoform of LmGAPDH on *L. major* differentiation to infective forms, infection of macrophages, and pathogenesis in mice, and thus, uncovered an important insight into parasite biology. Our data indicate that the number of HKO parasites in macrophage diminished over time, suggesting that a normal level of LmGAPDH is required for *L. major* persistence in macrophage. Due to the impaired capacity of KO parasites to persist in murine macrophages, we evaluated the effects of the deleted gene on virulence in mice. We found that the HKO promastigotes developed mild cutaneous lesions compared to mice infected with WT or OE *L. major* metacyclic promastigotes. Thus, HKO cells showed a lower level of infectivity both *in vitro* and *in vivo*. Although additional functional verification studies are ongoing, the findings in this chapter indicate that LmGAPDH is essential for the survival of *L. major* parasites within macrophages and for virulence in mice.

CHAPTER 3

"LmGAPDH contained in the extracellular vesicles modulate host immune response through post-transcriptional regulation of TNF-α expression"

RESULTS (Chapter 3)

"LmGAPDH contained in the extracellular vesicles modulate host immune response through post-transcriptional regulation of TNF-α expression"

3.3.1 Background

Multiple genes involved in immune response, particularly cytokines and pattern recognition receptors, were downregulated by leishmanial parasites. Extracellular vesicles (EVs) have been studied extensively in the *Leishmania*-host interaction in recent years, and it has already been documented that leishmanial EVs influence macrophage cell signaling and function [203]. Previous research has found that infection-like stresses (37°C pH 5.5) increased EV production by more than two fold and changed the protein composition of EVs. Incubation of macrophages with leishmanial extracellular vesicles selectively enhanced IL-8 production, but not TNF- α, according to evidence [204]. TNF- α is a pleiotropic cytokine that is produced by a variety of cells throughout the body such as macrophages, astroglia, microglia, Langerhans cells, Kupffer cells [205-207]. However macrophages are the primary producers of TNF- α and surprisingly, macrophages are also highly responsive to TNF- α [208]. This macrophage-produced protein has a wide range of biological functions and may have a role in inflammatory processes [209, 210]. TNF- α has been found to play a key role in orchestrating the cytokine cascade in a variety of inflammatory disorders, and it has been considered as a therapeutic target for a variety of diseases due to its position as a "master-regulator" of inflammatory cytokine production [211-213].

In our previous chapters, we have shown we have found that LmGAPDH is localized in the EVs isolated from *L. major* during infection. Now in this chapter, to check whether leishmanial derived LmGAPDH present in the EVs has any immunomodulatory properties, TNF- α expression in CT, OE, HKO and CM infected host cells were determined by RT-PCR, ELISA, and western blot analysis. Furthermore, by performing various molecular biology techniques like *in vitro* protein transfection, *in vitro* translation, immunofluorescence, confocal imaging and RNA-EMSA, we have unraveled a novel mechanism by LmGAPDH present in the EVs from *Leishmania* modulate the host immune response

3.3.2. Comparative study of TNF- α expression in mRNA and protein level in macrophage infected with CT, OE, HKO and CM cells by Real time PCR, ELISA, and Western Blotting

The pro-inflammatory cytokine TNF- α seems to have a crucial role in the regulation of infection. Real-time PCR, ELISA, and western blotting were used to evaluate the expression of the pro-inflammatory cytokine TNF- α at various time points 2hrs, 12hrs, 24hrs, and 48hrs. TNF- α mRNA expression in infected macrophages was measured using quantitative real time PCR after RAW 264.7 macrophages were infected with various types of *Leishmania* parasites (CT, OE, CM and HKO). TNF- α mRNA expression in HKO infected macrophage was unaffected compared to CT, OE or CM infected cells after 72 hours of infection, according to Quantitative real time PCR results **(Fig.26A).** In contrast, ELISA data showed that, like the LPS-treated control, HKO infected macrophage had a significant increase in TNF- α expression as compared to CT, OE and CM **(Fig.26B).** To corroborate these findings, a western blot was done using anti TNF- α antibody and the results we got were almost equivalent to the ELISA data **(Fig.26C).** Altogether, these results suggest that the expression of TNF- α protein but not mRNA was altered in HKO infected macrophages.

3.3.3. Comparative study of TNF- α expression in extracellular vesicles (from CT, OE, HKO and CM cells) treated un-induced and induced macrophage

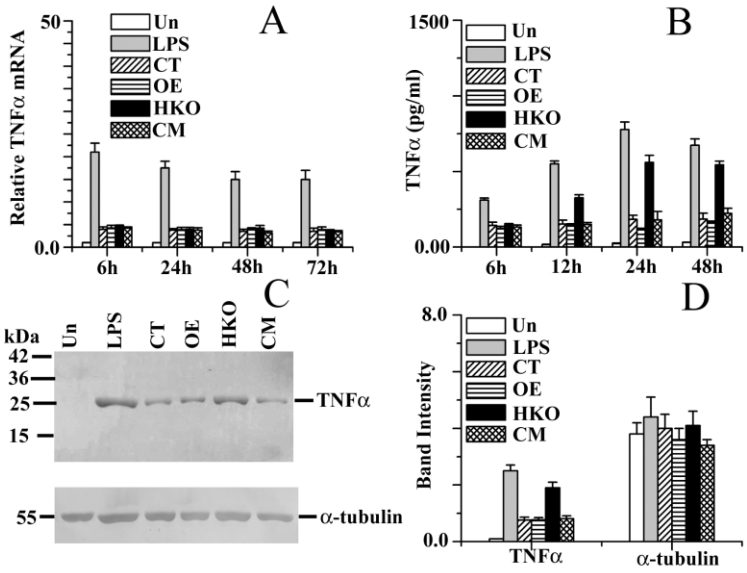

Fig. 26. The mRNA and protein expression of TNF-α production in stationary phase *Leishmania* promastigote infected macrophage. (A) Measurement of gene transcript abundance was analysed by using quantitative real-time PCR as described in materials and methods. All data were normalized using beta-actin as the endogenous control. (B) Levels of TNF-α production were measured by ELISA in the cell culture supernatants after infection. (C) TNF-α protein levels were measured by Western blot analysis of protein lysates from RAW264.7 cells. Alpha tubulin was used as loading control. (D) Densitometric analysis of all bands was done using ImageJ software (from NIH). (Adapted from Das et al, *J Biol Chem*, 2021)

We assessed TNF- α expression in extracellular vesicles (from OE, CT, CM or HKO) treated macrophages by ELISA and Western blot to see if the LmGAPDH deficient extracellular vesicles (EVs) had an influence on the host TNF- α expression. Extracellular vesicles from HKO treated un-induced macrophages showed very little change in TNF- α expression compared to extracellular vesicles from CT or CM treated cells up to 48 hours incubation periods, according to ELISA results **(Fig.27A)**. In case of LPS (0.1 μg/ml) pre-induced macrophage, the EVs from OE, CT or CM cells suppressed the TNF-α expression, whereas the EVs from HKO cells fails to represses TNF-α expression **(Fig.27B).** To further confirm this data, Western blot analysis was performed and the outcomes were nearly identical to the ELISA data **(Fig.27C).** Altogether, these results suggest that the GAPDH in parasite's EVs may regulate TNF-α expression when they interacted with the host macrophage. The EVs from OE, CT or CM cells inhibited TNF- α expression in LPS (0.1 μg/ml) pre-induced macrophages, whereas the EVs from HKO cells failed to suppress TNF- α expression. Western blot analysis was used to confirm this data, and the results were almost equivalent to the ELISA results. Overall, these findings imply that when parasite EVs and macrophage interact, LmGAPDH in the EVs may influence TNF- α production.

3.3.4. Confocal microscopy ensures macrophage *in-vitro* transfection with purified LmGAPDH, showing altered TNF- α expression

Given that extracellular vesicles contain a variety of components, including LmGAPDH, we investigated whether recombinant LmGAPDH could inhibit host TNF- α expression. The DAPI stained LmGAPDH transfected macrophages were co-stained with rabbit anti-LmGAPDH as primary antibody and Alexa Fluor 488-conjugated anti-rabbit secondary antibody to ensure recombinant LmGAPDH transfection within the macrophage. The presence

of recombinant LmGAPDH in the cytosol was confirmed by **Fig.28A and B**. In the presence of LPS, LmGAPDH transfected RAW 264.7 cells had lower levels of TNF- α expression than bovine serum albumin (BSA) transfected RAW 264.7 cells, according to Western blot analysis **(Fig.28C)**. These findings established that LmGAPDH is a significant factor that suppresses TNF- α expression.

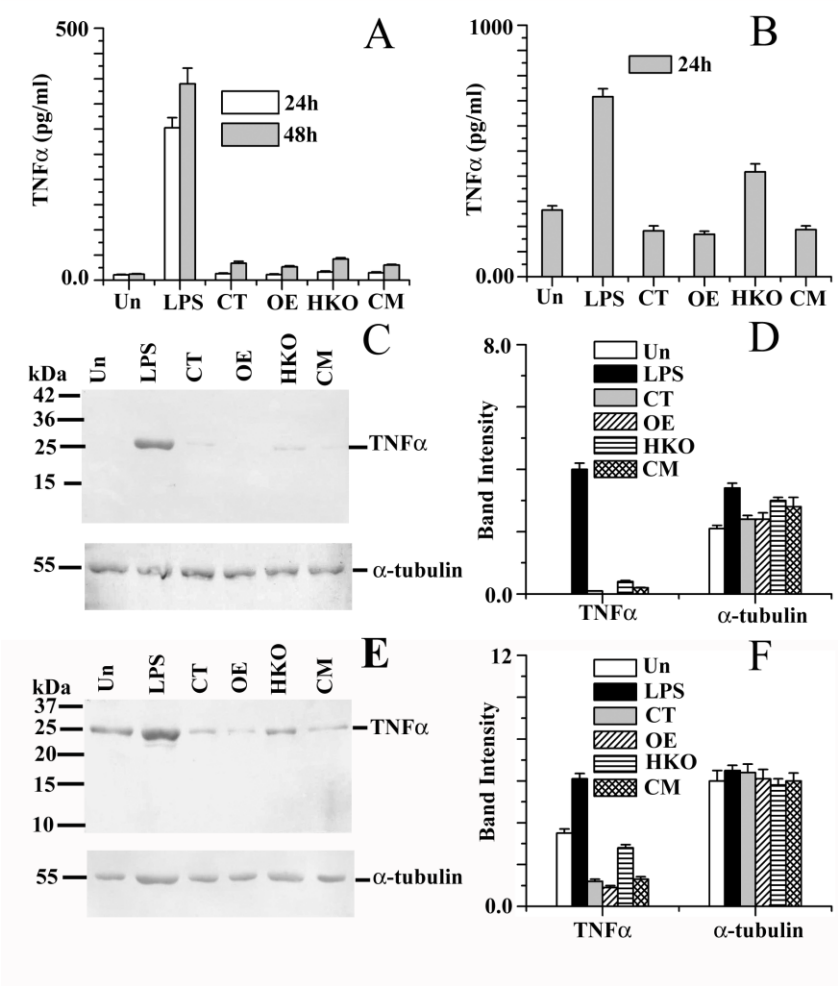

Fig. 27. **The TNF-α expression in the extracellular vesicles-treated un-induced and induced macrophages**. (A) Levels of TNF-α secretion were measured by ELISA in the cell culture supernatants of extracellular vesicles-treated un-induced macrophage. (B) Levels of TNF-α secretion were measured by ELISA in the cell culture supernatants of extracellular vesicles-treated 0.1 μg/ml pre-induced macrophage. (C) TNF-α protein levels were measured by Western blot analysis of protein lysates from extracellular vesicles-treated un-induced RAW264.7 cells. Alpha tubulin was used as loading control. (D) Densitometric analysis of all bands of panel C was done using ImageJ software (from NIH). (E) TNF-α protein levels were measured by Western blot analysis in extracellular vesicles-treated LPS pre-induced RAW264.7 cells. Alpha tubulin was used as loading control. (F) Densitometric analysis of all bands of panel E was done using ImageJ software (from NIH) (Adapted from Das et al, *J BiolChem*, 2021)

3.3.5. In-vitro translation followed by autoradiography shows LmGAPDH mediated hindrance in TNF- α protein expression

Translational silencing occurs in eukaryotes when trans-acting proteins bind to untranslated regions of particular mRNAs to prevent translation at the initiation or elongation stages. We performed in vitro protein translation of TNF- α utilizing LPS generated total mRNA and cell free reticulocyte lysates in the presence and absence of pure LmGAPDH to study the probable role of LmGAPDH as a potential inhibitory trans-factor in TNF-α translation. To validate the experimental result, LPS-induced total mRNA was chosen to enhance the TNF-α transcript pool. The standard 50μl *in vitro* translational reaction mixture contains the LPS induced total mRNA, rabbit reticulocyte lysate (Promega), amino acid mixture (containing radioactive S35-methionine) and increasing amount of purified

LmGAPDH protein. Following the 90 minutes incubation at 30°C, 45µl of reaction mixture

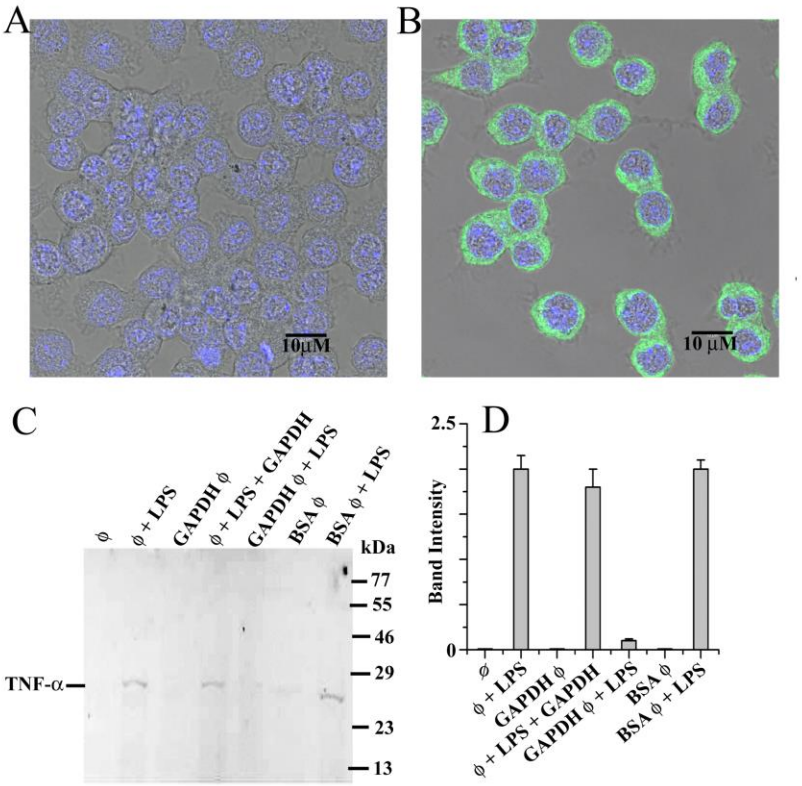

Fig. 28. In vitro transfection of LmGAPDH in macrophage: Visualization of normal macrophage (A) and LmGAPDH transfected macrophage (B) by confocal microscope. Anti-rabbit GAPDH antibody and Alexa Fluor 488-conjugated anti-rabbit secondary antibody were used for visualization of LmGAPDH. (C) The levels of TNF-α protein expression were measured from LmGAPDH transfected RAW264.7 cells in presence of LPS. Φ, GAPDH φ and BSA φ denoted as macrophage, LmGAPDH transfected macrophage and BSA transfected macrophage cells. (D) Densitometric analysis of all bands of panel C was done using ImageJ software (from NIH). (Adapted from Das et al, *J Biol Chem*, 2021)

was immunoprecipitated against TNF-α antibody and resolved on 13% SDS-PAGE. The results demonstrated that *in vitro* TNF-α translation was hindered in the presence of pure LmGAPDH and that expression is inversely related to LmGAPDH concentration. Unlike LmGAPDH, in-vitro TNF-α protein translation could not be suppressed by BSA protein **(Fig. 29B)**. Total or general translated S35-met-labelled proteins were detected by resolving a small aliquot of the respective translated samples on 10% SDS-PAGE and autoradiogram. The total *in vitro* protein synthesis represent the overall or general translation pattern showing the protein synthesis band pattern in all lanes are similar **(Fig. 29A),** indicating that *in vitro* protein translation is occurred in presence or absence of purified LmGAPDH.

3.3.6. LmGAPDH binding to TNF- α 3’ UTR and not to 5’ UTR results in translational blockage of TNF- α transcript

GAPDH is also an mRNA-binding protein that interacts with the 5' or 3'-UTR regions of mRNA, positively or negatively regulating gene expression at the post-transcriptional stage. Our findings suggest that LmGAPDH is accountable for the reduction in TNF-α protein expression. We used an RNA electrophoretic mobility shift (REMSA) test to look at the binding of TNF-α 5'-UTR mRNA's or 3'-UTR with LmGAPDH to further prove that this drop in cytokine production is due to post-transcriptional regulation. With LmGAPDH, a biotin tagged oligonucleotide corresponding to the 3'-UTR of TNF-α mRNA produced a retarded band, which could be an inactive form of mRNA-LmGAPDH complexes. A 200-fold molar excess of the unlabelled homologous oligonucleotide might compete for this retarded band.

When anti-LmGAPDH antibody was added to the REMSA mixture, the mRNA-LmGAPDH-

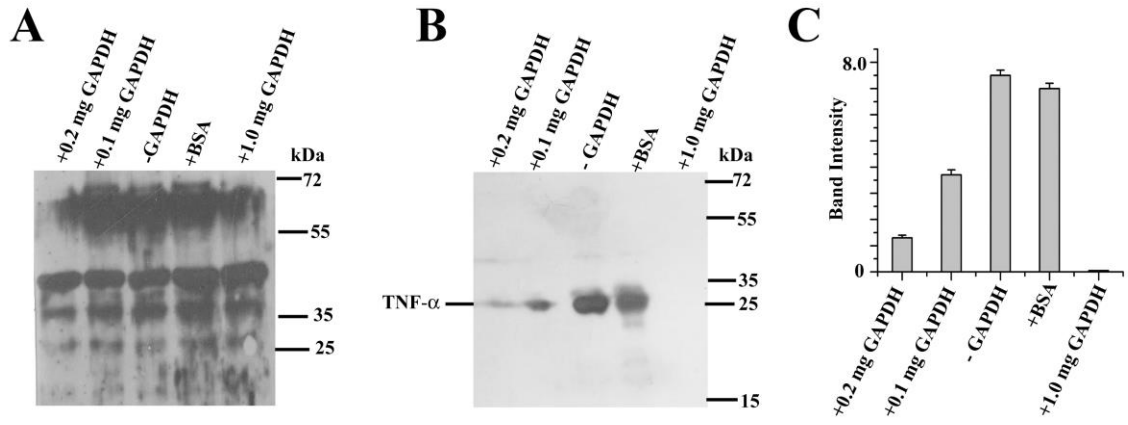

Fig. 29. Quantitation of TNF-α repression by purified LmGAPDH. (A) The autoradiographic image of in vitro general translation pattern. (B) The autoradiographic image of in vitro TNF-α translation with respect to various concentrations of LmGAPDH. (C) Densitometric analysis of all bands of panel B was done using ImageJ software (from NIH). (Adapted from Das et al, *J Biol Chem*, 2021)

antibody complex moved more slowly down the REMSA gel, indicating that the complex was more likely to be super shifted **(Fig.30C).** The displaced band was not noticed in the 5'-UTR of TNF-α mRNA oligonucleotide in contrast to the 3'-UTR of TNF-mRNA. The binding of the 3'-UTR of TNF-α mRNA with LmGAPDH is concentration dependent, as seen in **Fig.30A**. TNF-α 5'-UTR, mRNAs on the other hand, could not form a complex with LmGAPDH at greater concentrations **(Fig.30B).** These data imply that LmGAPDH binds to the 3'-UTR of TNF-α mRNA, preventing it from being translated and hence reducing TNF-cytokine production. The competitive test with cofactor NAD^+/NADH or ATP in 3'-UTR-LmGAPDH complexes **(Fig.30D)** was used to identify the interaction site of the LmGAPDH with the 3'-UTR of TNF-α mRNA. GAPDH's binding capacity to the 3′-UTR was reduced as NAD^+, NADH, and ATP concentrations were increased. These findings finally suggest that LmGAPDH's cofactor NAD^+ interaction site present in the protein is responsible for 3'-UTR binding.

3.3.7. Discussion

Several researches have demonstrated that extracellular vesicles (EVs) are used by *Leishmania* to transfer effector molecules to host cells and to communicate with the host cellular environment [214, 215]. In this paper, we show how the *Leishmania* parasite affects host TNF- protein expression through a method that has never been seen before in macrophages. The key discovery is that extracellular vesicles (EVs) generated from *Leishmania* promastigotes downregulate host TNF-production selectively, inhibiting the immune system of the host. In

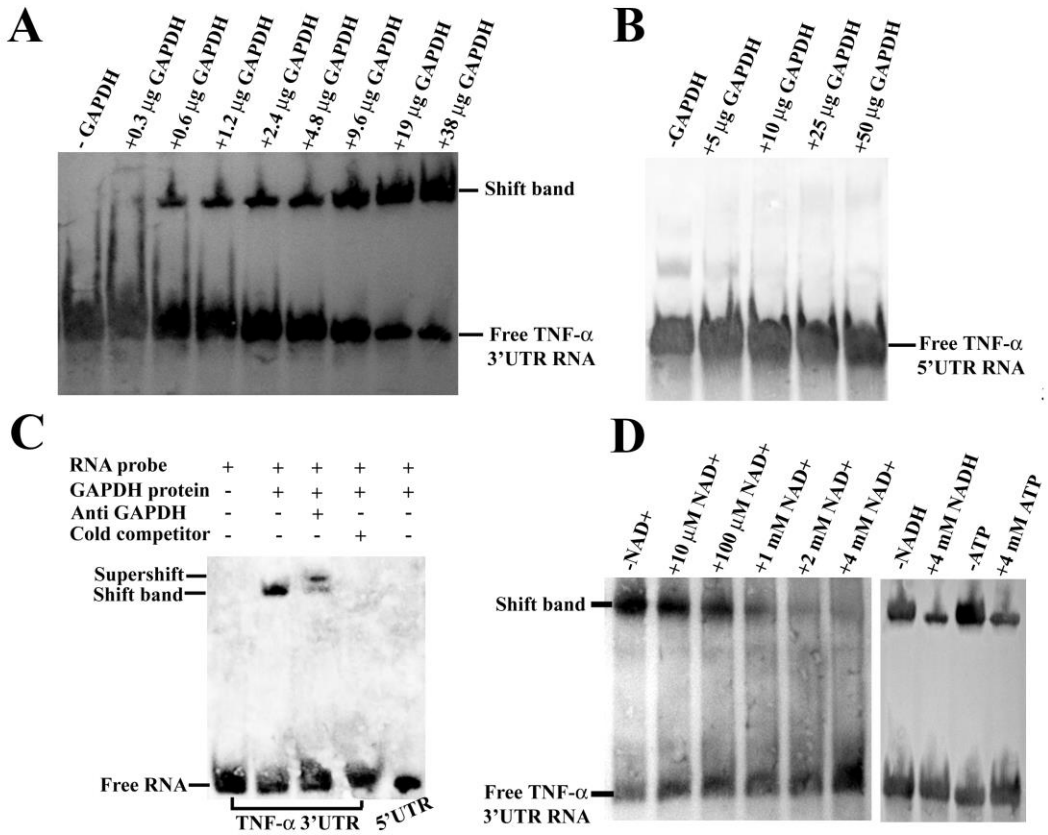

Fig. 30. Binding LmGAPDH to the 3' UTR region of TNF-α mRNA. (*A*) The REMSA measurement for LmGAPDH binding to the 3′UTR region of TNF-α mRNA. (*B*) The RNA electrophoretic mobility shift assay image for LmGAPDH–3′UTR TNF-α mRNA complexes with respect to various concentrations of LmGAPDH. (*C*) The RNA electrophoretic mobility shift assay image for the binding pattern of 5′UTR TNF-α mRNA with various concentrations of LmGAPDH. (*D*)Inhibition of 3′UTR TNF-α mRNA binding of LmGAPDH by NAD^+, NADH, and ATP.(Adapted from Das et al, *J Biol Chem*, 2021)

the presence of LPS, LmGAPDH transfected macrophages had reduced levels of TNF- expression, while naked LmGAPDH could not decrease TNF-expression in LPS-treated macrophages. These findings show that LmGAPDH must permeate the host membrane in order to inhibit TNF-expression. Most intracellular infections release virulence factors that target the host's cytosolic components in order to alter host cell function. One question that comes right away is which phase appears to be engaged in TNF-suppression. The RT-PCR results from comparative investigations of *Leishmania* (OE, CT, HKO, CM) infected macrophages with varying concentrations of GAPDH reveal that the transcription of TNF-mRNA from host DNA is unaffected by LmGAPDH concentration. As a result, we can rule out the first option. ELISA and immunoblot findings, on the other hand, reveal that TNF- protein expression in infected

host cells is inversely proportional to LmGAPDH levels. Thus infected host cells exhibit a considerable change in TNF-protein expression despite no alteration in TNF-mRNA. These findings quickly highlighted the importance of TNF-mRNA post-transcriptional suppression. GAPDH has recently been demonstrated to bind to AU-rich regions of the untranslated region of mRNA, which are responsible for posttranscriptional regulation of IFN-γ [216] and TNF-α expression, blocking translation and restricting IFN-γ and TNF-α cytokine secretion [217-220]. According to our mRNA (AU-rich elements of untranslated region) binding experiment, LmGAPDH bind to AU-rich parts of TNF-'s 3' UTR. This automatically raises another question of which LmGAPDH domain is involved in binding to AU-rich regions of TNF-'s 3' UTR. Our competition analyses with varying concentration of NAD^+, NADH, and ATP finally show that dinucleotide-binding area in the Rossmann fold of LmGAPDH can act as a 3' UTR-binding domain.

“Everything comes to us that belongs to us, if we create the capacity to receive it.”

_ Rabindranath Tagore

Conclusion & Perspectives

CONCLUSION & PERSPECTIVE

An improved understanding of mechanism by which *Leishmania* parasites replicates and persists in, and disperse from macrophages may identify new therapeutic targets for the treatment of leishmaniasis. GAPDH is studied as a model protein for enzyme kinetic analyses and considered as "moonlighting" protein, but the function of leishmanial GAPDH is completely unknown except its glycolytic activity. In this research we have shown the possible non glycolytic role of leishmanial GAPDH (LmGAPDH). We have demonstrated how LmGAPDH participates in infection and disease progression by translocating itself inside the host cell and regulating host immune system by suppressing one of the most crucial proinfalmmatory cytokine TNF-α.

In order to explain the possible mechanism for the suppression of TNF-α in *Leishmania* infected macrophage cells, we postulate a strategy (shown schematically in **Fig.31**) based on a unique virulence role of EV mediated LmGAPDH that is translocated from parasite to the cytosol of host macrophage during infection and binds specifically to 3' UTR region of TNF- α mRNA and blocks its translation and then suppresses host immune response resulting in disease progression. Our result further zooms into the mechanism and confirm that the dinucleotide-binding region in the Rossmann fold of LmGAPDH might serve as a 3' UTR -binding domain.

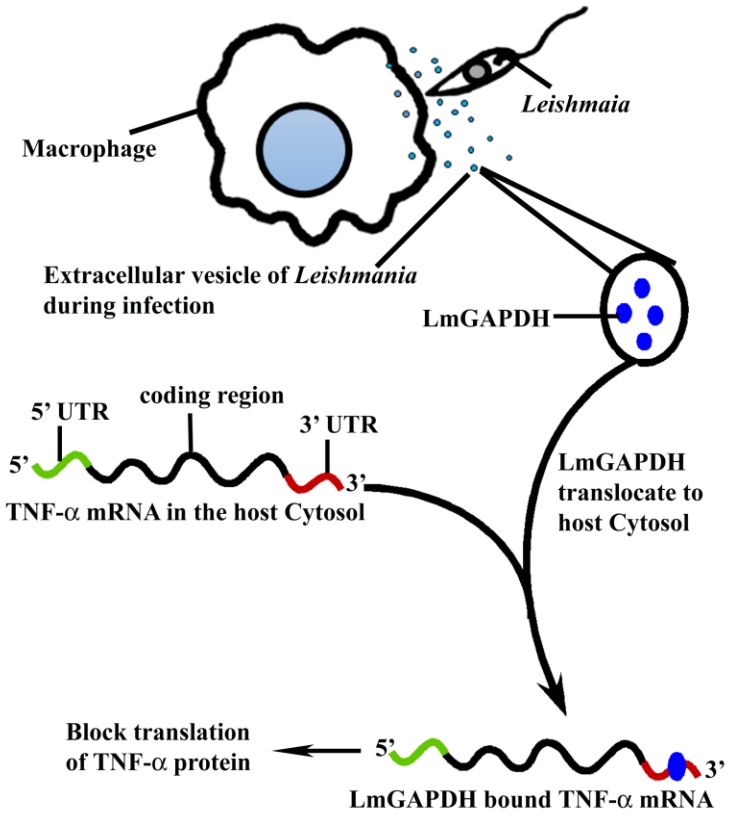

Fig. 31. A possible schematic diagram for a novel virulence function of LmGAPDH contained in extracellular vesicle. (Adapted from Das et al, *J Biol Chem*, 2021)

The NAD^+ binding site in GAPDH is located in the N-terminal domain, which exhibits the typical Rossmann-fold. Homology alignment studies suggest that the NAD^+ molecule may bind to residues 9–16 (NGFGRIGR), A39, 112-113 (TG), and N336 - binding site in LmGAPDH (data not shown). The NAD+ pyrophosphate moiety binds to the glycine-rich loop (residues 10–16). Asp39 forms two hydrogen bonds with the adenosine ribose. The nicotinamide carbonyl oxygen is hydrogen bonded to Asn316. As of now, we do not know which residues of LmGAPDH are responsible for TNF-α 3′-UTR binding. So

identifying the specific amino acid residues accountable for the binding can show a new direction the research.

So, our findings indicate for the first time that the leishmanial glycolytic enzyme LmGAPDH affects host immune system by post-transcriptionally regulating macrophage pro-inflammatory function [221]. Thus, targeting the EV mediated LmGAPDH protein could be a promising area for drug development in the battle against leishmaniasis in the near future.

Bibliography

1. Perez, J. M. (2009) Parasites, Pests, and Pets in a Global World: New Perspectives and Challenges, *J Exot Pet Med.* **18**, 248-253.
2. Hotez, P. J., Brindley, P. J., Bethony, J. M., King, C. H., Pearce, E. J. & Jacobson, J. (2008) Helminth infections: the great neglected tropical diseases, *J Clin Invest.* **118**, 1311-21.
3. Cross, G. A., Holder, A. A., Allen, G. & Boothroyd, J. C. (1980) An introduction to antigenic variation in trypanosomes, *Am J Trop Med Hyg.* **29**, 1027-32.
4. De Lange, T. (1986) The molecular biology of antigenic variation in trypanosomes: gene rearrangements and discontinuous transcription, *Int Rev Cytol.* **99**, 85-117.
5. Gull, K. (2001) The biology of kinetoplastid parasites: insights and challenges from genomics and post-genomics, *Int J Parasitol.* **31**, 443-52.
6. El-Sayed, N. M., Myler, P. J., Bartholomeu, D. C., Nilsson, D., Aggarwal, G., et al. (2005) The genome sequence of Trypanosoma cruzi, etiologic agent of Chagas disease, *Science.* **309**, 409-15.
7. Perry, K. & Agabian, N. (1991) mRNA processing in the Trypanosomatidae, *Experientia.* **47**, 118-28.
8. Levick, M. P., Blackwell, J. M., Connor, V., Coulson, R. M., Miles, A., Smith, H. E., Wan, K. L. & Ajioka, J. W. (1996) An expressed sequence tag analysis of a full-length, spliced-leader cDNA library from *Leishmania major* promastigotes, *Mol Biochem Parasitol.* **76**, 345-8.
9. Handman, E., Greenblatt, C. L. & Goding, J. W. (1984) An amphipathic sulphated glycoconjugate of *Leishmania*: characterization with monoclonal antibodies, *EMBO J.* **3**, 2301-6.
10. Brandao, A., Urmenyi, T., Rondinelli, E., Gonzalez, A., de Miranda, A. B. & Degrave, W. (1997) Identification of transcribed sequences (ESTs) in the Trypanosoma cruzi genome project, *Mem Inst Oswaldo Cruz.* **92**, 863-6.
11. Martin, W. (2010) Evolutionary origins of metabolic compartmentalization in eukaryotes, *Philos Trans R Soc Lond B Biol Sci.* **365**, 847-55.
12. Ullman, B. & Carter, D. (1997) Molecular and biochemical studies on the hypoxanthine-guanine phosphoribosyltransferases of the pathogenic haemoflagellates, *Int J Parasitol.* **27**, 203-13.
13. Stuart, K., Brun, R., Croft, S., Fairlamb, A., Gurtler, R. E., McKerrow, J., Reed, S. & Tarleton, R. (2008) Kinetoplastids: related protozoan pathogens, different diseases, *J Clin Invest.* **118**, 1301-10.
14. Horn, D. (2014) Antigenic variation in African trypanosomes, *Mol Biochem Parasitol.* **195**, 123-9.
15. Bruhn, D. F., Sammartino, M. P. & Klingbeil, M. M. (2011) Three mitochondrial DNA polymerases are essential for kinetoplast DNA replication and survival of bloodstream form Trypanosoma brucei, *Eukaryot Cell.* **10**, 734-43.
16. Bates, P. A. (2007) Transmission of *Leishmania* metacyclic promastigotes by phlebotomine sand flies, *Int J Parasitol.* **37**, 1097-106.
17. Desjeux, P. (1996) Leishmaniasis. Public health aspects and control, *Clin Dermatol.* **14**, 417-23.
18. Stockdale, L. & Newton, R. (2013) A review of preventative methods against human leishmaniasis infection, *PLoS Negl Trop Dis.* **7**, e2278.
19. Steverding, D. (2017) The history of leishmaniasis, *Parasit Vectors.* **10**, 82.

20. Pratlong, F., Dedet, J. P., Marty, P., Portus, M., Deniau, M., Dereure, J., Abranches, P., Reynes, J., Martini, A., Lefebvre, M. & et al. (1995) *Leishmania*-human immunodeficiency virus coinfection in the Mediterranean basin: isoenzymatic characterization of 100 isolates of the *Leishmania infantum* complex, *J Infect Dis.* **172**, 323-6.
21. Levine, N. D., Corliss, J. O., Cox, F. E., Deroux, G., Grain, J., Honigberg, B. M., Leedale, G. F., Loeblich, A. R., 3rd, Lom, J., Lynn, D., Merinfeld, E. G., Page, F. C., Poljansky, G., Sprague, V., Vavra, J. & Wallace, F. G. (1980) A newly revised classification of the protozoa, *J Protozool.* **27**, 37-58.
22. Saporito, L., Giammanco, G. M., De Grazia, S. & Colomba, C. (2013) Visceral leishmaniasis: host-parasite interactions and clinical presentation in the immunocompetent and in the immunocompromised host, *Int J Infect Dis.* **17**, e572-6.
23. Herrero, M., Orfanos, G., Argaw, D., Mulugeta, A., Aparicio, P., Parreno, F., Bernal, O., Rubens, D., Pedraza, J., Lima, M. A., Flevaud, L., Palma, P. P., Bashaye, S., Alvar, J. & Bern, C. (2009) Natural history of a visceral leishmaniasis outbreak in highland Ethiopia, *Am J Trop Med Hyg.* **81**, 373-7.
24. Chapman, L. A., Dyson, L., Courtenay, O., Chowdhury, R., Bern, C., Medley, G. F. & Hollingsworth, T. D. (2015) Quantification of the natural history of visceral leishmaniasis and consequences for control, *Parasit Vectors.* **8**, 521.
25. Weigle, K. A., Santrich, C., Martinez, F., Valderrama, L. & Saravia, N. G. (1993) Epidemiology of cutaneous leishmaniasis in Colombia: environmental and behavioral risk factors for infection, clinical manifestations, and pathogenicity, *J Infect Dis.* **168**, 709-14.
26. Karami, M., Doudi, M. & Setorki, M. (2013) Assessing epidemiology of cutaneous leishmaniasis in Isfahan, Iran, *J Vector Borne Dis.* **50**, 30-7.
27. Abadias-Granado, I., Diago, A., Cerro, P. A., Palma-Ruiz, A. M. & Gilaberte, Y. (2021) Cutaneous and Mucocutaneous Leishmaniasis, *Actas Dermosifiliogr (Engl Ed).*
28. Monge-Maillo, B., Norman, F. F., Chamorro-Tojeiro, S., Gioia, F., Perez-Molina, J. A., Chicharro, C., Moreno, J. & Lopez-Velez, R. (2021) Post-kala-azar dermal leishmaniasis due to *Leishmania infantum* in an HIV-negative patient treated with miltefosine, *J Travel Med*.
29. Nieves, E. & Pimenta, P. F. (2000) Development of *Leishmania* (Viannia) *braziliensis* and *Leishmania* (*Leishmania*) *amazonensis* in the sand fly Lutzomyia migonei (Diptera: Psychodidae), *J Med Entomol.* **37**, 134-40.
30. Nieves, E. & Pimenta, P. F. (2002) Influence of vertebrate blood meals on the development of *Leishmania* (Viannia) braziliensis and *Leishmania* (*Leishmania*) amazonensis in the sand fly Lutzomyia migonei (Diptera: Psychodidae), *Am J Trop Med Hyg.* **67**, 640-7.
31. Bates, P. A. (1994) The developmental biology of *Leishmania* promastigotes, *Exp Parasitol.* **79**, 215-8.
32. Quinnell, R. J. & Courtenay, O. (2009) Transmission, reservoir hosts and control of zoonotic visceral leishmaniasis, *Parasitology.* **136**, 1915-34.
33. Harhay, M. O., Olliaro, P. L., Costa, D. L. & Costa, C. H. (2011) Urban parasitology: visceral leishmaniasis in Brazil, *Trends Parasitol.* **27**, 403-9.
34. Sharma, U. & Singh, S. (2008) Insect vectors of *Leishmania*: distribution, physiology and their control, *J Vector Borne Dis.* **45**, 255-72.

35. Chong, S. Z., Evrard, M. & Ng, L. G. (2013) Lights, camera, and action: vertebrate skin sets the stage for immune cell interaction with arthropod-vectored pathogens, *Front Immunol.* **4**, 286.
36. Lainson, R., Ward, R. D. & Shaw, J. J. (1977) *Leishmania* in phlebotomid sandflies: VI. Importance of hindgut development in distinguishing between parasites of the *Leishmania mexicana* and *L. braziliensis* complexes, *Proc R Soc Lond B Biol Sci.* **199**, 309-20.
37. Dostalova, A. & Volf, P. (2012) *Leishmania* development in sand flies: parasite-vector interactions overview, *Parasit Vectors.* **5**, 276.
38. Walters, L. L. (1993) *Leishmania* differentiation in natural and unnatural sand fly hosts, *J Eukaryot Microbiol.* **40**, 196-206.
39. Kamhawi, S. (2006) Phlebotomine sand flies and *Leishmania* parasites: friends or foes?, *Trends Parasitol.* **22**, 439-45.
40. Sadlova, J. & Volf, P. (1999) Occurrence of *Leishmania major* in sandfly urine, *Parasitology.* **118 (Pt 5)**, 455-60.
41. Warburg, A. & Schlein, Y. (1986) The effect of post-bloodmeal nutrition of Phlebotomus papatasi on the transmission of *Leishmania major*, *Am J Trop Med Hyg.* **35**, 926-30.
42. Schlein, Y., Jacobson, R. L. & Shlomai, J. (1991) Chitinase secreted by *Leishmania* functions in the sandfly vector, *Proc Biol Sci.* **245**, 121-6.
43. McConville, M. J. & Blackwell, J. M. (1991) Developmental changes in the glycosylated phosphatidylinositols of *Leishmania donovani*. Characterization of the promastigote and amastigote glycolipids, *J Biol Chem.* **266**, 15170-9.
44. de Menezes, J. P., Saraiva, E. M. & da Rocha-Azevedo, B. (2016) The site of the bite: *Leishmania* interaction with macrophages, neutrophils and the extracellular matrix in the dermis, *Parasit Vectors.* **9**, 264.
45. McConville, M. J., de Souza, D., Saunders, E., Likic, V. A. & Naderer, T. (2007) Living in a phagolysosome; metabolism of Leishmania amastigotes, *Trends Parasitol.* **23**, 368-75.
46. Real, F. & Mortara, R. A. (2012) The diverse and dynamic nature of Leishmania parasitophorous vacuoles studied by multidimensional imaging, *PLoS Negl Trop Dis.* **6**, e1518.
47. Wilson, J., Huynh, C., Kennedy, K. A., Ward, D. M., Kaplan, J., Aderem, A. & Andrews, N. W. (2008) Control of parasitophorous vacuole expansion by LYST/Beige restricts the intracellular growth of *Leishmania amazonensis*, *PLoS Pathog.* **4**, e1000179.
48. McConville, M. J. & Naderer, T. (2011) Metabolic pathways required for the intracellular survival of *Leishmania*, *Annu Rev Microbiol.* **65**, 543-61.
49. Ndjamen, B., Kang, B. H., Hatsuzawa, K. & Kima, P. E. (2010) *Leishmania* parasitophorous vacuoles interact continuously with the host cell's endoplasmic reticulum; parasitophorous vacuoles are hybrid compartments, *Cell Microbiol.* **12**, 1480-94.
50. Rubin-Bejerano, I., Fraser, I., Grisafi, P. & Fink, G. R. (2003) Phagocytosis by neutrophils induces an amino acid deprivation response in Saccharomyces cerevisiae and Candida albicans, *Proc Natl Acad Sci U S A.* **100**, 11007-12.
51. Naderer, T., Wee, E. & McConville, M. J. (2008) Role of hexosamine biosynthesis in *Leishmania* growth and virulence, *Mol Microbiol.* **69**, 858-69.

52. Scott, D. A., Hickerson, S. M., Vickers, T. J. & Beverley, S. M. (2008) The role of the mitochondrial glycine cleavage complex in the metabolism and virulence of the protozoan parasite *Leishmania major*, *J Biol Chem.* **283**, 155-165.
53. Carter, N. S., Yates, P. A., Gessford, S. K., Galagan, S. R., Landfear, S. M. & Ullman, B. (2010) Adaptive responses to purine starvation in *Leishmania donovani*, *Mol Microbiol.* **78**, 92-107.
54. Alvar, J., Aparicio, P., Aseffa, A., Den Boer, M., Canavate, C., Dedet, J. P., Gradoni, L., Ter Horst, R., Lopez-Velez, R. & Moreno, J. (2008) The relationship between leishmaniasis and AIDS: the second 10 years, *Clin Microbiol Rev.* **21**, 334-59, table of contents.
55. Lindoso, J. A., Cunha, M. A., Queiroz, I. T. & Moreira, C. H. (2016) Leishmaniasis-HIV coinfection: current challenges, *HIV AIDS (Auckl).* **8**, 147-156.
56. White, S. W., Hendricks, L. D. & Chulay, J. D. (1980) Leishmaniasis: a case history and treatment failure with rifampin, *Arch Dermatol.* **116**, 620-1.
57. Wyllie, S., Cunningham, M. L. & Fairlamb, A. H. (2004) Dual action of antimonial drugs on thiol redox metabolism in the human pathogen *Leishmania donovani*, *J Biol Chem.* **279**, 39925-32.
58. Roatt, B. M., de Oliveira Cardoso, J. M., De Brito, R. C. F., Coura-Vital, W., de Oliveira Aguiar-Soares, R. D. & Reis, A. B. (2020) Recent advances and new strategies on leishmaniasis treatment, *Appl Microbiol Biotechnol.* **104**, 8965-8977.
59. Mutiso, J. M., Macharia, J. C., Kiio, M. N., Ichagichu, J. M., Rikoi, H. & Gicheru, M. M. (2013) Development of *Leishmania* vaccines: predicting the future from past and present experience, *J Biomed Res.* **27**, 85-102.
60. Evans, K. J. & Kedzierski, L. (2012) Development of Vaccines against Visceral Leishmaniasis, *J Trop Med.* **2012**, 892817.
61. Khamesipour, A., Rafati, S., Davoudi, N., Maboudi, F. & Modabber, F. (2006) Leishmaniasis vaccine candidates for development: a global overview, *Indian J Med Res.* **123**, 423-38.
62. Okwor, I., Mou, Z., Liu, D. & Uzonna, J. (2012) Protective immunity and vaccination against cutaneous leishmaniasis, *Front Immunol.* **3**, 128.
63. Genaro, O., de Toledo, V. P., da Costa, C. A., Hermeto, M. V., Afonso, L. C. & Mayrink, W. (1996) Vaccine for prophylaxis and immunotherapy, Brazil, *Clin Dermatol.* **14**, 503-12.
64. Okwor, I., Kuriakose, S. & Uzonna, J. (2010) Repeated inoculation of killed *Leishmania major* induces durable immune response that protects mice against virulent challenge, *Vaccine.* **28**, 5451-7.
65. Sinha, S., Sundaram, S., Singh, A. P. & Tripathi, A. (2011) A gp63 based vaccine candidate against Visceral Leishmaniasis, *Bioinformation.* **5**, 320-5.
66. Alvar, J., Croft, S. L., Kaye, P., Khamesipour, A., Sundar, S. & Reed, S. G. (2013) Case study for a vaccine against leishmaniasis, *Vaccine.* **31 Suppl 2**, B244-9.
67. Depledge, D. P., MacLean, L. M., Hodgkinson, M. R., Smith, B. A., Jackson, A. P., Ma, S., Uliana, S. R. & Smith, D. F. (2010) *Leishmania*-specific surface antigens show sub-genus sequence variation and immune recognition, *PLoS Negl Trop Dis.* **4**, e829.
68. Beaumier, C. M., Gillespie, P. M., Hotez, P. J. & Bottazzi, M. E. (2013) New vaccines for neglected parasitic diseases and dengue, *Transl Res.* **162**, 144-55.

69. Doroud, D., Zahedifard, F., Vatanara, A., Najafabadi, A. R., Taslimi, Y., Vahabpour, R., Torkashvand, F., Vaziri, B. & Rafati, S. (2011) Delivery of a cocktail DNA vaccine encoding cysteine proteinases type I, II and III with solid lipid nanoparticles potentiate protective immunity against *Leishmania major* infection, *J Control Release.* **153**, 154-62.
70. Martin, W. F. & Cerff, R. (2017) Physiology, phylogeny, early evolution, and GAPDH, *Protoplasma.* **254**, 1823-1834.
71. Sirover, M. A. (2011) On the functional diversity of glyceraldehyde-3-phosphate dehydrogenase: biochemical mechanisms and regulatory control, *Biochim Biophys Acta.* **1810**, 741-51.
72. Sirover, M. A. (2014) Structural analysis of glyceraldehyde-3-phosphate dehydrogenase functional diversity, *Int J Biochem Cell Biol.* **57**, 20-6.
73. Backlund, M., Paukku, K., Daviet, L., De Boer, R. A., Valo, E., Hautaniemi, S., Kalkkinen, N., Ehsan, A., Kontula, K. K. & Lehtonen, J. Y. (2009) Posttranscriptional regulation of angiotensin II type 1 receptor expression by glyceraldehyde 3-phosphate dehydrogenase, *Nucleic Acids Res.* **37**, 2346-58.
74. Bonafe, N., Gilmore-Hebert, M., Folk, N. L., Azodi, M., Zhou, Y. & Chambers, S. K. (2005) Glyceraldehyde-3-phosphate dehydrogenase binds to the AU-Rich 3' untranslated region of colony-stimulating factor-1 (CSF-1) messenger RNA in human ovarian cancer cells: possible role in CSF-1 posttranscriptional regulation and tumor phenotype, *Cancer Res.* **65**, 3762-71.
75. Rodriguez-Pascual, F., Redondo-Horcajo, M., Magan-Marchal, N., Lagares, D., Martinez-Ruiz, A., Kleinert, H. & Lamas, S. (2008) Glyceraldehyde-3-phosphate dehydrogenase regulates endothelin-1 expression by a novel, redox-sensitive mechanism involving mRNA stability, *Mol Cell Biol.* **28**, 7139-55.
76. Zhou, Y., Yi, X., Stoffer, J. B., Bonafe, N., Gilmore-Hebert, M., McAlpine, J. & Chambers, S. K. (2008) The multifunctional protein glyceraldehyde-3-phosphate dehydrogenase is both regulated and controls colony-stimulating factor-1 messenger RNA stability in ovarian cancer, *Mol Cancer Res.* **6**, 1375-84.
77. Kaneda, M., Takeuchi, K., Inoue, K. & Umeda, M. (1997) Localization of the phosphatidylserine-binding site of glyceraldehyde-3-phosphate dehydrogenase responsible for membrane fusion, *J Biochem.* **122**, 1233-40.
78. Puder, M. & Soberman, R. J. (1997) Glutathione conjugates recognize the Rossmann fold of glyceraldehyde-3-phosphate dehydrogenase, *J Biol Chem.* **272**, 10936-40.
79. Hara, M. R., Cascio, M. B. & Sawa, A. (2006) GAPDH as a sensor of NO stress, *Biochim Biophys Acta.* **1762**, 502-9.
80. Nakajima, H., Amano, W., Fujita, A., Fukuhara, A., Azuma, Y. T., Hata, F., Inui, T. & Takeuchi, T. (2007) The active site cysteine of the proapoptotic protein glyceraldehyde-3-phosphate dehydrogenase is essential in oxidative stress-induced aggregation and cell death, *J Biol Chem.* **282**, 26562-74.
81. Hara, M. R. & Snyder, S. H. (2006) Nitric oxide-GAPDH-Siah: a novel cell death cascade, *Cell Mol Neurobiol.* **26**, 527-38.
82. Brown, V. M., Krynetski, E. Y., Krynetskaia, N. F., Grieger, D., Mukatira, S. T., Murti, K. G., Slaughter, C. A., Park, H. W. & Evans, W. E. (2004) A novel CRM1-mediated nuclear export signal governs nuclear accumulation of glyceraldehyde-3-phosphate dehydrogenase following genotoxic stress, *J Biol Chem.* **279**, 5984-92.

83. White, M. R. & Garcin, E. D. (2017) D-Glyceraldehyde-3-Phosphate Dehydrogenase Structure and Function, *Subcell Biochem.* **83**, 413-453.
84. Huang, L., Zhu, Y. N., Yang, J. Y., Li, D. W., Li, Y., Bian, L. M. & Ye, J. R. (2018) Shoot Blight on Chinese Fir (Cunninghamia lanceolata) is Caused by Bipolaris oryzae, *Plant Dis.* **102**, 500-506.
85. Madhavan, A., Pandey, A. & Sukumaran, R. K. (2017) Expression system for heterologous protein expression in the filamentous fungus Aspergillus unguis, *Bioresour Technol.* **245**, 1334-1342.
86. Prielhofer, R., Barrero, J. J., Steuer, S., Gassler, T., Zahrl, R., Baumann, K., Sauer, M., Mattanovich, D., Gasser, B. & Marx, H. (2017) GoldenPiCS: a Golden Gate-derived modular cloning system for applied synthetic biology in the yeast Pichia pastoris, *BMC Syst Biol.* **11**, 123.
87. Sirover, M. A. (1999) New insights into an old protein: the functional diversity of mammalian glyceraldehyde-3-phosphate dehydrogenase, *Biochim Biophys Acta.* **1432**, 159-84.
88. Zheng, L., Roeder, R. G. & Luo, Y. (2003) S phase activation of the histone H2B promoter by OCA-S, a coactivator complex that contains GAPDH as a key component, *Cell.* **114**, 255-66.
89. McKnight, S. (2003) Gene switching by metabolic enzymes--how did you get on the invitation list?, *Cell.* **114**, 150-2.
90. Tisdale, E. J. (2001) Glyceraldehyde-3-phosphate dehydrogenase is required for vesicular transport in the early secretory pathway, *J Biol Chem.* **276**, 2480-6.
91. Tisdale, E. J. (2002) Glyceraldehyde-3-phosphate dehydrogenase is phosphorylated by protein kinase Ciota /lambda and plays a role in microtubule dynamics in the early secretory pathway, *J Biol Chem.* **277**, 3334-41.
92. Tisdale, E. J., Kelly, C. & Artalejo, C. R. (2004) Glyceraldehyde-3-phosphate dehydrogenase interacts with Rab2 and plays an essential role in endoplasmic reticulum to Golgi transport exclusive of its glycolytic activity, *J Biol Chem.* **279**, 54046-52.
93. Tisdale, E. J. & Artalejo, C. R. (2006) Src-dependent aprotein kinase C iota/lambda (aPKCiota/lambda) tyrosine phosphorylation is required for aPKCiota/lambda association with Rab2 and glyceraldehyde-3-phosphate dehydrogenase on pre-golgi intermediates, *J Biol Chem.* **281**, 8436-42.
94. Tisdale, E. J. & Artalejo, C. R. (2007) A GAPDH mutant defective in Src-dependent tyrosine phosphorylation impedes Rab2-mediated events, *Traffic.* **8**, 733-41.
95. Tisdale, E. J., Azizi, F. & Artalejo, C. R. (2009) Rab2 utilizes glyceraldehyde-3-phosphate dehydrogenase and protein kinase C{iota} to associate with microtubules and to recruit dynein, *J Biol Chem.* **284**, 5876-84.
96. Harada, N., Yasunaga, R., Higashimura, Y., Yamaji, R., Fujimoto, K., Moss, J., Inui, H. & Nakano, Y. (2007) Glyceraldehyde-3-phosphate dehydrogenase enhances transcriptional activity of androgen receptor in prostate cancer cells, *J Biol Chem.* **282**, 22651-61.
97. Raje, C. I., Kumar, S., Harle, A., Nanda, J. S. & Raje, M. (2007) The macrophage cell surface glyceraldehyde-3-phosphate dehydrogenase is a novel transferrin receptor, *J Biol Chem.* **282**, 3252-61.
98. Sundararaj, K. P., Wood, R. E., Ponnusamy, S., Salas, A. M., Szulc, Z., Bielawska, A., Obeid, L. M., Hannun, Y. A. & Ogretmen, B. (2004) Rapid shortening of telomere length

in response to ceramide involves the inhibition of telomere binding activity of nuclear glyceraldehyde-3-phosphate dehydrogenase, *J Biol Chem.* **279**, 6152-62.

99. Demarse, N. A., Ponnusamy, S., Spicer, E. K., Apohan, E., Baatz, J. E., Ogretmen, B. & Davies, C. (2009) Direct binding of glyceraldehyde 3-phosphate dehydrogenase to telomeric DNA protects telomeres against chemotherapy-induced rapid degradation, *J Mol Biol.* **394**, 789-803.
100. Azam, S., Jouvet, N., Jilani, A., Vongsamphanh, R., Yang, X., Yang, S. & Ramotar, D. (2008) Human glyceraldehyde-3-phosphate dehydrogenase plays a direct role in reactivating oxidized forms of the DNA repair enzyme APE1, *J Biol Chem.* **283**, 30632-41.
101. Pierce, A., Mirzaei, H., Muller, F., De Waal, E., Taylor, A. B., Leonard, S., Van Remmen, H., Regnier, F., Richardson, A. & Chaudhuri, A. (2008) GAPDH is conformationally and functionally altered in association with oxidative stress in mouse models of amyotrophic lateral sclerosis, *J Mol Biol.* **382**, 1195-210.
102. Baek, D., Jin, Y., Jeong, J. C., Lee, H. J., Moon, H., Lee, J., Shin, D., Kang, C. H., Kim, D. H., Nam, J., Lee, S. Y. & Yun, D. J. (2008) Suppression of reactive oxygen species by glyceraldehyde-3-phosphate dehydrogenase, *Phytochemistry.* **69**, 333-8.
103. Barbini, L., Rodriguez, J., Dominguez, F. & Vega, F. (2007) Glyceraldehyde-3-phosphate dehydrogenase exerts different biologic activities in apoptotic and proliferating hepatocytes according to its subcellular localization, *Mol Cell Biochem.* **300**, 19-28.
104. Du, Z. X., Wang, H. Q., Zhang, H. Y. & Gao, D. X. (2007) Involvement of glyceraldehyde-3-phosphate dehydrogenase in tumor necrosis factor-related apoptosis-inducing ligand-mediated death of thyroid cancer cells, *Endocrinology.* **148**, 4352-61.
105. Tarze, A., Deniaud, A., Le Bras, M., Maillier, E., Molle, D., Larochette, N., Zamzami, N., Jan, G., Kroemer, G. & Brenner, C. (2007) GAPDH, a novel regulator of the pro-apoptotic mitochondrial membrane permeabilization, *Oncogene.* **26**, 2606-20.
106. Benhar, M. & Stamler, J. S. (2005) A central role for S-nitrosylation in apoptosis, *Nat Cell Biol.* **7**, 645-6.
107. Hara, M. R., Agrawal, N., Kim, S. F., Cascio, M. B., Fujimuro, M., Ozeki, Y., Takahashi, M., Cheah, J. H., Tankou, S. K., Hester, L. D., Ferris, C. D., Hayward, S. D., Snyder, S. H. & Sawa, A. (2005) S-nitrosylated GAPDH initiates apoptotic cell death by nuclear translocation following Siah1 binding, *Nat Cell Biol.* **7**, 665-74.
108. Colell, A., Ricci, J. E., Tait, S., Milasta, S., Maurer, U., Bouchier-Hayes, L., Fitzgerald, P., Guio-Carrion, A., Waterhouse, N. J., Li, C. W., Mari, B., Barbry, P., Newmeyer, D. D., Beere, H. M. & Green, D. R. (2007) GAPDH and autophagy preserve survival after apoptotic cytochrome c release in the absence of caspase activation, *Cell.* **129**, 983-97.
109. Song, S. & Finkel, T. (2007) GAPDH and the search for alternative energy, *Nat Cell Biol.* **9**, 869-70.
110. Nishikawa, T., Edelstein, D., Du, X. L., Yamagishi, S., Matsumura, T., Kaneda, Y., Yorek, M. A., Beebe, D., Oates, P. J., Hammes, H. P., Giardino, I. & Brownlee, M. (2000) Normalizing mitochondrial superoxide production blocks three pathways of hyperglycaemic damage, *Nature.* **404**, 787-90.
111. Reusch, J. E. (2003) Diabetes, microvascular complications, and cardiovascular complications: what is it about glucose?, *J Clin Invest.* **112**, 986-8.
112. Szabo, C. (2009) Role of nitrosative stress in the pathogenesis of diabetic vascular dysfunction, *Br J Pharmacol.* **156**, 713-27.

113. Blatnik, M., Thorpe, S. R. & Baynes, J. W. (2008) Succination of proteins by fumarate: mechanism of inactivation of glyceraldehyde-3-phosphate dehydrogenase in diabetes, *Ann N Y Acad Sci.* **1126**, 272-5.
114. Mazzola, J. L. & Sirover, M. A. (2002) Alteration of intracellular structure and function of glyceraldehyde-3-phosphate dehydrogenase: a common phenotype of neurodegenerative disorders?, *Neurotoxicology.* **23**, 603-9.
115. Butterfield, D. A., Hardas, S. S. & Lange, M. L. (2010) Oxidatively modified glyceraldehyde-3-phosphate dehydrogenase (GAPDH) and Alzheimer's disease: many pathways to neurodegeneration, *J Alzheimers Dis.* **20**, 369-93.
116. Daubenberger, C. A., Tisdale, E. J., Curcic, M., Diaz, D., Silvie, O., Mazier, D., Eling, W., Bohrmann, B., Matile, H. & Pluschke, G. (2003) The N'-terminal domain of glyceraldehyde-3-phosphate dehydrogenase of the apicomplexan Plasmodium falciparum mediates GTPase Rab2-dependent recruitment to membranes, *Biol Chem.* **384**, 1227-37.
117. Fugier, E., Salcedo, S. P., de Chastellier, C., Pophillat, M., Muller, A., Arce-Gorvel, V., Fourquet, P. & Gorvel, J. P. (2009) The glyceraldehyde-3-phosphate dehydrogenase and the small GTPase Rab 2 are crucial for Brucella replication, *PLoS Pathog.* **5**, e1000487.
118. Butera, G., Mullappilly, N., Masetto, F., Palmieri, M., Scupoli, M. T., Pacchiana, R. & Donadelli, M. (2019) Regulation of Autophagy by Nuclear GAPDH and Its Aggregates in Cancer and Neurodegenerative Disorders, *Int J Mol Sci.* **20**.
119. Sirover, M. A. (1997) Role of the glycolytic protein, glyceraldehyde-3-phosphate dehydrogenase, in normal cell function and in cell pathology, *J Cell Biochem.* **66**, 133-40.
120. Huberts, D. H. & van der Klei, I. J. (2010) Moonlighting proteins: an intriguing mode of multitasking, *Biochim Biophys Acta.* **1803**, 520-5.
121. Jeffery, C. J. (2018) Protein moonlighting: what is it, and why is it important?, *Philos Trans R Soc Lond B Biol Sci.* **373**.
122. Nicholls, C., Li, H. & Liu, J. P. (2012) GAPDH: a common enzyme with uncommon functions, *Clin Exp Pharmacol Physiol.* **39**, 674-9.
123. Kawamoto, R. M. & Caswell, A. H. (1986) Autophosphorylation of glyceraldehydephosphate dehydrogenase and phosphorylation of protein from skeletal muscle microsomes, *Biochemistry.* **25**, 657-61.
124. Durrieu, C., Bernier-Valentin, F. & Rousset, B. (1987) Binding of glyceraldehyde 3-phosphate dehydrogenase to microtubules, *Mol Cell Biochem.* **74**, 55-65.
125. Glaser, P. E. & Gross, R. W. (1995) Rapid plasmenylethanolamine-selective fusion of membrane bilayers catalyzed by an isoform of glyceraldehyde-3-phosphate dehydrogenase: discrimination between glycolytic and fusogenic roles of individual isoforms, *Biochemistry.* **34**, 12193-203.
126. Hessler, R. J., Blackwood, R. A., Brock, T. G., Francis, J. W., Harsh, D. M. & Smolen, J. E. (1998) Identification of glyceraldehyde-3-phosphate dehydrogenase as a Ca2+-dependent fusogen in human neutrophil cytosol, *J Leukoc Biol.* **63**, 331-6.
127. Brune, B. & Lapetina, E. G. (1996) Nitric oxide-induced covalent modification of glycolytic enzyme glyceraldehyde-3-phosphate dehydrogenase, *Methods Enzymol.* **269**, 400-7.
128. Morgenegg, G., Winkler, G. C., Hubscher, U., Heizmann, C. W., Mous, J. & Kuenzle, C. C. (1986) Glyceraldehyde-3-phosphate dehydrogenase is a nonhistone protein and a possible activator of transcription in neurons, *J Neurochem.* **47**, 54-62.

129. Singh, R. & Green, M. R. (1993) Sequence-specific binding of transfer RNA by glyceraldehyde-3-phosphate dehydrogenase, *Science.* **259**, 365-8.
130. Meyer-Siegler, K., Mauro, D. J., Seal, G., Wurzer, J., deRiel, J. K. & Sirover, M. A. (1991) A human nuclear uracil DNA glycosylase is the 37-kDa subunit of glyceraldehyde-3-phosphate dehydrogenase, *Proc Natl Acad Sci U S A.* **88**, 8460-4.
131. Baxi, M. D. & Vishwanatha, J. K. (1995) Uracil DNA-glycosylase/glyceraldehyde-3-phosphate dehydrogenase is an Ap4A binding protein, *Biochemistry.* **34**, 9700-7.
132. Nagy, E. & Rigby, W. F. (1995) Glyceraldehyde-3-phosphate dehydrogenase selectively binds AU-rich RNA in the NAD(+)-binding region (Rossmann fold), *J Biol Chem.* **270**, 2755-63.
133. Chakravarti, R., Aulak, K. S., Fox, P. L. & Stuehr, D. J. (2010) GAPDH regulates cellular heme insertion into inducible nitric oxide synthase, *Proc Natl Acad Sci U S A.* **107**, 18004-9.
134. Sen, N., Hara, M. R., Kornberg, M. D., Cascio, M. B., Bae, B. I., Shahani, N., Thomas, B., Dawson, T. M., Dawson, V. L., Snyder, S. H. & Sawa, A. (2008) Nitric oxide-induced nuclear GAPDH activates p300/CBP and mediates apoptosis, *Nat Cell Biol.* **10**, 866-73.
135. Sirover, M. A. (2020) Moonlighting glyceraldehyde-3-phosphate dehydrogenase: posttranslational modification, protein and nucleic acid interactions in normal cells and in human pathology, *Crit Rev Biochem Mol Biol.* **55**, 354-371.
136. Sirover, M. A. (2018) Pleiotropic effects of moonlighting glyceraldehyde-3-phosphate dehydrogenase (GAPDH) in cancer progression, invasiveness, and metastases, *Cancer Metastasis Rev.* **37**, 665-676.
137. Sirover, M. A. (2012) Subcellular dynamics of multifunctional protein regulation: mechanisms of GAPDH intracellular translocation, *J Cell Biochem.* **113**, 2193-200.
138. Nicholls, C., Pinto, A. R., Li, H., Li, L., Wang, L., Simpson, R. & Liu, J. P. (2012) Glyceraldehyde-3-phosphate dehydrogenase (GAPDH) induces cancer cell senescence by interacting with telomerase RNA component, *Proc Natl Acad Sci U S A.* **109**, 13308-13.
139. Lin, K. W. & Yan, J. (2005) The telomere length dynamic and methods of its assessment, *J Cell Mol Med.* **9**, 977-89.
140. Smith, E. M., Pendlebury, D. F. & Nandakumar, J. (2020) Structural biology of telomeres and telomerase, *Cell Mol Life Sci.* **77**, 61-79.
141. Demple, B. & Harrison, L. (1994) Repair of oxidative damage to DNA: enzymology and biology, *Annu Rev Biochem.* **63**, 915-48.
142. Jayaraman, L., Murthy, K. G., Zhu, C., Curran, T., Xanthoudakis, S. & Prives, C. (1997) Identification of redox/repair protein Ref-1 as a potent activator of p53, *Genes Dev.* **11**, 558-70.
143. Thakur, S., Sarkar, B., Cholia, R. P., Gautam, N., Dhiman, M. & Mantha, A. K. (2014) APE1/Ref-1 as an emerging therapeutic target for various human diseases: phytochemical modulation of its functions, *Exp Mol Med.* **46**, e106.
144. Thakur, S., Dhiman, M., Tell, G. & Mantha, A. K. (2015) A review on protein-protein interaction network of APE1/Ref-1 and its associated biological functions, *Cell Biochem Funct.* **33**, 101-12.
145. Chambers, S. K. (2009) Role of CSF-1 in progression of epithelial ovarian cancer, *Future Oncol.* **5**, 1429-40.

146. Miyauchi, T. & Masaki, T. (1999) Pathophysiology of endothelin in the cardiovascular system, *Annu Rev Physiol.* **61**, 391-415.
147. Reimunde, F. M., Castanares, C., Redondo-Horcajo, M., Lamas, S. & Rodriguez-Pascual, F. (2005) Endothelin-1 expression is strongly repressed by AU-rich elements in the 3'-untranslated region of the gene, *Biochem J.* **387**, 763-72.
148. Schultz, D. E., Hardin, C. C. & Lemon, S. M. (1996) Specific interaction of glyceraldehyde 3-phosphate dehydrogenase with the 5'-nontranslated RNA of hepatitis A virus, *J Biol Chem.* **271**, 14134-42.
149. Tang, A. H., Neufeld, T. P., Kwan, E. & Rubin, G. M. (1997) PHYL acts to down-regulate TTK88, a transcriptional repressor of neuronal cell fates, by a SINA-dependent mechanism, *Cell.* **90**, 459-67.
150. Li, S., Li, Y., Carthew, R. W. & Lai, Z. C. (1997) Photoreceptor cell differentiation requires regulated proteolysis of the transcriptional repressor Tramtrack, *Cell.* **90**, 469-78.
151. Hu, G., Chung, Y. L., Glover, T., Valentine, V., Look, A. T. & Fearon, E. R. (1997) Characterization of human homologs of the Drosophila seven in absentia (sina) gene, *Genomics.* **46**, 103-11.
152. Zhang, Q., Wang, Z., Hou, F., Harding, R., Huang, X., Dong, A., Walker, J. R. & Tong, Y. (2017) The substrate binding domains of human SIAH E3 ubiquitin ligases are now crystal clear, *Biochim Biophys Acta Gen Subj.* **1861**, 3095-3105.
153. Dutta, S., Teresinski, H. J. & Smith, M. D. (2014) A split-ubiquitin yeast two-hybrid screen to examine the substrate specificity of atToc159 and atToc132, two Arabidopsis chloroplast preprotein import receptors, *PLoS One.* **9**, e95026.
154. Zaffagnini, M., Fermani, S., Costa, A., Lemaire, S. D. & Trost, P. (2013) Plant cytoplasmic GAPDH: redox post-translational modifications and moonlighting properties, *Front Plant Sci.* **4**, 450.
155. Ortiz-Ortiz, M. A., Moran, J. M., Ruiz-Mesa, L. M., Bravo-San Pedro, J. M. & Fuentes, J. M. (2010) Paraquat exposure induces nuclear translocation of glyceraldehyde-3-phosphate dehydrogenase (GAPDH) and the activation of the nitric oxide-GAPDH-Siah cell death cascade, *Toxicol Sci.* **116**, 614-22.
156. Liiv, I., Haljasorg, U., Kisand, K., Maslovskaja, J., Laan, M. & Peterson, P. (2012) AIRE-induced apoptosis is associated with nuclear translocation of stress sensor protein GAPDH, *Biochem Biophys Res Commun.* **423**, 32-7.
157. Mustafa Rizvi, S. H., Shao, D., Tsukahara, Y., Pimentel, D. R., Weisbrod, R. M., Hamburg, N. M., McComb, M. E., Matsui, R. & Bachschmid, M. M. (2021) Oxidized GAPDH transfers S-glutathionylation to a nuclear protein Sirtuin-1 leading to apoptosis, *Free Radic Biol Med.* **174**, 73-83.
158. Kornberg, M. D., Sen, N., Hara, M. R., Juluri, K. R., Nguyen, J. V., Snowman, A. M., Law, L., Hester, L. D. & Snyder, S. H. (2010) GAPDH mediates nitrosylation of nuclear proteins, *Nat Cell Biol.* **12**, 1094-100.
159. Ventura, M., Mateo, F., Serratosa, J., Salaet, I., Carujo, S., Bachs, O. & Pujol, M. J. (2010) Nuclear translocation of glyceraldehyde-3-phosphate dehydrogenase is regulated by acetylation, *Int J Biochem Cell Biol.* **42**, 1672-80.
160. Bae, B. I., Hara, M. R., Cascio, M. B., Wellington, C. L., Hayden, M. R., Ross, C. A., Ha, H. C., Li, X. J., Snyder, S. H. & Sawa, A. (2006) Mutant huntingtin: nuclear translocation and cytotoxicity mediated by GAPDH, *Proc Natl Acad Sci U S A.* **103**, 3405-9.

161. Galluzzi, L. Vitale, I. Aaronson, S. A. Abrams, J. M. Adam, D, et al. (2018) Molecular mechanisms of cell death: recommendations of the Nomenclature Committee on Cell Death 2018, *Cell Death Differ.* **25**, 486-541.
162. Glick, D., Barth, S. & Macleod, K. F. (2010) Autophagy: cellular and molecular mechanisms, *J Pathol.* **221**, 3-12.
163. Levine, B. & Klionsky, D. J. (2004) Development by self-digestion: molecular mechanisms and biological functions of autophagy, *Dev Cell.* **6**, 463-77.
164. Bernard, A., Jin, M., Xu, Z. & Klionsky, D. J. (2015) A large-scale analysis of autophagy-related gene expression identifies new regulators of autophagy, *Autophagy.* **11**, 2114-2122.
165. Henry, E., Fung, N., Liu, J., Drakakaki, G. & Coaker, G. (2015) Beyond glycolysis: GAPDHs are multi-functional enzymes involved in regulation of ROS, autophagy, and plant immune responses, *PLoS Genet.* **11**, e1005199.
166. Huang, J. & Klionsky, D. J. (2007) Autophagy and human disease, *Cell Cycle.* **6**, 1837-49.
167. Racker, E. (1972) Bioenergetics and the problem of tumor growth, *Am Sci.* **60**, 56-63.
168. Colell, A., Green, D. R. & Ricci, J. E. (2009) Novel roles for GAPDH in cell death and carcinogenesis, *Cell Death Differ.* **16**, 1573-81.
169. Coley, A. F., Dodson, H. C., Morris, M. T. & Morris, J. C. (2011) Glycolysis in the african trypanosome: targeting enzymes and their subcellular compartments for therapeutic development, *Mol Biol Int.* **2011**, 123702.
170. Parsons, M. (2004) Glycosomes: parasites and the divergence of peroxisomal purpose, *Mol Microbiol.* **53**, 717-24.
171. Hannaert, V. & Michels, P. A. (1994) Structure, function, and biogenesis of glycosomes in kinetoplastida, *J Bioenerg Biomembr.* **26**, 205-12.
172. Opperdoes, F. R. & Borst, P. (1977) Localization of nine glycolytic enzymes in a microbody-like organelle in Trypanosoma brucei: the glycosome, *FEBS Lett.* **80**, 360-4.
173. Gualdron-Lopez, M., Brennand, A., Hannaert, V., Quinones, W., Caceres, A. J., Bringaud, F., Concepcion, J. L. & Michels, P. A. (2012) When, how and why glycolysis became compartmentalised in the Kinetoplastea. A new look at an ancient organelle, *Int J Parasitol.* **42**, 1-20.
174. Hannaert, V., Bringaud, F., Opperdoes, F. R. & Michels, P. A. (2003) Evolution of energy metabolism and its compartmentation in Kinetoplastida, *Kinetoplastid Biol Dis.* **2**, 11.
175. Albert, M. A., Haanstra, J. R., Hannaert, V., Van Roy, J., Opperdoes, F. R., Bakker, B. M. & Michels, P. A. (2005) Experimental and in silico analyses of glycolytic flux control in bloodstream form Trypanosoma brucei, *J Biol Chem.* **280**, 28306-15.
176. Aronov, A. M., Suresh, S., Buckner, F. S., Van Voorhis, W. C., Verlinde, C. L., Opperdoes, F. R., Hol, W. G. & Gelb, M. H. (1999) Structure-based design of submicromolar, biologically active inhibitors of trypanosomatid glyceraldehyde-3-phosphate dehydrogenase, *Proc Natl Acad Sci U S A.* **96**, 4273-8.
177. Zhang, W. W., McCall, L. I. & Matlashewski, G. (2013) Role of cytosolic glyceraldehyde-3-phosphate dehydrogenase in visceral organ infection by *Leishmania donovani*, *Eukaryot Cell.* **12**, 70-7.
178. Michels, P. A., Poliszczak, A., Osinga, K. A., Misset, O., Van Beeumen, J., Wierenga, R. K., Borst, P. & Opperdoes, F. R. (1986) Two tandemly linked identical genes code for the

glycosomal glyceraldehyde-phosphate dehydrogenase in Trypanosoma brucei, *EMBO J.* **5**, 1049-56.

179. Lambeir, A. M., Loiseau, A. M., Kuntz, D. A., Vellieux, F. M., Michels, P. A. & Opperdoes, F. R. (1991) The cytosolic and glycosomal glyceraldehyde-3-phosphate dehydrogenase from Trypanosoma brucei. Kinetic properties and comparison with homologous enzymes, *Eur J Biochem.* **198**, 429-35.
180. Hannaert, V., Blaauw, M., Kohl, L., Allert, S., Opperdoes, F. R. & Michels, P. A. (1992) Molecular analysis of the cytosolic and glycosomal glyceraldehyde-3-phosphate dehydrogenase in *Leishmania mexicana*, *Mol Biochem Parasitol.* **55**, 115-26.
181. Misset, O., Van Beeumen, J., Lambeir, A. M., Van der Meer, R. & Opperdoes, F. R. (1987) Glyceraldehyde-phosphate dehydrogenase from Trypanosoma brucei. Comparison of the glycosomal and cytosolic isoenzymes, *Eur J Biochem.* **162**, 501-7.
182. Peacock, C. S., Seeger, K., Harris, D., Murphy, L., Ruiz, J. C., et. al. (2007) Comparative genomic analysis of three *Leishmania* species that cause diverse human disease, *Nat Genet.* **39**, 839-47.
183. Michels, P. A., Marchand, M., Kohl, L., Allert, S., Wierenga, R. K. & Opperdoes, F. R. (1991) The cytosolic and glycosomal isoenzymes of glyceraldehyde-3-phosphate dehydrogenase in Trypanosoma brucei have a distant evolutionary relationship, *Eur J Biochem.* **198**, 421-8.
184. Vikeved, E., Backlund, A. & Alsmark, C. (2016) The Dynamics of Lateral Gene Transfer in Genus *Leishmania* - A Route for Adaptation and Species Diversification, *PLoS Negl Trop Dis.* **10**, e0004326.
185. Adhikari, A., Biswas, S., Mukherjee, A., Das, S. & Adak, S. (2019) PAS domain-containing phosphoglycerate kinase deficiency in *Leishmania major* results in increased autophagosome formation and cell death, *Biochem J.* **476**, 1303-1321.
186. Biswas, S., Adhikari, A., Mukherjee, A., Das, S. & Adak, S. (2020) Regulation of *Leishmania major* PAS domain-containing phosphoglycerate kinase by cofactor Mg(2+) ion at neutral pH, *FEBS J.* **287**, 5183-5195.
187. Mukherjee, A., Adhikari, A., Das, P., Biswas, S., Mukherjee, S. & Adak, S. (2018) Loss of virulence in NAD(P)H cytochrome b5 oxidoreductase deficient *Leishmania major*, *Biochem Biophys Res Commun.* **503**, 371-377.
188. Gilles-Gonzalez, M. A., Gonzalez, G., Sousa, E. H. & Tuckerman, J. (2008) Oxygen-sensing histidine-protein kinases: assays of ligand binding and turnover of response-regulator substrates, *Methods Enzymol.* **437**, 173-89.
189. Bradford, M. M. (1976) A rapid and sensitive method for the quantitation of microgram quantities of protein utilizing the principle of protein-dye binding, *Anal Biochem.* **72**, 248-54.
190. Kapler, G. M., Coburn, C. M. & Beverley, S. M. (1990) Stable transfection of the human parasite *Leishmania major* delineates a 30-kilobase region sufficient for extrachromosomal replication and expression, *Mol Cell Biol.* **10**, 1084-94.
191. Dolai, S., Yadav, R. K., Pal, S. & Adak, S. (2008) *Leishmania major* ascorbate peroxidase overexpression protects cells against reactive oxygen species-mediated cardiolipin oxidation, *Free Radic Biol Med.* **45**, 1520-9.
192. Pal, S., Dolai, S., Yadav, R. K. & Adak, S. (2010) Ascorbate peroxidase from *Leishmania major* controls the virulence of infective stage of promastigotes by regulating oxidative stress, *PLoS One.* **5**, e11271.

193. Colasante, C., Voncken, F., Manful, T., Ruppert, T., Tielens, A. G. M., van Hellemond, J. J. & Clayton, C. (2013) Proteins and lipids of glycosomal membranes from *Leishmania tarentolae* and *Trypanosoma brucei*, *F1000Res.* **2**, 27.
194. Gomez, M. A., Contreras, I., Halle, M., Tremblay, M. L., McMaster, R. W. & Olivier, M. (2009) *Leishmania* GP63 alters host signaling through cleavage-activated protein tyrosine phosphatases, *Sci Signal.* **2**, ra58.
195. Joshi, P. B., Kelly, B. L., Kamhawi, S., Sacks, D. L. & McMaster, W. R. (2002) Targeted gene deletion in *Leishmania major* identifies leishmanolysin (GP63) as a virulence factor, *Mol Biochem Parasitol.* **120**, 33-40.
196. Hubel, A., Krobitsch, S., Horauf, A. & Clos, J. (1997) *Leishmania major* Hsp100 is required chiefly in the mammalian stage of the parasite, *Mol Cell Biol.* **17**, 5987-95.
197. Klein, C., Gopfert, U., Goehring, N., Stierhof, Y. D. & Ilg, T. (1999) Proteophosphoglycans of *Leishmania mexicana*. Identification, purification, structural and ultrastructural characterization of the secreted promastigote proteophosphoglycan pPPG2, a stage-specific glycoisoform of amastigote aPPG, *Biochem J.* **344 Pt 3**, 775-86.
198. Vannier-Santos, M. A., Martiny, A., Meyer-Fernandes, J. R. & de Souza, W. (1995) Leishmanial protein kinase C modulates host cell infection via secreted acid phosphatase, *Eur J Cell Biol.* **67**, 112-9.
199. Lancaster, G. I. & Febbraio, M. A. (2005) Exosome-dependent trafficking of HSP70: a novel secretory pathway for cellular stress proteins, *J Biol Chem.* **280**, 23349-55.
200. Nandan, D., Yi, T., Lopez, M., Lai, C. & Reiner, N. E. (2002) *Leishmania* EF-1alpha activates the Src homology 2 domain containing tyrosine phosphatase SHP-1 leading to macrophage deactivation, *J Biol Chem.* **277**, 50190-7.
201. Nandan, D., Tran, T., Trinh, E., Silverman, J. M. & Lopez, M. (2007) Identification of *Leishmania* fructose-1,6-bisphosphate aldolase as a novel activator of host macrophage Src homology 2 domain containing protein tyrosine phosphatase SHP-1, *Biochem Biophys Res Commun.* **364**, 601-7.
202. Millet, P., Vachharajani, V., McPhail, L., Yoza, B. & McCall, C. E. (2016) GAPDH Binding to TNF-alpha mRNA Contributes to Posttranscriptional Repression in Monocytes: A Novel Mechanism of Communication between Inflammation and Metabolism, *J Immunol.* **196**, 2541-51.
203. Silverman, J. M., Clos, J., Horakova, E., Wang, A. Y., Wiesgigl, M., Kelly, I., Lynn, M. A., McMaster, W. R., Foster, L. J., Levings, M. K. & Reiner, N. E. (2010) *Leishmania* exosomes modulate innate and adaptive immune responses through effects on monocytes and dendritic cells, *J Immunol.* **185**, 5011-22.
204. Silverman, J. M., Clos, J., de'Oliveira, C. C., Shirvani, O., Fang, Y., Wang, C., Foster, L. J. & Reiner, N. E. (2010) An exosome-based secretion pathway is responsible for protein export from *Leishmania* and communication with macrophages, *J Cell Sci.* **123**, 842-52.
205. Gehr, G., Gentz, R., Brockhaus, M., Loetscher, H. & Lesslauer, W. (1992) Both tumor necrosis factor receptor types mediate proliferative signals in human mononuclear cell activation, *J Immunol.* **149**, 911-7.
206. Pfeffer, K., Matsuyama, T., Kundig, T. M., Wakeham, A., Kishihara, K., Shahinian, A., Wiegmann, K., Ohashi, P. S., Kronke, M. & Mak, T. W. (1993) Mice deficient for the 55 kd tumor necrosis factor receptor are resistant to endotoxic shock, yet succumb to L. monocytogenes infection, *Cell.* **73**, 457-67.

207. Flynn, J. L., Goldstein, M. M., Chan, J., Triebold, K. J., Pfeffer, K., Lowenstein, C. J., Schreiber, R., Mak, T. W. & Bloom, B. R. (1995) Tumor necrosis factor-alpha is required in the protective immune response against Mycobacterium tuberculosis in mice, *Immunity.* **2**, 561-72.
208. Theodos, C. M., Povinelli, L., Molina, R., Sherry, B. & Titus, R. G. (1991) Role of tumor necrosis factor in macrophage leishmanicidal activity in vitro and resistance to cutaneous leishmaniasis in vivo, *Infect Immun.* **59**, 2839-42.
209. Liew, F. Y., Parkinson, C., Millott, S., Severn, A. & Carrier, M. (1990) Tumour necrosis factor (TNF alpha) in leishmaniasis. I. TNF alpha mediates host protection against cutaneous leishmaniasis, *Immunology.* **69**, 570-3.
210. Berry, M. A., Hargadon, B., Shelley, M., Parker, D., Shaw, D. E., Green, R. H., Bradding, P., Brightling, C. E., Wardlaw, A. J. & Pavord, I. D. (2006) Evidence of a role of tumor necrosis factor alpha in refractory asthma, *N Engl J Med.* **354**, 697-708.
211. Parameswaran, N. & Patial, S. (2010) Tumor necrosis factor-alpha signaling in macrophages, *Crit Rev Eukaryot Gene Expr.* **20**, 87-103.
212. Lombardo, E., Alvarez-Barrientos, A., Maroto, B., Bosca, L. & Knaus, U. G. (2007) TLR4-mediated survival of macrophages is MyD88 dependent and requires TNF-alpha autocrine signalling, *J Immunol.* **178**, 3731-9.
213. Maini, R. N., Breedveld, F. C., Kalden, J. R., Smolen, J. S., Davis, D., Macfarlane, J. D., Antoni, C., Leeb, B., Elliott, M. J., Woody, J. N., Schaible, T. F. & Feldmann, M. (1998) Therapeutic efficacy of multiple intravenous infusions of anti-tumor necrosis factor alpha monoclonal antibody combined with low-dose weekly methotrexate in rheumatoid arthritis, *Arthritis Rheum.* **41**, 1552-63.
214. Silverman, J. M. & Reiner, N. E. (2011) *Leishmania* exosomes deliver preemptive strikes to create an environment permissive for early infection, *Front Cell Infect Microbiol.* **1**, 26.
215. Silverman, J. M., Chan, S. K., Robinson, D. P., Dwyer, D. M., Nandan, D., Foster, L. J. & Reiner, N. E. (2008) Proteomic analysis of the secretome of *Leishmania donovani*, *Genome Biol.* **9**, R35.
216. Chang, C. H., Curtis, J. D., Maggi, L. B., Jr., Faubert, B., Villarino, A. V., O'Sullivan, D., Huang, S. C., van der Windt, G. J., Blagih, J., Qiu, J., Weber, J. D., Pearce, E. J., Jones, R. G. & Pearce, E. L. (2013) Posttranscriptional control of T cell effector function by aerobic glycolysis, *Cell.* **153**, 1239-51.
217. Caput, D., Beutler, B., Hartog, K., Thayer, R., Brown-Shimer, S. & Cerami, A. (1986) Identification of a common nucleotide sequence in the 3'-untranslated region of mRNA molecules specifying inflammatory mediators, *Proc Natl Acad Sci U S A.* **83**, 1670-4.
218. Chen, C. Y. & Shyu, A. B. (1995) AU-rich elements: characterization and importance in mRNA degradation, *Trends Biochem Sci.* **20**, 465-70.
219. Guhaniyogi, J. & Brewer, G. (2001) Regulation of mRNA stability in mammalian cells, *Gene.* **265**, 11-23.
220. Wu, X. & Brewer, G. (2012) The regulation of mRNA stability in mammalian cells: 2.0, *Gene.* **500**, 10-21.
221. Das, P., Mukherjee, A. & Adak, S. (2021) Glyceraldehyde-3-phosphate dehydrogenase present in extracellular vesicles from *Leishmania major* suppresses host TNF-alpha expression, *J Biol Chem.* **297**, 101198.

Publications

List of publications

1. **Das, P**., Mukherjee, A. & Adak, S. (2021) **Glyceraldehyde-3-phosphate dehydrogenase present in extracellular vesicles from *Leishmania major* suppresses host TNF-alpha expression**, *J Biol Chem.* **297**, 101198.

2. Mukherjee, A., Adhikari, A., **Das, P**., Biswas, S., Mukherjee, S. & Adak, S. (2018**)** **Loss of virulence in NAD(P)H cytochrome b5 oxidoreductase deficient *Leishmania major***, *Biochem Biophys Res Commun.* **503**, 371-377

JBC RESEARCH ARTICLE

Glyceraldehyde-3-phosphate dehydrogenase present in extracellular vesicles from *Leishmania major* suppresses host TNF-alpha expression

Received for publication, August 16, 2021, and in revised form, September 8, 2021 Published, Papers in Press, September 15, 2021,
https://doi.org/10.1016/j.jbc.2021.101198

Priya Das, Aditi Mukherjee, and Subrata Adak*

From the Division of Structural Biology & Bio-informatics, CSIR-Indian Institute of Chemical Biology, Kolkata, India

Edited by Peter Cresswell

Glyceraldehyde-3-phosphate dehydrogenase (GAPDH) fulfills various physiological roles that are unrelated to its glycolytic function. However, to date, the nonglycolytic function of GAPDH in trypanosomal parasites is absent from the literature. Exosomes secreted from *Leishmania*, like entire parasites, were found to have a significant impact on macrophage cell signaling and function, indicating cross talk with the host immune system. In this study, we demonstrate that the *Leishmania* GAPDH (LmGAPDH) protein is highly enriched within the extracellular vesicles (EVs) secreted during infection. To understand the function of LmGAPDH in EVs, we generated control, overexpressed, half-knockout (HKO), and complement cell lines. HKO cells displayed lower virulence compared with control cells when macrophages and BALB/c mice were infected with them, implying a crucial role for LmGAPDH in *Leishmania* infection and disease progression. Furthermore, upon infection of macrophages with HKO mutant *Leishmania* and its EVs, despite no differences in *TNFA* mRNA expression, there was a considerable increase in TNF-α protein expression compared with control, overexpressed, and complement parasites as determined by ELISA, RT-PCR, and immunoblot data. *In vitro* protein translation studies suggest that LmGAPDH-mediated TNF-α suppression occurs in a concentration-dependent manner. Moreover, mRNA binding assays also verified that LmGAPDH binds to the AU-rich 3′-UTR region of *TNFA* mRNA, limiting its production. Together, these findings confirmed that the LmGAPDH contained in EVs inhibits TNF-α expression in macrophages during infection *via* post-transcriptional repression.

Leishmania spp., the organism causing leishmaniasis in humans, divides its life cycle between the sand fly vector and the mammalian host. Earlier researchers revealed that extracellular vesicles (EVs)-based secretion by *Leishmania* is involved in the delivery of proteins into host cells (1, 2). Comparative quantitative proteomics studies unambiguously identified numerous proteins in *Leishmania* EVs (1, 3). *Leishmania* EVs and EV mediate proteins were detected in the cytosolic compartment of infected macrophages, and the incubation of macrophages with EVs selectively regulated the secretion of different cytokines (2, 4). However, the exact functions of parasite-derived EV mediate proteins in host parasite interaction are far from being elucidated.

Earlier, glyceraldehyde-3-phosphate dehydrogenase (GAPDH) has been considered simply as a housekeeping glycolytic enzyme. Recent studies indicate GAPDH as a multifunctional protein displaying numerous physiological roles that are unrelated to its glycolytic function. For example, GAPDH shows phosphotransferase/kinase activity, autophosphorylation, or phosphorylation of other proteins, thus acting as a cellular kinase (5). It can interact with tubulin and catalyzes tubulin polymerization into microtubules (6), assists membrane fusion in a highly plasmenylethanolamine- and cholesterol-specific manner (7) and shows Ca^{2+}-dependent fusogen activity (8). It has been identified as a target protein for nitric oxide (9) and a binding protein for nucleic acids, DNA (10), and nuclear tRNA (11). It has also been identified as a uracil DNA glycosylase (12) and as an Ap4A-binding protein (13), implying that it is involved in DNA replication and repair. GAPDH also acts as a specific mRNA-binding protein interacting with 5′-UTR or 3′-UTR mRNA sequences that are important for translational regulation of gene expression (14). Other known activities of GAPDH are the regulation of heme insertion in hemoproteins and nitrosylation of nuclear proteins (15–17). Furthermore, new and novel studies also indicate that moonlighting GAPDH has a fundamental role in a variety of pathologies including diabetes, age-related neurodegenerative disorders, and tumorigenesis (18, 19).

In some pathogens, GAPDH has been designated as a protein virulence factor (20, 21) owing to its ability to interact with several host proteins (22). Like *Trypanosoma brucei*, two copies of glycosomal GAPDH genes in tandem array and one copy of the cytosolic GAPDH genes have been identified in *Leishmania infantum*, *Leishmania mexicana*, and *Leishmania donovani*. The activity measurement data suggest that GAPDH in *T. brucei* and *L. mexicana* has also been detected in the cytosol (23–25). However, *Leishmania major* and *Leishmania braziliensis* have only two copies of the active form of glycosomal GAPDH and lack the cytosolic GAPDH genes (26, 27). A group of workers demonstrated that the cytosolic GAPDH enzyme in *L. donovani* plays a role in the parasite's ability to

* For correspondence: Subrata Adak, adaks@iicb.res.in.

thrive in visceral organs (28). Although, GAPDHs from *T. brucei*, *Trypanosoma cruzi*, and *L. mexicana* have been purified, crystalized, and biochemically characterized (29–31), nonglycolytic role of GAPDH is still unknown in the trypanosomatid parasites, *Trypanosome* and *Leishmania*.

In this article, we have unraveled a possible nonglycolytic role of GAPDH from *L. major* (LmGAPDH), which is localized in the glycosome as well as in the EVs. To understand the nonglycolytic function of this protein, we have made different types of *Leishmania* cell lines (overexpressed [OE], control [CT], half knockout [HKO], and complement [CM] system for GAPDH). By performing various *in vitro* and *in vivo* experiments with these cell lines, we are trying to bridge between two phenomena: EVs–mediated LmGAPDH secretion during *Leishmania* infection and the regulation of the first line of host defense.

Results

Localization of LmGAPDH in Leishmania *promastigotes*

It is well established that the cytosolic human GAPDH enzymes are targeted to the plasma membrane (21, 32) and the nucleus (33) for showing moonlighting activity. Although both LmGAPDH copies contain the predicted C-terminal glycosomal tri-peptide (PKL) signal sequence, the enzyme may be present in other organelles for displaying nonglycolytic functions. To ascertain whether the mature LmGAPDH protein was localized in any specific organelles other than the glycosome as a native protein, homogenates of *L. major* cells were fractionated by differential centrifugation, glycosomes were isolated from *L. major* promastigotes using Colasante *et al.*'s (34) technique, and *Leishmania*-secreted microvesicles were harvested following the conventional EVs isolation protocol from conditioned medium subjecting to ultracentrifugation with prior incubation of the promastigotes at 37 °C for ∼2 h.

Then, we verified the morphology and size of the EVs *via* atomic force microscopy (AFM) (Fig. 1, *A* and *B*). Two-dimensional (tapping mode topographic and phase AFM) and three-dimensional views confirmed the spherical morphology and size of the vesicles to around 65 ± 5 nm in diameter, which were identical to EVs' previously recognized form (35). To further confirm these data, dynamic light scattering (DLS) analysis was performed. The results obtained from DLS confirmed that the mean diameter of the EVs derived from *Leishmania* was ∼65 nm with high homogeneity (96%) (Fig. 1*C*). Western blot results showed that the LmGAPDH protein band was recovered from both glycosomal and EVs fractions, where the glycosomal PAS domain containing phosphoglycerate kinase and the EVs GP63 protein (as a marker protein) were concentrated (Fig. 1*D*), indicating that the enzyme is localized in both the glycosome and the EV of *Leishmania*. On the other hand, the LmGAPDH protein band was absent in the cytosol, mitochondria, and nucleus fractions, where the cytosolic adenosine kinase, mitochondrial ascorbate peroxidase, and nuclear histone H2B (as a marker protein) were concentrated. Similarly, the GAPDH activity in the crude extract was recovered from both the glycosomal and the EVs fraction, suggesting that the enzyme is almost entirely localized in the glycosome and the EV of *Leishmania* (Fig. 1*E*).

Analysis of EV mediate LmGAPDH in overexpressed, control, half knockout, and complement cells

L. major Gene DB reveals that the LmGAPDH gene has its two identical copies in tandem array. To investigate the nonglycolytic role of LmGAPDH gene in *L. major*, a gene replacement technique was carried out. Since the LmGAPDH is an essential gene for the survival of *Leishmania* parasite, two copies of the gene cannot be deleted. Thus, we knocked out only one of the two copies of the gene, denoted as HKO. We generated LmGAPDH HKO constructs by gene replacement of hygromycin and neomycin selectable markers (Fig. 2*A*). After two rounds of transfection and selection with neomycin and hygromycin drugs, both the alleles of a single copy of LmGAPDH gene in cells had been replaced. To screen the HKO mutants, we first performed a PCR analysis on genomic DNA with primers generated from the 5′- and 3′-flanking regions (Fig. 2*B*); then Western blot analysis with anti-LmGAPDH antibody further confirmed the presence of ∼50% LmGAPDH in the HKO cell line (Fig. 2, *C* and *D*). These results suggested that both alleles of a single copy of LmGAPDH gene had been knocked out in the *L. major* cell line that is resistant to both neomycin and hygromycin drugs. On the other hand, the results of Western blot technique demonstrated higher level of LmGAPDH protein expression (4.5-fold) in OE cells compared with CT, even though the amount of LmGAPDH in CM and CT is equivalent (Fig. 2, *C* and *D*). Next, we investigated whether the level of LmGAPDH was changed in the EVs isolated from HKO and OE cells compared with CT and CM. Western blotting confirmed that the EVs from HKO cells had negligible amount of LmGAPDH protein (Fig. 2, *E* and *F*), whereas the EVs from the OE cell line had expressed an ∼2.3 times higher amount of LmGAPDH compared with CT or CM.

Characteristics of OE, CT, HKO, and CM cells

To investigate whether the growth rate of HKO mutants is similar to CT, CM, or OE promastigotes, microscopically viable cell counting analysis was performed. The growth curve showed that the HKO population had no significant change in the growth rate compared with CT, CM, or OE cells (Fig. 3*A*). Thus, a single copy of GAPDH in HKO expresses sufficient amounts of proteins that maintain glycolytic function of promastigotes for growth. Because *L. major* promastigotes can infect host macrophages, we investigated the interaction of promastigotes with the macrophages. We explored to what extent HKO, CT, CM, and OE cells were endocytosed by the macrophages. The adhering rates of all promastigotes were more or less same after 2 h of incubation period (Fig. 3*B*). HKO promastigotes, on the other hand, internalized at a substantially lower rate than WT, OE, or CM cells after 24 and

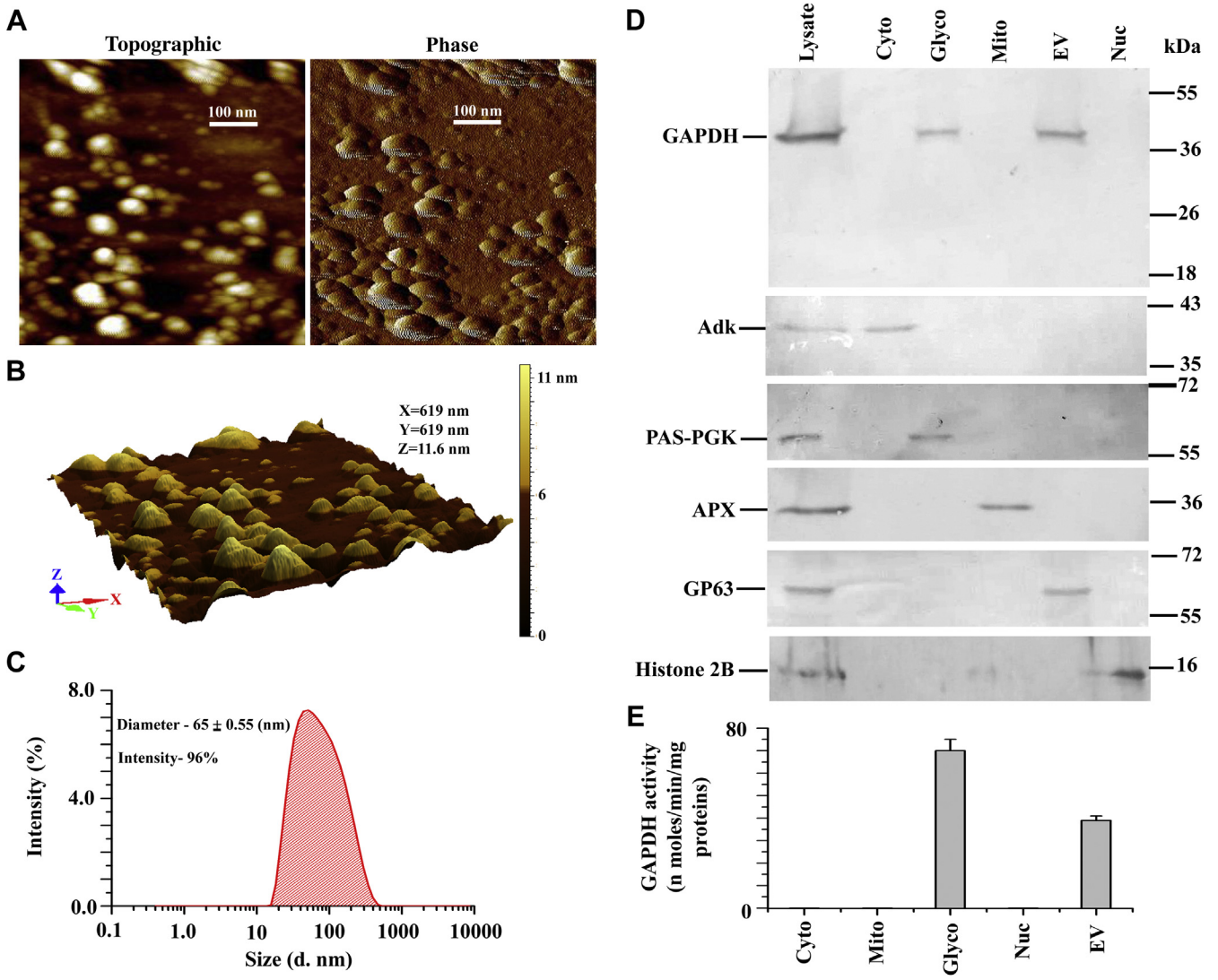

Figure 1. Localization of LmGAPDH. *A*, the shape and size of extracellular vesicles (EVs) extracted from *L. major* were identified through atomic force microscopy (topography and phase mode). *B*, three-D image of same EVs as in *A*. *C*, the average diameter of *Leishmania* EVs was determined by dynamic light scattering. *D*, subcellular localization of LmGAPDH was performed by Western blotting. Lanes: 1, cell lysate; 2, cytosolic; 3, glycosomal; 4, mitochondrial; 5, EVs; and 6, nuclear fraction. Adenosine kinase, PAS domain containing phosphoglycerate kinase, ascorbate peroxidase, GP63, and histone 2B were used in the subcellular fractions as cytosolic, glycosomal, mitochondrial, EVs and nuclear markers, respectively. *E*, the enzymatic activity of LmGAPDH in different subcellular fractions. Cyto, glyco, mito, ev, and nue denote as cytosolic, glycosomal, mitochondrial, EVs, and nuclear fraction, respectively.

48 h of incubation. Most infected macrophages still had parasites 72 h after phagocytosing WT and CM promastigotes, whereas the percentage of parasites in HKO infected macrophages dropped considerably. These results indicate that the HKO parasites were killed more easily inside the macrophages. In addition, the percentage of macrophages infected with OE increased considerably (Fig. 3*C*) compared with CT infection. Similarly, mice infection results suggested that HKO cells could not develop a severe disease, with an earlier onset of footpad necrosis, compared with CT or CM promastigotes (Fig. 3*D*). These results were supported by the OE promastigotes, showing increased virulence in *in vivo* mice model. The result of parasite burden during 6 weeks post infection indicated that HKO parasites, compared with CT or CM, had about 2.6-fold less parasite burden (Fig. 3*D* inset) in 1 mg of footpad tissue. These findings indicated that the GAPDH gene in parasites plays an important role in macrophage infection and disease development in mice.

Deletion of single copy of LmGAPDH gene leads to changed expression of TNF-α in host macrophage

TNF-α, a proinflammatory cytokine, appears to have a crucial role in the regulation of infection. GAPDH has been found to influence inflammatory TNF-α and immunological responses by modulating macrophage activity (36). TNF-α expression in OE, CT, CM, and HKO infected macrophages was determined by quantitative real-time PCR assay (Fig. 4*A*), ELISA (Fig. 4*B*), and Western blot analysis (Fig. 4, *C* and *D*). Quantitative real-time PCR assay showed that the TNF-α mRNA expression in the HKO infected macrophage was unaltered compared with CT, OE, and CM infected cells (Fig. 4*A*)

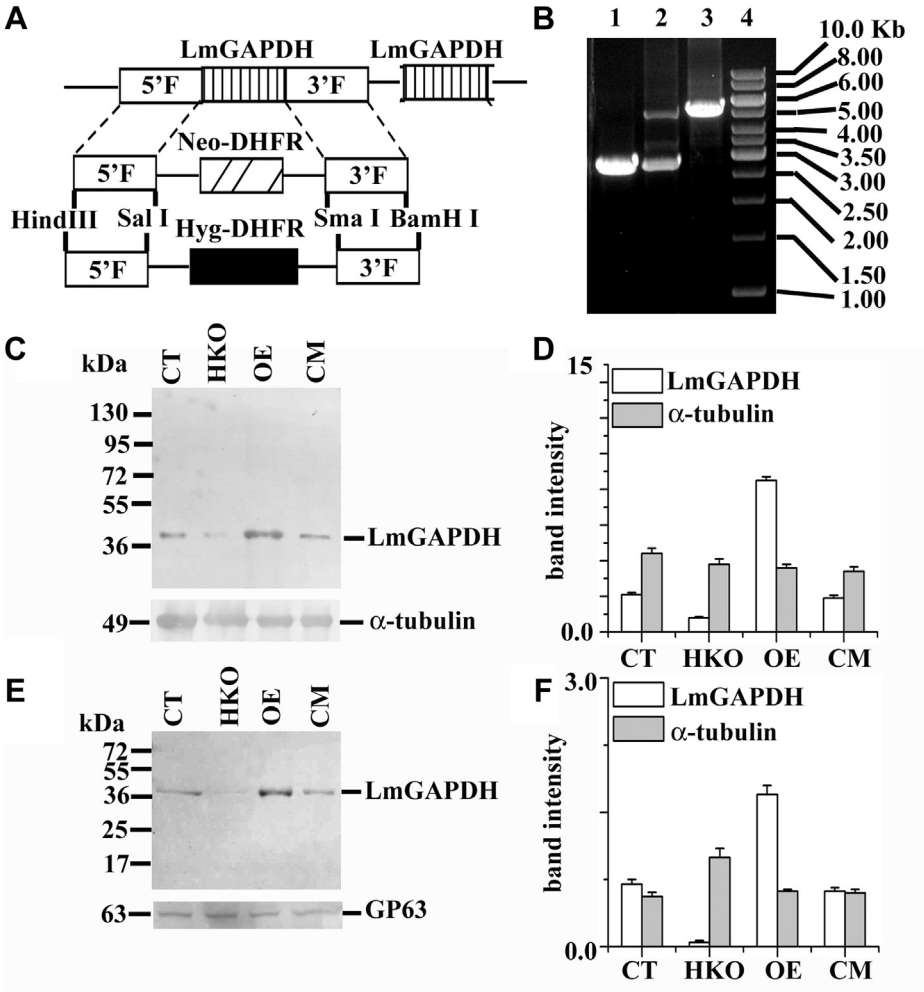

Figure 2. Targeted gene replacement of single copy of LmGAPDH gene. *A*, schematic representation of the LmGAPDH locus and the plasmid constructs used for gene replacement. DHFR denotes dihydrofolate reductase. *B*, agarose gel analysis of PCR-amplified products of LmGAPDH gene. Lane 4 shows the molecular mass marker, lanes 1, 2, and 3 correspond to PCR with genomic DNA from CT, +/− allele, and HKO mutants, respectively, with external (5′ and 3′ flanking region) primers to the LmGAPDH gene. The expected sizes of the LmGAPDH, NEO, and HYG gene PCR product are 2.75, 5.3, and 5.7 kb, respectively. *C*, *L. major* lysate was used for Western blotting. Western blot results using rabbit anti-LmGAPDH and mouse anti-tubulin antibody are shown. *D*, bar diagram depicted as the percentage of band intensities in *C*. *E*, *L. major* extracellular vesicles were used for Western blotting. Western blot results using rabbit anti-LmGAPDH and mouse anti-GP63 antibody are shown. *F*, bar diagram denoted as the percentage of band intensities in *E*. Band intensity was quantified by ImageJ software (NIH). OE, CT, CM, and HKO denote overexpressed, control, complement, and half knockout cell lines.

up to 72 h infection period. Conversely, ELISA data suggested that the HKO infected macrophage cells produced a higher amount of TNF-α (∼3-fold) expression (Fig. 4*B*) compared with CT and CM cells. As expected, lipopolysaccharide (LPS) (1 μg/ml) induced both mRNA and protein level of TNF-α expression in macrophages. To further confirm these data, Western blot analysis was performed (Fig. 4, *C* and *D*), and the results we got were almost similar to the ELISA data. Altogether, these results suggest that the LmGAPDH regulates the host TNF-α expression at the translation level.

To check the effect of the LmGAPDH-deficient EVs in the host TNF-α expression, we measured the TNF-α expression in EVs (from OE, CT, CM, or HKO) treated macrophages by ELISA (Fig. 5, *A* and *B*) and Western blot (Fig. 5, *C*–*F*). ELISA data suggested that the EVs from HKO treated uninduced macrophage showed very little change in TNF-α expression compared with the EVs from CT or CM treated cells (Fig. 5*A*) up to 48 h incubation periods. In case of 0.1 μg/ml LPS preinduced macrophage, the EVs from OE, CT, or CM cells suppressed the TNF-α expression, whereas the EVs from HKO cells fail to represses TNF-α expression (Fig. 5*B*). To further confirm these data, Western blot analysis was performed (Fig. 5, *C*–*F*), and the outcomes were nearly identical to the ELISA data. Altogether, these results suggest that the GAPDH in parasite's EVs may regulate TNF-α expression when they interacted with the host macrophage.

It is well defined that EV has a lot of components including LmGAPDH; thus, we checked whether recombinant LmGAPDH itself could block the host TNF-α expression. To ensure recombinant LmGAPDH transfection within the macrophage, the DAPI-stained LmGAPDH-transfected macrophages were costained with rabbit anti-LmGAPDH as primary antibody and Alexa Fluor 488–conjugated anti-rabbit secondary antibody (Fig. 6, *A* and *B*). Figure 6*B* confirmed the presence of recombinant LmGAPDH in the cytosol. Western

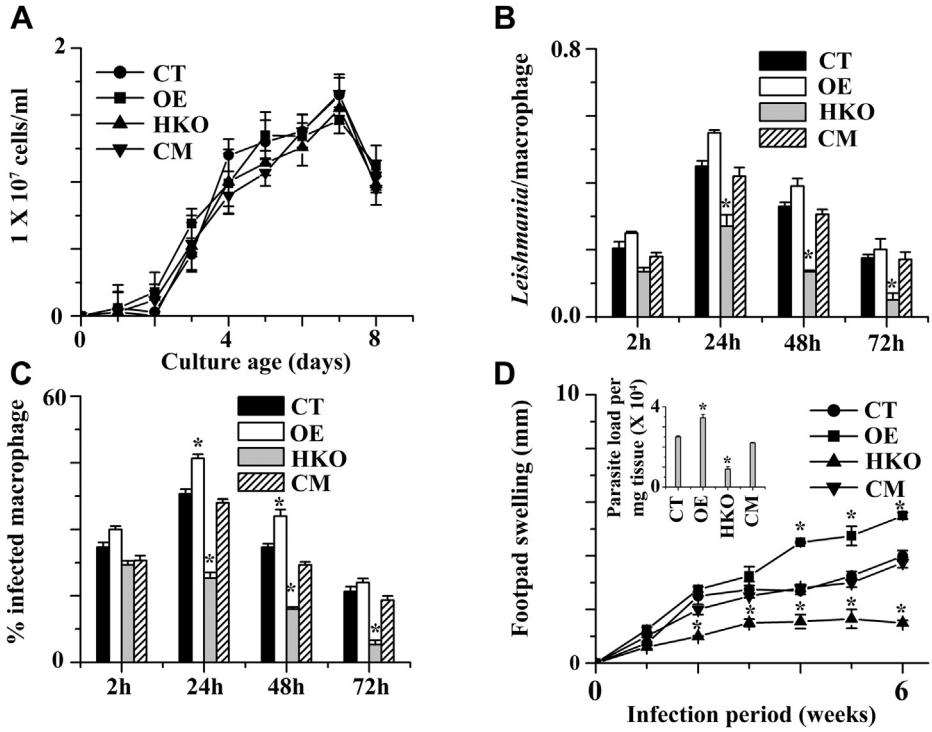

Figure 3. Functional characterization of LmGAPDH variant *L. major* cells. *A*, the growth curves of CT, OE, CM, and HKO cells. *B*, the percentage of macrophages infected with CT, OE, CM, and HKO parasites. For each time point, 200 macrophages were counted. *C*, the number of *Leishmania* within each infected macrophage was counted. For each time point and cell type, 200 infected macrophages were analyzed. *D*, infection in BALB/c mice. Footpad swelling of CT, OE, CM, and HKO was observed for the three groups (15 mice/group). *D*, *inset*, parasite burden in the footpad after 6 weeks post infection in CT, OE, CM, and HKO cells. *Statistically significant value of less than 0.05. OE, CT, CM, and HKO denote overexpressed, control, complement, and half knockout cell lines.

blot analysis confirmed that LmGAPDH-transfected RAW 264.7 cells showed lower level of TNF-α expression in the presence of LPS (Fig. 6, *C* and *D*) compared with bovine serum albumin (BSA)-transfected RAW 264.7 cells. These results directly proved that LmGAPDH is the actual factor for the suppression of TNF-α expression. Then, we investigated *in vitro* protein translation of TNF-α in the presence or absence of purified LmGAPDH (Fig. 6, *E* and *F*). The gel autoradiography analysis showed that the protein synthesis band pattern in all lanes is similar (Fig. 6*E*), indicating that *in vitro* protein translation occurred in the presence or absence of purified LmGAPDH. After immunoprecipitation with TNF-α monoclonal antibody, the gel showed the TNF-α expression is inversely proportional to the LmGAPDH concentration (Fig. 6, *F* and *G*). In contrast to LmGAPDH, BSA protein could not suppress *in vitro* TNF-α protein translation. GAPDH also acts as a specific mRNA-binding protein that interacts with 5′ or 3′-UTR regions of mRNA regulating gene expression positively or negatively at the posttranscriptional level (14). Our data already indicate that LmGAPDH is responsible for the decrease in TNF-α protein expression. To further demonstrate that this decrease in cytokine production is due to posttranscriptional repression, we examined the binding of 5′-UTR or 3′-UTR of TNF-α mRNA by LmGAPDH (Fig. 6*H*) using an RNA electrophoretic mobility shift assay (REMSA). A labeled oligonucleotide corresponding to the 3′-UTR of TNF-α mRNA produced a retarded band with LmGAPDH that may be an inactive form of mRNA–LmGAPDH complexes (Fig. 6*H*). This retarded band could be competed with a 200-fold molar excess of the unlabeled homologous oligonucleotide. When anti-LmGAPDH antibody was added to the REMSA mixture, the 3′-UTR of TNF-α mRNA–LmGAPDH–anti-LmGAPDH antibody complex moved more slowly down the REMSA gel, indicating that the complex was more likely to be super shifted. In comparison with 3′-UTR of TNF-α mRNA, the shifted band was not observed in case of 5′-UTR of TNF-α mRNA oligonucleotide. Figure 6*I* showed that the binding of 3′-UTR of TNF-α mRNA with LmGAPDH is concentration dependent. Conversely, 5′-UTR of TNF-α mRNA could not form complex with LmGAPDH at higher concentrations also (Fig. 6*J*). These findings suggest that LmGAPDH binds with the 3′-UTR of TNF-α mRNA, preventing the transcript from being translated and hence decreasing TNF-α cytokine production. To identify the interaction site of LmGAPDH with 3′-UTR of TNF-α mRNA, we examined the competitive assay with cofactor NAD^+/NADH or ATP in 3′-UTR–LmGAPDH complexes (Fig. 6*K*) by RNA electrophoretic mobility shift assay. Increasing concentrations of NAD^+, NADH, and ATP decreased GAPDH binding ability toward 3′-UTR. These results indicate that cofactor NAD^+-interacting site of LmGAPDH is responsible for 3′-UTR binding.

Discussion

Recently several studies demonstrated that GAPDH is translocated to different subcellular organelles for exhibiting

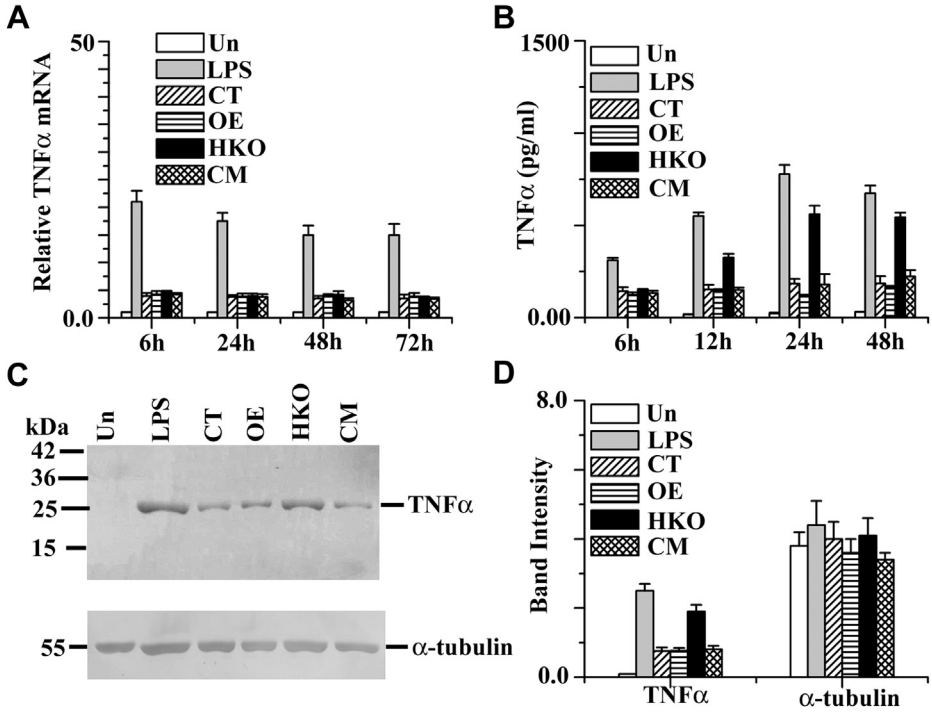

Figure 4. mRNA and protein expression of TNF-α production in stationary-phase *Leishmania* promastigote-infected macrophage. *A*, measurement of gene transcript abundance was analyzed by using quantitative real-time PCR as described in Experimental procedures. All data were normalized using beta-actin as the endogenous control. *B*, levels of TNF-α production were measured by ELISA in the cell culture supernatants after infection. *C*, TNF-α protein levels were measured by Western blot analysis of protein lysates from RAW264.7 cells. Alpha tubulin was used as loading control. *D*, densitometric analysis of all bands was done using ImageJ software (from NIH). All data are representative of three independent experiments. Error bars represent the SD from three independent experiments. "Un" denotes uninfected macrophage (-*Leishmania*). LPS denotes induced macrophage with LPS (1 μg/ml). OE, CT, CM, and HKO denote overexpressed, control, complement, and half knockout cell lines.

nonglycolytic function (18). Hence a precise knowledge about the localization of LmGAPDH will aid in predicting the potential role of this protein and enabling us to correlate its functions with those of other proteins that may be engaged in a different cellular signaling pathway for parasite survival. It is well known that the glycosomal and the cytosolic GAPDH play a major role in glycolytic function in trypanosomatid. Here we have shown for the first time by using various molecular approaches (including Western blot analysis, and activity measurement of protein) that the localization of LmGAPDH is in the glycosomal fraction as well as in the EV fraction, similar to where the leishmanial GP63 protein is found (37). Hence, EV mediate LmGAPDH is likely to affect the host defense system directly. The existence of an EV mediate LmGAPDH raises the question how this protein is translocated to EVs. LmGAPDH lacks an N-terminal secretion signal peptide and is thus thought to be secreted *via* nonconventional mechanisms. A similar type of result was found in proteomic study on *Leishmania*, where majority of the temperature shift–induced secreted proteins lacked the N-terminal signal peptide (36).

During the past two decades, several secretory virulent proteins have been identified in *Leishmania* EVs, including GP63 (37, 38), heat shock protein 100 (39), proteophosphoglycan pPPG2 (40), acid phosphatase (41), heat shock protein 70 (42), EF1alpha (43), and fructose-1,6-bisphosphate aldolase (44). In addition, a group of workers have demonstrated that leishmanial EVs from the extracellular environment is taken up by naive host cells, which selectively induced IL8 secretion (1). These data suggest that *Leishmania* use EVs to deliver effector molecules to host cells as well as to communicate with the host cellular environment. In this study, we describe how *Leishmania* parasite influences host TNF-α protein expression through a mechanism not previously observed in the macrophage. Here, the main finding is that the EVs-derived LmGAPDH from *Leishmania* promastigotes selectively downregulate host TNF-α production suppressing the host immune system. Furthermore, our data on *Leishmania*-infected macrophages and mouse models also indicate that LmGAPDH is essential for the survival of *L. major* parasites within macrophage and virulence in mice.

EVs released from promastigotes have freedom to interact with host cells, by receptor binding, fusion with the plasma membrane, or through endocytosis. So LmGAPDH may be active in host cells on the surface of the host plasma membrane, in the cytosol, or within the host phagolysosome. LmGAPDH-transfected macrophage showed a lower level of TNF-α expression in the presence of LPS (lane 5 in Fig. 6*C*) compared with BSA-transfected RAW 264.7 cells (lane 7 in Fig. 6*C*), but naked LmGAPDH cannot suppress TNF-α expression in LPS-treated macrophages (lane 4 in Fig. 6*C*). These results suggest that LmGAPDH has to penetrate the host membrane for blocking TNF-α expression. The general

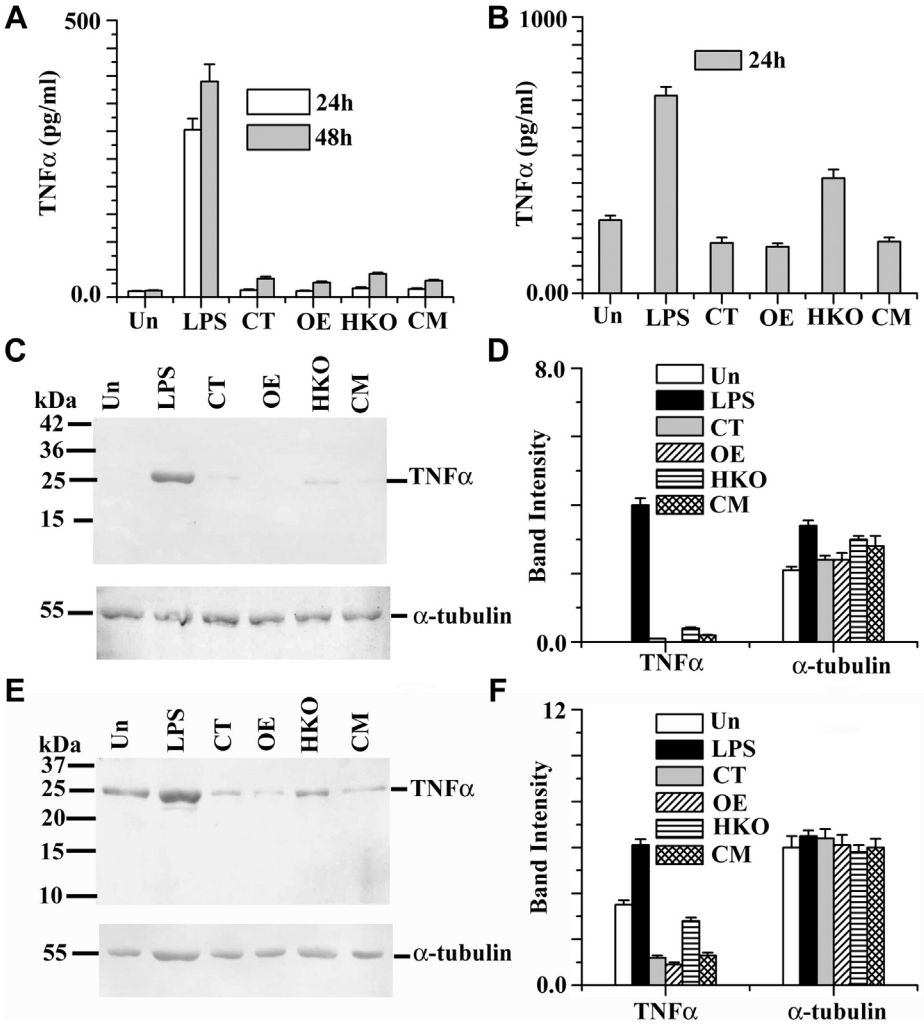

Figure 5. TNF-α expression in the extracellular vesicles–treated uninduced and induced macrophages. *A*, levels of TNF-α secretion were measured by ELISA in the cell culture supernatants of extracellular vesicles–treated uninduced macrophage. *B*, levels of TNF-α secretion were measured by ELISA in the cell culture supernatants of extracellular vesicles-treated 0.1 μg/ml LPS preinduced macrophage. *C*, TNF-α protein levels were measured by Western blot analysis of protein lysates from extracellular vesicles–treated uninduced RAW264.7 cells. Alpha tubulin was used as loading control. *D*, densitometric analysis of all bands of C was done using ImageJ software (from NIH). *E*, TNF-α protein levels were measured by Western blot analysis in extracellular vesicles–treated 0.1 μg/ml LPS preinduced RAW264.7 cells. Alpha tubulin was used as loading control. *F*, densitometric analysis of all bands of *E* was done using ImageJ software (from NIH). All data are representative of three independent experiments. Error bars represent the SD from three independent experiments. "Un" denotes macrophage lysate without extracellular vesicles treatment. LPS denotes LPS-induced macrophage (1 μg/ml). OE, CT, CM, and HKO denote overexpressed, control, complement, and half knockout cell lines.

concept is that the virulence factors secreted by most of intracellular pathogens target the host's cytosolic molecules for remodeling host cell function (45, 46). Now one question that immediately arises is which step is apparently involved in TNF-α suppression. First, *Leishmania*-derived GAPDH may either interact with a host transcription factor or bind to the promoter region of TNF-α gene and as a result suppress host TNF-α at the level of transcription. The second possibility is that the regulation of TNF-α expression might be affected at the posttranscriptional level. Like LPS, RT-PCR results suggest that *Leishmania*-infected macrophage produces a higher amount of TNF-α mRNA compared with uninfected cells. The RT-PCR results from the comparative studies among various concentrations of GAPDH containing *Leishmania* (OE, CT, HKO, CM)-infected macrophages suggest that the transcription of TNF-α mRNA from host DNA did not depend on LmGAPDH concentration. So we can rule out the first possibility. On the other hand, ELISA assay and immunoblot data suggest that the protein expression of TNF-α in infected host cells is inversely proportional to the LmGAPDH concentration. Despite showing no difference in TNF-α mRNA, however, infected host cells show a significant change in TNF-α protein expression. These results immediately demonstrated the relevance of posttranscriptional repression of TNF-α mRNA. Recently, it was shown that GAPDH could bind with AU-rich elements of the untranslated region of mRNA that is responsible for posttranscriptional regulation of IFN-γ (47) and TNF-α expression, inhibiting translation and limiting IFN-γ and TNF-α cytokine production (48–50). Our mRNA (AU-rich elements of untranslated region)-binding assay suggests that LmGAPDH can bind with AU-rich elements of 3′ UTR of TNF-α.

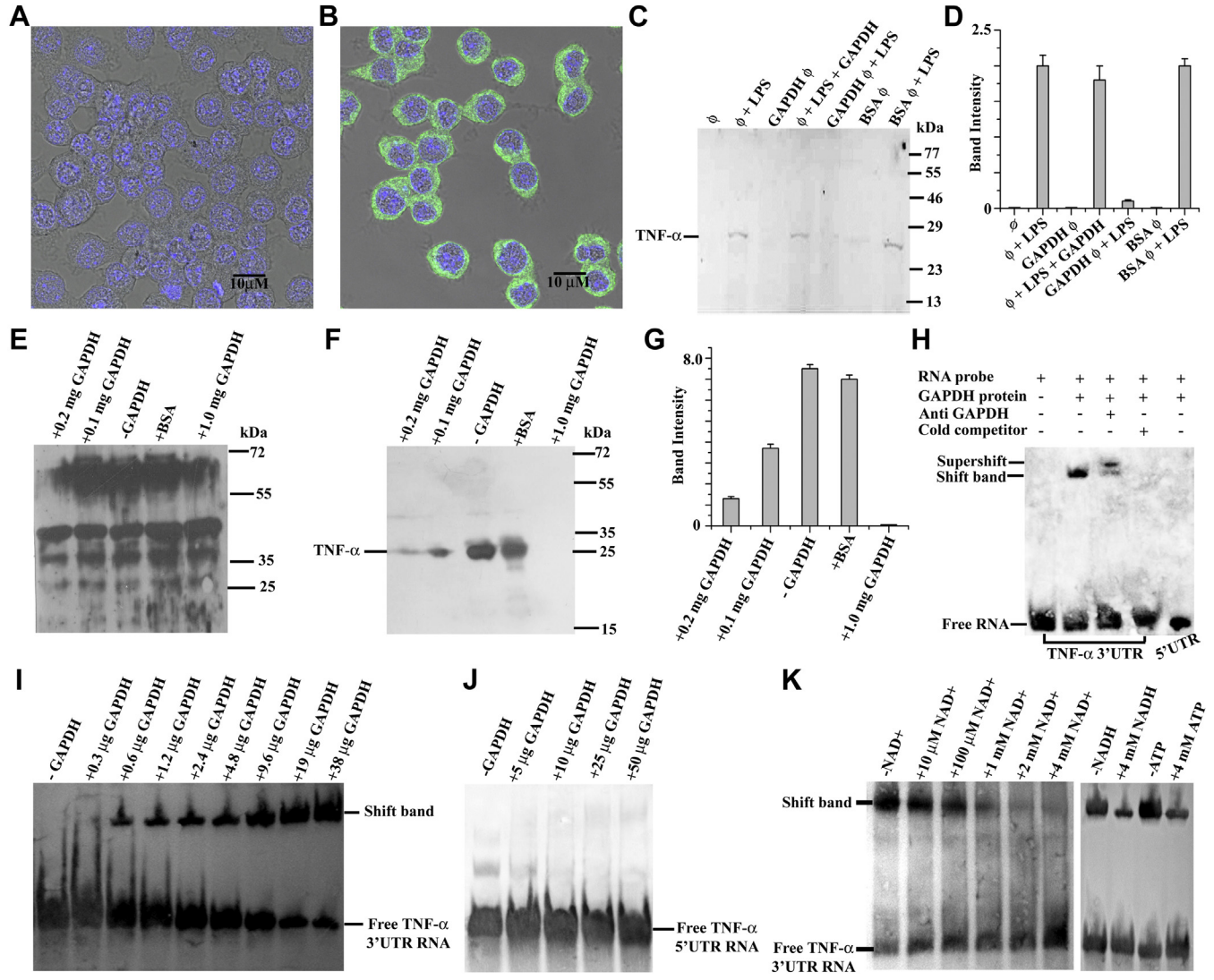

Figure 6. Quantitation of TNF-α repression by purified LmGAPDH and its binding to the 3′ UTR region of TNF-α mRNA. Visualization of normal macrophage (*A*) and LmGAPDH-transfected macrophage (*B*) by confocal microscope in bright field background. Nucleus was stained with DAPI (*blue*). Anti-rabbit LmGAPDH antibody and Alexa Fluor 488–conjugated anti-rabbit secondary antibody (Thermo Scientific) were used for visualization of LmGAPDH. *C*, the levels of TNF-α protein expression were measured from LmGAPDH-transfected RAW264.7 cells in presence of LPS. Φ, GAPDH φ, and BSA φ denote macrophage, LmGAPDH-transfected macrophage, and BSA-transfected macrophage cells. *D*, densitometric analysis of all bands of C was done using ImageJ software (from NIH). *E*, the autoradiographic image of *in vitro* general translation pattern. *F*, the autoradiographic image of *in vitro* TNF-α translation with respect to various concentrations of LmGAPDH. *G*, densitometric analysis of all bands of *F* was done using ImageJ software (from NIH). *H*, the REMSA measurement for LmGAPDH binding to the 3′UTR region of TNF-α mRNA. *I*, the RNA electrophoretic mobility shift assay image for LmGAPDH–3′UTR TNF-α mRNA complexes with respect to various concentrations of LmGAPDH. *J*, the RNA electrophoretic mobility shift assay image for the binding pattern of 5′UTR TNF-α mRNA with various concentrations of LmGAPDH. *K*, inhibition of 3′UTR TNF-α mRNA binding of LmGAPDH by NAD^+, NADH, and ATP.

This raises the question as to which region of LmGAPDH is implicated in binding to AU-rich elements of 3′ UTR of TNF-α. It is known that incubation of GAPDH with NAD+ decreases its RNA-binding activity (14). Our competition studies suggest that NAD+, NADH, and ATP were able to diminish the specific 3′ UTR binding of LmGAPDH indicating that the dinucleotide-binding region in the Rossmann fold of LmGAPDH might serve as a 3′ UTR–binding domain. Our data predict that the Rossmann fold of LmGAPDH might be reciprocally regulated between its 3′ UTR binding (inactive in glycolysis) and NAD+ binding (active in glycolysis) states within the macrophage. This mechanism would favor glycolytic activity of LmGAPDH in the parasite glycosome (where the concentration of NAD+ is high). Conversely, LmGAPDH may bind host TNF-α mRNA during *Leishmania* infection due to metabolic reprogramming of *Leishmania*-infected human macrophage, which results in increased oxidative phosphorylation relative to glycolysis and to lower concentrations of NAD+/NADH (51).

How do the LmGAPDH–TNF-α mRNA complexes inhibit translation of the transcript and limiting TNF-α production? *In vitro* protein translation results suggest that the protein expression of TNF-α decreases with increasing LmGAPDH concentration. On the other hand, BSA fails to repress *in vitro*

TNF-α protein translation. These results confirm that the LmGAPDH–TNF-α mRNA complexes inhibit translation of TNF-α expression.

In order to explain the possible mechanism for the suppression of TNF-α in *Leishmania*-infected macrophage cells, we propose a mechanism (shown schematically in Fig. 7) based on a novel virulence function of LmGAPDH contained in EV that is translocated from parasite to host macrophage during infection. Our results show for the first time that the glycolytic enzyme LmGAPDH posttranscriptionally regulates macrophage proinflammatory function by binding to the AU-rich region in the 3′ UTR of TNF-α mRNA and reducing protein translation and thereby modulates host immune response. Thus, targeting LmGAPDH gene present in EV could be a potential arena for medication development in the near future in the fight against leishmaniasis.

Experimental procedures

Reagents

L. major (strain 5ASKH) was procured from the *Leishmania* strain bank of our Institute. All reagents and materials were purchased from Sigma or sources reported previously (52–54).

Ethics statement

All BALB/c mice and rabbits were obtained from and maintained in our institutional animal facility (Kolkata, India). The research project was approved by the IICB Animal Ethical Committee (Registration No.147/1999, CPCSEA) and registered with the Committee for the Purpose of Control and Supervision on Experiments on Animals (CPCSEA), Government of India. The BALB/c mice and rabbits were handled according to their guidelines.

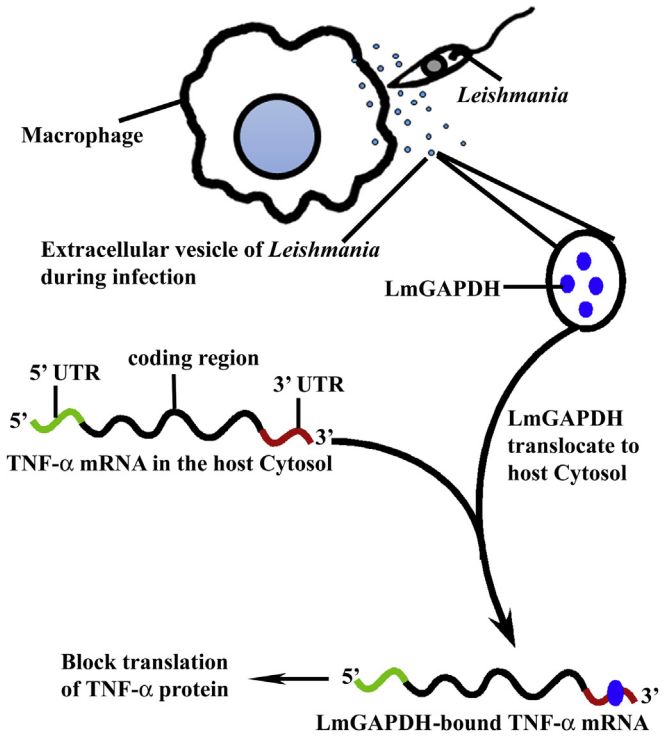

Figure 7. A possible schematic diagram for a novel virulence function of LmGAPDH contained in extracellular vesicle.

Parasite culture

L. major wildtype parasites were routinely cultured at 22 °C in M199 medium (Invitrogen) supplemented with 40 mM Hepes (pH 7.4, Amresco), 200 μM adenine (Sigma), 1% penicillin–streptomycin (v/v), 50 μg/ml gentamycin (Abott), and 10% heat-inactivated fetal bovine serum (Invitrogen).

Macrophage culture

The murine macrophage cell line RAW 264.7 maintained in RPMI-1640 medium (Gibco) containing 10% heat-inactivated fetal bovine serum at 37 °C in a humidified atmosphere containing 5% CO_2 was routinely passaged using a cell scraper and replated in tissue culture flasks at a ratio of 1:6 when they reached ∼80% confluence.

Genomic DNA isolation from L. major

Genomic DNA was isolated from *L. major* logarithmic phase promastigotes by using Qiagen genomic DNA isolation kit at room temperature (25 °C). The concentration was 25 ng/μl.

Cloning of LmGAPDH

Using the forward primer 5′- AAAACATATGATGG CTCCTATCAAGGTCGG-3′ and reverse primer 5′-AAAA GGATCCCTACATCTTGGCGCTCGCAG-3′, the entire ORF of the GAPDH (accession no: Lmjf.30.2970) was amplified to get a 1083-bp fragment that was digested and cloned within the pET15B vector in NdeI/BamHI restriction sites. DNA sequencing was performed to confirm the ORF.

Expression and purification of LmGAPDH

Recombinant pET15B/LmGAPDH were transformed into *Escherichia coli* BL21(DE3) and were grown overnight in 100 ml of Luria–Bertani broth containing 100 μg/ml ampicillin at 37 °C shaking. The overnight grown culture was then inoculated in 1 L of terrific broth. When the culture reached an absorbance of around 0.8 to 1.0 at 600 nm, 0.25 mM isopropyl β-D-1-thiogalactopyranoside was added and bacteria were further grown at 28 °C for around 18 h. Cells were then harvested by centrifugation at 6000*g* for 10 min and washed two times with 1× PBS. Purification of the recombinant LmGAPDH was achieved by a chromatographic step, which used nickel–nitrilotriacetic acid–agarose. The protein compositions of samples obtained from the various purification steps are shown in Figure 8*A*. As expected, purification yielded a single protein band of approximately 39 kDa. No other protein band could be detected in the gel stained with Coomassie brilliant blue.

Production of polyclonal antibodies against LmGAPDH

Polyclonal antibodies against the purified recombinant LmGAPDH (20 μg) were raised by subcutaneous injection in

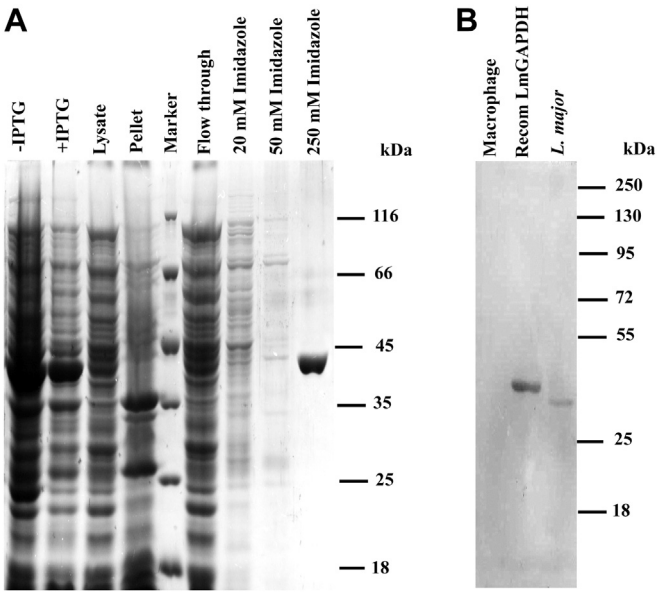

Figure 8. Measurement of specificity of polyclonal anti-LmGAPDH antibodies against LmGAPDH. *A*, SDS–PAGE during recombinant LmGAPDH purification. *B*, Western blot for macrophage cell lysate and *L. major* cell lysate by using polyclonal anti-LmGAPDH antibodies.

6-month-old female rabbit using Freund's complete adjuvant. This was followed by three booster doses of recombinant LmGAPDH (15 μg) with incomplete adjuvant at 2-week intervals. The rabbit were bled 2 weeks after the last booster, and sera were collected and used for Western blot analysis (Fig. 8*B*).

Enzyme assay using UV–visible spectroscopy

LmGAPDH activity was measured spectrophotometrically at 25 °C using Shimadzu UV-2550 spectrophotometer by monitoring NADH generation at 340 nm wavelength. The assay mixture was composed of 40 mM Tris-HCl buffer (pH 7.5), 50 mM K_2PO_4, 0.15 mM NAD^+, and 2.5 mM glyceraldehyde 3-phosphate. After incubating in a 1.0-ml cuvette at 25 °C for 5 min to achieve temperature equilibrium and establish blank values, the reaction was initiated with the addition of enzyme. Absorbance from 0 to 3 min was recorded.

Construction of overexpression system for LmGAPDH in Leishmania

Primers 5′-AAAACCCGGGATGGCTCCTATCAAGG TCGG-3′ (forward) and 5′-AAAAGGATCCCTACATCTTGG CGCTCGCAG-3′ (reverse) were used to amplify the ORF of *L. major* GAPDH gene by PCR. The amplified portion was then cloned into the SmaI/BamHI site of pXG-B2863 vector, which was transfected in *L. major* by electroporation (55). Overexpressed cells were maintained at 200 μg/ml neomycin.

Preparation of control cell lines

Only pXG-B2863 vector was transfected in *L. major* by electroporation. Control cells were maintained at 200 μg/ml neomycin.

Generation of half knockout strain for LmGAPDH alleles

Modified pXG-neo and pXG-hyg vectors were used to generate the HKO constructs of LmGAPDH gene. Primers 5′-AAAAAAGCTTAGCTGACCGGCATGTCC-3′ and 5′-AAAAGTCGACCGACCTTGATAGGAGCC-3′ were used for amplifying 5′ flank, and primers 5′-AAAACCC GGGTATGATAGCAGCGCAGCTG-3′ and 5′-AAAAGGAT CCCTGCCTCATTGTGCATGTGC-3′ were used for amplifying 3′ flank of the gene. The 5′F and 3′F DNA fragments were cloned on either side (at HindIII/SalI and SmaI/BamHI site) of the neomycin and hygromycin genes of pXG-neo and pXG-hyg vectors, respectively. Both constructs were then digested with HindIII and BamHI to get linear fragments of gene deletion constructs LmGAPDH::NEO and LmGAPDH::HYG and were transfected into *L. major* sequentially as described (56). The knock out strain was cultured in the presence of 50 μg/ml neomycin and 100 μg/ml hygromycin drug.

Complementation of LmGAPDH in null mutants

To restore LmGAPDH in the HKO parasites, LmGAPDH ORF was PCR amplified using an LmGAPDH-containing plasmid as template and the following forward primer 5′-AAAAGGATCCATGGCTCCTATCAAGGTCGG-3′ and reverse primer 5′-AAAAGGATCCCTACATCTTGGCGCTC GCAG-3. The amplified product was cloned at the BamHI site of pXG-PHLEO vector, and 10 μg of the pXG-PHLEO-LmGAPDH was transfected into the HKO promastigotes. Transfected promastigotes were selected with minimal doses of phleomycin (5 μg/ml) and finally were maintained in the presence of 60 μg/ml neomycin, 100 μg/ml hygromycin, and 10 μg/ml phleomycin drug.

Isolation of extracellular vesicles from CT, OE, HKO, and CM cell lines

For all EVs-related experiments, EVs-depleted fetal bovine serum (FBS) was used. EVs-depleted FBS was prepared by ultracentrifugation of the FBS used at 110,000*g* for 5 h. For EV isolation, cells were grown in media made from EVs-depleted FBS. The cell culture having 2×10^8 cells was taken and then centrifuged first at 300*g* for 10 min, then at 2000*g* for 15 min, followed by centrifugation at 10,000*g* for 30 min. All centrifugations were done at 4 °C. The supernatant was then filtered through a 0.22-μm filter unit. This supernatant was overlaid on a 30% sucrose cushion and then centrifuged at 100,000*g* for 90 min at 4 °C. After centrifugation, the supernatant just above the sucrose cushion was discarded leaving behind a narrow layer of medium with EVs at the interface. EVs were resuspended with 1× PBS (filtered) and again centrifuged at 100,000*g* for 90 min at 4 °C. The pellet was used as the EVs.

Isolation of glycosomal fractions

Glycosome was isolated from *L. major* promastigotes using Colasante *et al.*'s (34) technique with slight modifications. *L. major* promastigotes were harvested by centrifugation for 10 min at 2000*g* and were washed once in 10 ml of wash buffer (25 mM Tris, 1 mM EDTA, 1 mM DTT, 250 mM sucrose, pH

7.8). After centrifugation, the cell pellet was resuspended in 2 ml homogenization medium (250 mM sucrose, 1 mM EDTA, 0.1% (v/v) ethanol, 5 mM MOPS, pH 7.2) containing protease inhibitor (complete EDTA-free, Roche Applied Science) and was lysed using syringe (needle gauge-0.30 × 12.5 mm). Cell lysis was confirmed by light microscopy. The cell lysate was centrifuged sequentially for 5 min each at 100*g* and 3000*g* to remove cell debri and cell nuclei. The resulting supernatant was centrifuged at 17,000*g* for 15 min to obtain glycosomal-enriched pellet. This pellet was resuspended in 1.0 ml homogenizing buffer and was loaded on top of a 24-ml linear 20% to 40% (v/v) optiprep gradient (Sigma), mounted on 50% 2.5 ml optiprep cushion and centrifuged at 170,000*g* for 1 h. Nine fractions (1.0 ml each) were collected from the bottom of the tube. They were centrifuged at 30,000*g* to obtain the pellet. The pellet was resuspended in homogenizing buffer and again centrifuged at 30,000*g* to obtain the purified glycosomal pellet. The purity of the fraction was checked by Western blotting using the glycosome-specific rabbit LmPAS-PGK antibody (1:50).

Subcellular fractionation

Subcellular fractionation was performed to isolate mitochondria, nuclei, and cytosolic fractions using the mitochondria isolation kit (Qiagen). EVs and glycosome were isolated by the method described above. The purity of each fraction was checked by Western blot analysis with organelle-specific marker antibodies. The primary antibodies used were as follows: rabbit anti-(*L. major*) GAPDH antibody (1:100), rabbit anti-(*L. major*) PAS-PGK antibody (1:50), rabbit anti-(*L. major*) ascorbate peroxidase (1:50), rabbit anti-(*L. donovani*)-adenosine kinase (1:50), rabbit anti-goat histone 2B antibody (1:2000), and mice anti-(*L. donovani*) GP63 antibody (1:200). The alkaline phosphatase–conjugated anti-rabbit secondary antibody (Sigma) was used at a dilution 1:15,000.

In vitro *promastigote growth profile analysis*

A total of 10^6 mid-log phase cells were inoculated in 10 ml of M199 medium supplemented with 10% FBS. Growth rates were measured at a 24-h interval by counting cell number in an improved Neubauer chamber (hemocytometer) for eight consecutive days. Experiments were done in triplicate for each cell type.

In vitro *macrophage infection*

Stationary phase CT, OE, CM, and KO promastigotes were used to infect cultures of the adherent murine macrophage cell line RAW264.7 on glass cover slips (22 mm; 5×10^5 macrophages/cover slip) in 0.5 ml of RPMI 1640/10% FBS mixture at a parasite to cell ratio of 10:1. Following the incubation, unphagocytosed parasites were removed by washing with medium, and cells were resuspended in RPMI 1640/10% FCS mixture at 37 °C. A 2-h incubation period was used for the determination of parasite entry. Cultures were transferred to a CO_2 incubator at 37 °C for an infection period of 24, 48, and 72 h. Cells were then fixed in methanol and stained with propidium iodide. Cells were visualized and quantified using Olympus IX81 microscope.

Infection in mice

Female BALB/c mice 6 to 7 weeks old were infected subcutaneously with 5×10^6 stationary-phase promastigotes in their left hind footpads (eight mice per group). Disease progression was monitored by daily caliper measurement of footpad swelling. Parasite loads in footpad of mice containing WT, OE, CM, and HKO parasites were determined by limiting dilution assay with slight modification. Footpad tissue were sequentially immersed in 70% ethanol and sterile water before homogenization of weighed tissue in M199 medium supplemented with gentamycin and penicillin–streptomycin containing 10% heat-inactivated FBS. Each tissue homogenate was serially diluted in the same medium in a 96-well flat-bottomed tissue culture plate. The number of viable parasites per milligram of tissue was determined from the highest dilution at which promastigotes could be grown out after up to 10 to 15 days of incubation at 22 °C.

Real-time PCR for measuring mRNA expression of TNF-α cytokines in parasite-infected macrophage

Real-time PCR was performed to investigate the relative quantities of cytokines TNF-α mRNA. Briefly, RAW264.7 cells (1×10^6 cells/ml) were plated in six-well plates for around 24 h. The plates were then washed with RPMI-1640 and reincubated with LPS (1 μg/ml) or different type of *Leishmania* promastigotes (1:10 ratio) at different time periods. Total RNA was isolated from the parasite-infected RAW264.7 cells using Trizol reagent (Invitrogen Life Technologies) according to the manufacture's protocol. cDNA synthesis was then performed using High Capacity cDNA Reverse Transcription Kit (Applied Biosystems, ABI). Real-time quantitative PCR was performed on the StepOne Real-Time PCR system (Applied Biosystems, ABI) using Power SYBR Green PCR Master Mix (ABI). Relative expression levels of mRNA were normalized using control cells as reference sample and beta-actin as the endogenous control using a comparative ΔΔct method as described by the manufacturer. Primers 5′-GGATTATGGCTCAGGGTCCA-3′ (forward) and 5′-ACATTCGAGGTCCAGTGAA-3′ (reverse) for TNF-α and primers 5′-TTGTGATGGACTCCGGAGAC-3′ (forward) and 5′-TGATGTCACGCACGATTTCC-3′ (reverse) for beta-actin were used.

Cytokine measurement by ELISA

The cell culture supernatant from the *L. major*/macrophage coculture and EVs-treated macrophage was collected and centrifuged to remove noninternalized parasites and debris. The production of proinflammatory cytokine TNF-α was quantified using TNF-α Quantikine ELISA kits (R&D systems) according to the manufacturer's instructions.

Cytokine measurement by Western blotting

Cells were collected following infection for 24 h and lysed in lysis buffer (Cell Signaling Technology). The protein

concentrations in the cleared supernatants were estimated using a Bio-Rad protein assay mixture. Fifty micrograms of proteins was subjected to 10% SDS-PAGE, and proteins were transferred to a nitrocellulose membrane (Millipore) and blocked for 2 h at 37 °C in TBS-T (20 mM Tris-HCl, 137 mM NaCl, 0.05% (v/v) Tween 20, pH 7.6) containing 5% BSA to prevent nonspecific binding of antibodies. Immunoblotting was performed by incubating in TNF-α monoclonal primary antibody (Abcam) at 1:1000 dilution overnight at 4 °C. Membranes were washed three times in TBS-T, followed by incubation with anti-rabbit IgG coupled to alkaline phosphatase (1:15,000). Again, after three washes with TBS-T, membranes were developed by NBT-BCIP (Roche) method.

In vitro *protein translation of TNF-α mRNA in presence or absence of purified leishmanial GAPDH*

Total RNA was isolated from the parasite-infected RAW264.7 cells using Trizol reagent (Invitrogen Life Technologies) according to the manufacture's protocol. LPS (20 μg)-induced mRNA expression in Raw 264.7 cells was subjected to *in vitro* translation by addition of 35 μl rabbit reticulocyte lysate (Promega), 20 mM methionine free amino acid mixture, 40 U of RNase inhibitor (Roche), and 20 μCi of ^{35}S methionine with or without LmGAPDH in a 50-μl reaction for 90 min at 30 °C. A 45-μl aliquot was subjected to immunoprecipitation with TNF-α monoclonal antibody (Abcam) and protein A/G plus agarose (Santa Cruz Biotechnology) in a buffer containing 50 mM Tris-Cl (pH 7.6), 50 mM NaCl, 1 mM PMSF, 1 mM DTT, 0.5% NP40, 1× protease inhibitor cocktail (Roche). Immunoprecipitated proteins were resolved on 10% SDS-PAGE. To analyze the general translation pattern, a 5-μl aliquot that was not subjected to immunoprecipitation was resolved by 10% SDS-PAGE. The gels were analyzed autoradiographically by fixing, drying, and exposing the gel on X-ray film as mentioned above.

In vitro *LmGAPDH protein transfection*

Adherent RAW 264.7 cells were grown on six-well plates in RPMI 1640 and 10% FBS. Recombinant LmGAPDH protein was purified according to the protocol mentioned above. Purified protein in a suitable buffer (10 mM Tris, 150 mM NaCl, pH 7.0) was transfected to the adherent RAW cells through Pierce Protein Transfection Reagent kit (Thermo Scientific) following manufacture's instruction.

Immunofluorescence and confocal microscopy

The transfected cells grown on glass cover slips were washed in 1× PBS and then the cells were fixed by 4% paraformaldehyde. Cells were then permeabilized with 1.0% Triton X 100 in 1× PBS with 50 μg/ml RNaseA (Calbiochem). The cover slips were air dried and blocked with 1.5% BSA for 2 h. The cover slips were then incubated with anti-rabbit GAPDH antibody (1:200) overnight at 4 °C. On the next day the cover slips were washed with 1× PBS and incubated with Alexa fluor 488-conjugated anti-rabbit secondary antibody (Life Technologies) at a dilution of 1:600 for 2 h. Finally, they were mounted on a slide with DAPI-containing antifade mounting media (Invitrogen) and observed under confocal microscope (Leica). The wavelengths used were DAPI, Ex_λ = 350 nm and Em_λ = 470 nm; Alexa Flour 488 secondary antibody, Ex_λ = 488 nm and Em_λ = 522 nm.

RNA electrophoretic mobility shift assay

For our experiment, we used AU-rich RNA derived from TNF-α 3′ UTR (ARE38 5′-GUGAUUAUUUAUUAUUU AUUUAUUAUUUAUUUAUUUAG-3′) and an arbitrary region derived from TNF-α 5′ UTR (5′-AGAACAUCUUGG AAAUAGCUCCCAGAAAAGCAAGCAGC-3′) synthesized and biotin end-labeled by using biotin at 3′ end by Biotech Desk Pvt. Ltd. RNA-EMSA was then performed with the Light Shift chemiluminescent RNA EMSA kit (Thermo Scientific) according to the manufacturer's instructions. For performing RNA binding reactions, purified LmGAPDH protein and 2 nM of biotin-labeled probe in a volume of 20 μl were incubated together for 30 min at room temperature along with 2 μg tRNA, 5% glycerol in 1× of REMSA binding buffer. For monitoring cold competition assays, unlabeled TNF-α 3′ UTR RNA oligonucleotides were added to the reaction mixture (∼200-fold excess) before addition of the labeled probes. The REMSA supershift is carried out using another lane loaded with labeled probe, LmGAPDH purified protein, and LmGAPDH antibody (raised) specific for the protein. Increasing concentrations of NAD+, NADH, and ATP were added to the reaction mixture to ensure their effect on LmGAPDH-mediated inhibition of TNF-α production. Samples were separated on native polyacrylamide gels (6%) in 0.5× Tris-borate-EDTA (TBE) buffer at 100 V at 4 °C that were prerun for 30 min. Then the gel was transferred into positively charged nylon membranes (Sigma) in Trans-Blot Semi dry apparatus (Bio-Rad). The biotin-labeled RNA on the membrane was cross-linked by a UV-light cross-linker (UVP HL-2000 HybriLinkerTM) and then detected using horseradish peroxidase–conjugated streptavidin. Band shifts were observed by exposure using iBright Imaging System (Invitrogen).

Atomic force microscopy for visualizing extracellular vesicles structure

For AFM imaging, purified EVs preparations were diluted with filtered PBS (1:100) and a 5 μl aliquot of the diluted sample solution was deposited on freshly cleaved mica sheet followed by incubation at room temperature for 10 min. The dried sample was then gently washed with 200 μl of Milli-Q water to remove salt and loosely bound moieties. AFM experiments were performed in intermittent contact mode (called "tapping" or AAC mode) to minimize tip-induced damage. AAC mode AFM was performed using a Pico plus 5500 inverted light microscope AFM (Agilent Technologies) with a Piezo scanner (maximum range 9 μm). Microfabricated silicon cantilevers 225 μm in length with a nominal spring force constant of 21 to 98 N/m were used (Nano Sensors). Cantilever oscillation frequency was tuned into resonance frequency. The cantilever resonance frequency was 150 to

300 kHz. The images (512 × 512 pixels) were captured with a scan size between 0.5 and 0.8 μm at a scan speed rate of 0.5 lines/s. Images were processed by flatten using Pico view1.1 version software (Agilent Technologies). Image manipulation was done using Pico Image Advanced version software (Agilent Technologies).

Dynamic light scattering Zeta potential measurements

The extracted EVs (100 μl) were diluted 10 times using 1 × PBS and then transferred into a disposable cuvette (40 μl), and then the EVs-containing cuvette was put into the DLS device to start measuring. All size distribution and ζ-potential experiments were conducted using the Nano-ZS instrument (Malvern Instruments) at 25 °C (5 mW, He–Ne laser, λ = 632 nm, scattering angle = 173°). For determining size distributions by DLS, the operation procedure was programmed using the DTS software supplied with the instrument to record the average of an automated number of runs. Every run was collected for 10 s, and an equilibration time of 5 min was used, prior to starting the measurement. For all ζ-potential measurements, samples were loaded into a folded capillary cell and average ζ-potential values obtained from an automated number of runs (maximum 100) were noted. The instrument measured ζ-potential from the electrophoretic mobility (μ), using a model described by the Smoluchowski equation.

Statistical analysis

All data were expressed as the mean ± SD from at least three independent experiments. Statistical analysis for parametric data was performed by Student's *t* test or analysis of variance (ANOVA) wherever applicable using Origin 7.0 software (Microcal software, Inc). A p value of less than 0.05 was considered statistically significant.

Data availability

All data generated and analyzed during this study are contained within the article.

Acknowledgments—We thank Dr S. M. Beverley (Washington University, St Louis, MO) for providing pXG-B2863, pXG-neo, pXG-hyg, and pXG-phleo vector as a gift; Dr Nahid Ali for *Leishmania donovani* GP63 antibody; and Dr A. K. Datta for *Leishmania donovani* adenosine kinase antibody.

Author contributions—S. A. conceptualization; P. D., A. M., and S. A. methodology; P. D., A. M., and S. A. formal analysis; P. D., S. A., and A. M. investigation; S. A. resources; P. D., A. M., and S. A. data curation; S. A. writing–original draft; P. D. visualization; S. A. supervision; S. A. project administration; S. A. funding acquisition.

Funding and additional information—This work was supported by Council of Scientific and Industrial Research (CSIR) NCP Project MLP-136, CSIR fellowships (to P. D. and A. M.).

Conflict of interest—The authors declare that they have no conflicts of interest with the content of this article.

Abbreviations—The abbreviations used are: AFM, atomic force microscopy; BSA, bovine serum albumin; CM, complement cell; CT, control cell; DLS, dynamic light scattering; EV, extracellular vesicle; FBS, fetal bovine serum; HKO, LmGAPDH half knockout cell; LmGAPDH, glyceraldehyde-3-phosphate dehydrogenase from *Leishmania major*; LPS, lipopolysaccharide; OE, LmGAPDH overexpressing cell; TNF-α, Tumor necrosis factor alpha; REMSA, RNA electrophoretic mobility shift assay.

References

1. Silverman, J. M., Clos, J., de'Oliveira, C. C., Shirvani, O., Fang, Y., Wang, C., Foster, L. J., and Reiner, N. E. (2010) An exosome-based secretion pathway is responsible for protein export from *Leishmania* and communication with macrophages. *J. Cell Sci.* **123**, 842–852
2. Silverman, J. M., Clos, J., Horakova, E., Wang, A. Y., Wiesgigl, M., Kelly, I., Lynn, M. A., McMaster, W. R., Foster, L. J., Levings, M. K., and Reiner, N. E. (2010) *Leishmania* exosomes modulate innate and adaptive immune responses through effects on monocytes and dendritic cells. *J. Immunol.* **185**, 5011–5022
3. Silverman, J. M., Chan, S. K., Robinson, D. P., Dwyer, D. M., Nandan, D., Foster, L. J., and Reiner, N. E. (2008) Proteomic analysis of the secretome of *Leishmania donovani*. *Genome Biol.* **9**, R35
4. Silverman, J. M., and Reiner, N. E. (2011) *Leishmania* exosomes deliver preemptive strikes to create an environment permissive for early infection. *Front. Cell. Infect. Microbiol.* **1**, 26
5. Kawamoto, R. M., and Caswell, A. H. (1986) Autophosphorylation of glyceraldehydephosphate dehydrogenase and phosphorylation of protein from skeletal muscle microsomes. *Biochemistry* **25**, 657–661
6. Durrieu, C., Bernier-Valentin, F., and Rousset, B. (1987) Binding of glyceraldehyde 3-phosphate dehydrogenase to microtubules. *Mol. Cell. Biochem.* **74**, 55–65
7. Glaser, P. E., and Gross, R. W. (1995) Rapid plasmenylethanolamine-selective fusion of membrane bilayers catalyzed by an isoform of glyceraldehyde-3-phosphate dehydrogenase: Discrimination between glycolytic and fusogenic roles of individual isoforms. *Biochemistry* **34**, 12193–12203
8. Hessler, R. J., Blackwood, R. A., Brock, T. G., Francis, J. W., Harsh, D. M., and Smolen, J. E. (1998) Identification of glyceraldehyde-3-phosphate dehydrogenase as a Ca2+-dependent fusogen in human neutrophil cytosol. *J. Leukoc. Biol.* **63**, 331–336
9. Brüne, B., and Lapetina, E. G. (1996) Nitric oxide-induced covalent modification of glycolytic enzyme glyceraldehyde-3-phosphate dehydrogenase. *Methods Enzymol.* **269**, 400–407
10. Morgenegg, G., Winkler, G. C., Hübscher, U., Heizmann, C. W., Mous, J., and Kuenzle, C. C. (1986) Glyceraldehyde-3-phosphate dehydrogenase is a nonhistone protein and a possible activator of transcription in neurons. *J. Neurochem.* **47**, 54–62
11. Singh, R., and Green, M. R. (1993) Sequence-specific binding of transfer RNA by glyceraldehyde-3-phosphate dehydrogenase. *Science* **259**, 365–368
12. Meyer-Siegler, K., Mauro, D. J., Seal, G., Wurzer, J., deRiel, J. K., and Sirover, M. A. (1991) A human nuclear uracil DNA glycosylase is the 37-kDa subunit of glyceraldehyde-3-phosphate dehydrogenase. *Proc. Natl. Acad. Sci. U. S. A.* **88**, 8460–8464
13. Baxi, M. D., and Vishwanatha, J. K. (1995) Uracil DNA-glycosylase/glyceraldehyde-3-phosphate dehydrogenase is an Ap4A binding protein. *Biochemistry* **34**, 9700–9707
14. Nagy, E., and Rigby, W. F. (1995) Glyceraldehyde-3-phosphate dehydrogenase selectively binds AU-rich RNA in the NAD(+)-binding region (Rossmann fold). *J. Biol. Chem.* **270**, 2755–2763
15. Chakravarti, R., Aulak, K. S., Fox, P. L., and Stuehr, D. J. (2010) GAPDH regulates cellular heme insertion into inducible nitric oxide synthase. *Proc. Natl. Acad. Sci. U. S. A.* **107**, 18004–18009
16. Hara, M. R., Agrawal, N., Kim, S. F., Cascio, M. B., Fujimuro, M., Ozeki, Y., Takahashi, M., Cheah, J. H., Tankou, S. K., Hester, L. D., Ferris, C. D., Hayward, S. D., Snyder, S. H., and Sawa, A. (2005) S-nitrosylated GAPDH

initiates apoptotic cell death by nuclear translocation following Siah1 binding. *Nat. Cell Biol.* **7**, 665–674
17. Sen, N., Hara, M. R., Kornberg, M. D., Cascio, M. B., Bae, B.-I., Shahani, N., Thomas, B., Dawson, T. M., Dawson, V. L., Snyder, S. H., and Sawa, A. (2008) Nitric oxide-induced nuclear GAPDH activates p300/CBP and mediates apoptosis. *Nat. Cell Biol.* **10**, 866–873
18. Sirover, M. A. (2020) Moonlighting glyceraldehyde-3-phosphate dehydrogenase: Posttranslational modification, protein and nucleic acid interactions in normal cells and in human pathology. *Crit. Rev. Biochem. Mol. Biol.* **55**, 354–371
19. Sirover, M. A. (2017) *Glyceraldehyde-3-Phosphate Dehydrogenase (GAPDH): The Quintessential Moonlighting Protein in Normal Cell Function and in Human Disease*, Illustrated Ed., Academic Press, London, UK
20. Madureira, P., Baptista, M., Vieira, M., Magalhães, V., Camelo, A., Oliveira, L., Ribeiro, A., Tavares, D., Trieu-Cuot, P., Vilanova, M., and Ferreira, P. (2007) *Streptococcus agalactiae* GAPDH is a virulence-associated immunomodulatory protein. *J. Immunol.* **178**, 1379–1387
21. Alvarez, R. A., Blaylock, M. W., and Baseman, J. B. (2003) Surface localized glyceraldehyde-3-phosphate dehydrogenase of *Mycoplasma genitalium* binds mucin. *Mol. Microbiol.* **48**, 1417–1425
22. Pancholi, V., and Fischetti, V. A. (1992) A major surface protein on group A *streptococci* is a glyceraldehyde-3-phosphate-dehydrogenase with multiple binding activity. *J. Exp. Med.* **176**, 415–426
23. Hannaert, V., Blaauw, M., Kohl, L., Allert, S., Opperdoes, F. R., and Michels, P. A. (1992) Molecular analysis of the cytosolic and glycosomal glyceraldehyde-3-phosphate dehydrogenase in *Leishmania mexicana*. *Mol. Biochem. Parasitol.* **55**, 115–126
24. Lambeir, A. M., Loiseau, A. M., Kuntz, D. A., Vellieux, F. M., Michels, P. A., and Opperdoes, F. R. (1991) The cytosolic and glycosomal glyceraldehyde-3-phosphate dehydrogenase from *Trypanosoma brucei*. Kinetic properties and comparison with homologous enzymes. *Eur. J. Biochem.* **198**, 429–435
25. Misset, O., Van Beeumen, J., Lambeir, A. M., Van der Meer, R., and Opperdoes, F. R. (1987) Glyceraldehyde-phosphate dehydrogenase from *Trypanosoma brucei*. Comparison of the glycosomal and cytosolic isoenzymes. *Eur. J. Biochem.* **162**, 501–507
26. Peacock, C. S., Seeger, K., Harris, D., Murphy, L., Ruiz, J. C., Quail, M. A., Peters, N., Adlem, E., Tivey, A., Aslett, M., Kerhornou, A., Ivens, A., Fraser, A., Rajandream, M.-A., Carver, T., *et al.* (2007) Comparative genomic analysis of three *Leishmania* species that cause diverse human disease. *Nat. Genet.* **39**, 839–847
27. Rogers, M. B., Hilley, J. D., Dickens, N. J., Wilkes, J., Bates, P. A., Depledge, D. P., Harris, D., Her, Y., Herzyk, P., Imamura, H., Otto, T. D., Sanders, M., Seeger, K., Dujardin, J.-C., Berriman, M., *et al.* (2011) Chromosome and gene copy number variation allow major structural change between species and strains of *Leishmania*. *Genome Res.* **21**, 2129–2142
28. Zhang, W.-W., McCall, L.-I., and Matlashewski, G. (2013) Role of cytosolic glyceraldehyde-3-phosphate dehydrogenase in visceral organ infection by *Leishmania donovani*. *Eukaryot. Cell.* **12**, 70–77
29. Kim, H., Feil, I. K., Verlinde, C. L., Petra, P. H., and Hol, W. G. (1995) Crystal structure of glycosomal glyceraldehyde-3-phosphate dehydrogenase from *Leishmania mexicana*: Implications for structure-based drug design and a new position for the inorganic phosphate binding site. *Biochemistry* **34**, 14975–14986
30. Souza, D. H. F., Garratt, R. C., Araújo, A. P. U., Guimarães, B. G., Jesus, W. D. P., Michels, P. A. M., Hannaert, V., and Oliva, G. (1998) *Trypanosoma cruzi* glycosomal glyceraldehyde-3-phosphate dehydrogenase: Structure, catalytic mechanism and targeted inhibitor design. *FEBS Lett.* **424**, 131–135
31. Vellieux, F. M., Hajdu, J., and Hol, W. G. (1995) Refined 3.2 A structure of glycosomal holo glyceraldehyde phosphate dehydrogenase from *Trypanosoma brucei* brucei. *Acta Crystallogr. D Biol. Crystallogr.* **51**, 575–589
32. Aguilera, L., Ferreira, E., Giménez, R., Fernández, F. J., Taulés, M., Aguilar, J., Vega, M. C., Badia, J., and Baldomà, L. (2012) Secretion of the housekeeping protein glyceraldehyde-3-phosphate dehydrogenase by the LEE-encoded type III secretion system in enteropathogenic *Escherichia coli*. *Int. J. Biochem. Cell Biol.* **44**, 955–962
33. Dastoor, Z., and Dreyer, J. L. (2001) Potential role of nuclear translocation of glyceraldehyde-3-phosphate dehydrogenase in apoptosis and oxidative stress. *J. Cell Sci.* **114**, 1643–1653
34. Colasante, C., Voncken, F., Manful, T., Ruppert, T., Tielens, A. G. M., van Hellemond, J. J., and Clayton, C. (2013) Proteins and lipids of glycosomal membranes from *Leishmania tarentolae* and *Trypanosoma brucei*. *F1000Res.* **2**, 27
35. Théry, C., Witwer, K. W., Aikawa, E., Alcaraz, M. J., Anderson, J. D., Andriantsitohaina, R., Antoniou, A., Arab, T., Archer, F., Atkin-Smith, G. K., Ayre, D. C., Bach, J.-M., Bachurski, D., Baharvand, H., Balaj, L., *et al.* (2018) Minimal information for studies of extracellular vesicles 2018 (MISEV2018): A position statement of the International Society for Extracellular Vesicles and update of the MISEV2014 guidelines. *J. Extracell. Vesicles.* **7**, 1535750
36. Millet, P., Vachharajani, V., McPhail, L., Yoza, B., and McCall, C. E. (2016) GAPDH binding to TNF-α mRNA contributes to post-transcriptional repression in monocytes: A novel mechanism of communication between inflammation and metabolism. *J. Immunol.* **196**, 2541–2551
37. Gomez, M. A., Contreras, I., Hallé, M., Tremblay, M. L., McMaster, R. W., and Olivier, M. (2009) *Leishmania* GP63 alters host signaling through cleavage-activated protein tyrosine phosphatases. *Sci. Signal.* **2**, ra58
38. Joshi, P. B., Kelly, B. L., Kamhawi, S., Sacks, D. L., and McMaster, W. R. (2002) Targeted gene deletion in *Leishmania major* identifies leishmanolysin (GP63) as a virulence factor. *Mol. Biochem. Parasitol.* **120**, 33–40
39. Hübel, A., Krobitsch, S., Hörauf, A., and Clos, J. (1997) *Leishmania major* Hsp100 is required chiefly in the mammalian stage of the parasite. *Mol. Cell. Biol.* **17**, 5987–5995
40. Klein, C., Göpfert, U., Goehring, N., Stierhof, Y. D., and Ilg, T. (1999) Proteophosphoglycans of *Leishmania mexicana*. Identification, purification, structural and ultrastructural characterization of the secreted promastigote proteophosphoglycan pPPG2, a stage-specific glycoisoform of amastigote aPPG. *Biochem. J.* **344 Pt 3**, 775–786
41. Vannier-Santos, M. A., Martiny, A., Meyer-Fernandes, J. R., and de Souza, W. (1995) Leishmanial protein kinase C modulates host cell infection via secreted acid phosphatase. *Eur. J. Cell Biol.* **67**, 112–119
42. Lancaster, G. I., and Febbraio, M. A. (2005) Exosome -dependent trafficking of HSP70: A novel secretory pathway for cellular stress proteins. *J. Biol. Chem.* **280**, 23349–23355
43. Nandan, D., Yi, T., Lopez, M., Lai, C., and Reiner, N. E. (2002) *Leishmania* EF-1alpha activates the Src homology 2 domain containing tyrosine phosphatase SHP-1 leading to macrophage deactivation. *J. Biol. Chem.* **277**, 50190–50197
44. Nandan, D., Tran, T., Trinh, E., Silverman, J. M., and Lopez, M. (2007) Identification of *Leishmania* fructose-1,6-bisphosphate aldolase as a novel activator of host macrophage Src homology 2 domain containing protein tyrosine phosphatase SHP-1. *Biochem. Biophys. Res. Commun.* **364**, 601–607
45. Marti, M., Good, R. T., Rug, M., Knuepfer, E., and Cowman, A. F. (2004) Targeting malaria virulence and remodeling proteins to the host erythrocyte. *Science* **306**, 1930–1933
46. Scianimanico, S., Desrosiers, M., Dermine, J. F., Méresse, S., Descoteaux, A., and Desjardins, M. (1999) Impaired recruitment of the small GTPase rab7 correlates with the inhibition of phagosome maturation by *Leishmania donovani* promastigotes. *Cell. Microbiol.* **1**, 19–32
47. Chang, C.-H., Curtis, J. D., Maggi, L. B., Faubert, B., Villarino, A. V., O'Sullivan, D., Huang, S. C.-C., van der Windt, G. J. W., Blagih, J., Qiu, J., Weber, J. D., Pearce, E. J., Jones, R. G., and Pearce, E. L. (2013) Post-transcriptional control of T cell effector function by aerobic glycolysis. *Cell* **153**, 1239–1251
48. Caput, D., Beutler, B., Hartog, K., Thayer, R., Brown-Shimer, S., and Cerami, A. (1986) Identification of a common nucleotide sequence in the 3′-untranslated region of mRNA molecules specifying inflammatory mediators. *Proc. Natl. Acad. Sci. U. S. A.* **83**, 1670–1674
49. Chen, C. Y., and Shyu, A. B. (1995) AU-rich elements: Characterization and importance in mRNA degradation. *Trends Biochem. Sci.* **20**, 465–470

50. Guhaniyogi, J., and Brewer, G. (2001) Regulation of mRNA stability in mammalian cells. *Gene* **265**, 11–23
51. Ty, M. C., Loke, P., Alberola, J., Rodriguez, A., and Rodriguez-Cortes, A. (2019) Immuno-metabolic profile of human macrophages after *Leishmania* and *Trypanosoma cruzi* infection. *PLoS One* **14**, e0225588
52. Biswas, S., Adhikari, A., Mukherjee, A., Das, S., and Adak, S. (2020) Regulation of *Leishmania major* PAS domain-containing phosphoglycerate kinase by cofactor Mg2+ ion at neutral pH. *FEBS J.* **287**, 5183–5195
53. Adhikari, A., Biswas, S., Mukherjee, A., Das, S., and Adak, S. (2019) PAS domain-containing phosphoglycerate kinase deficiency in *Leishmania major* results in increased autophagosome formation and cell death. *Biochem. J.* **476**, 1303–1321
54. Mukherjee, A., Adhikari, A., Das, P., Biswas, S., Mukherjee, S., and Adak, S. (2018) Loss of virulence in NAD(P)H cytochrome b5 oxidoreductase deficient *Leishmania major*. *Biochem. Biophys. Res. Commun.* **503**, 371–377
55. Dolai, S., Yadav, R. K., Pal, S., and Adak, S. (2008) *Leishmania major* ascorbate peroxidase overexpression protects cells against reactive oxygen species-mediated cardiolipin oxidation. *Free Radic. Biol. Med.* **45**, 1520–1529
56. Pal, S., Dolai, S., Yadav, R. K., and Adak, S. (2010) Ascorbate peroxidase from *Leishmania major* controls the virulence of infective stage of promastigotes by regulating oxidative stress. *PLoS One* **5**, e11271

Biochemical and Biophysical Research Communications xxx (2018) 1–7

Contents lists available at ScienceDirect

Biochemical and Biophysical Research Communications

journal homepage: www.elsevier.com/locate/ybbrc

Loss of virulence in NAD(P)H cytochrome *b*5 oxidoreductase deficient *Leishmania major*

Aditi Mukherjee, Ayan Adhikari, Priya Das, Saroj Biswas, Supratim Mukherjee, Subrata Adak*

From the Division of Structural Biology & Bio-informatics, CSIR-Indian Institute of Chemical Biology, 4, Raja S.C. Mullick Road, Kolkata, 700 032, India

ARTICLE INFO

Article history:
Received 17 May 2018
Accepted 9 June 2018
Available online xxx

Keywords:
Cytochrome *b*5 oxidoreductase
de novo linoleate synthesis
NF-κB activation
Cytokine expression
Leishmania

ABSTRACT

Leishmania promastigotes have the ability to synthesize essential polyunsaturated fatty acids *de novo* and can grow in lipid free media. Recently, we have shown that NAD(P)H cytochrome *b*5 oxidoreductase (Ncb5or) enzyme in *Leishmania* acts as the redox partner for Δ12 fatty acid desaturase, which catalyses the conversion of oleate to linoleate. So far, the exact role of *Leishmania* derived linoleate synthesis is still incomplete in the literature. The viability assay by flow cytometry as well as microscopic studies suggests that linoleate is an absolute requirement for *Leishmania* promastigote survival in delipidated media. Western blot analysis suggested that infection with log phase linoleate deficient mutant (KO) results in increased level of NF-κBp65, IκB and IKKβ phosphorylation in RAW264.7 cells. Similarly, the log phase KO infected RAW264.7 cells show dramatic increment of COX-2 expression and TNF-α secretion, compared to control or Ncb5or complement (CM) cell lines. The activation of inflammatory signaling pathways by KO mutant is significantly reduced when the RAW264.7 cells are pre-treated with BSA bound linoleate. Together, these findings confirmed that the leishmanial linoleate inhibits both COX-2 and TNF-α expression in macrophage via the inactivation of NF-κB signaling pathway. The stationary phase of KO promastigotes shows avirulence after infection in macrophages as well as inoculation into BALB/c mice; whereas CM cell lines show virulence. Collectively, these data provide strong evidence that *de novo* linoleate synthesis in *Leishmania* is an essential for parasite survival at extracellular promastigote stage as well as intracellular amastigote stage.

1. Introduction

Cytochrome *b*-type NAD(P)H oxidoreductase (Ncb5or), comprising of cytochrome *b*5 and cytochrome *b*5 reductase domains, has been demonstrated to be involved in many physiological processes, including lipid metabolism and diabetes [1–4]. The C-terminal cytochrome *b*5 reductase (*cb*5r) domain contains a single flavin adenine dinucleotide prosthetic group and catalyzes the transfer of electron from NAD(P)H to N-terminal cytochrome *b*5 heme (*cb*5) domain. After taking electron from the cb5r domain, the *cb*5 domain donates electron to various electron acceptors including Δ9-, Δ6-, and Δ5-acyl CoA desaturases [5].

Leishmania spp., the organism causing leishmaniasis in human, divides its life cycle between the sand fly vector and the mammalian host. Earlier researchers revealed that *Leishmania* promastigotes possess the capacity to synthesize fatty acids (FAs) *de novo* and can grow in lipid depleted media [6]. Linoleic acid and linolenic acid are the most common unsaturated fatty acid components of *Leishmania* [7]. These organisms can synthesize these essential polyunsaturated fatty acids (PUFAs) by fatty acid desaturases (FADs) [8,9]. All FADs require a redox partner for transferring electron from NAD(P)H [10]. Recently, the measurement of free fatty acid profile in Ncb5or knock-out (KO) cells revealed marked deficiency in linoleate and linolenate when compared with wild type (WT) cells. These findings suggest that Ncb5or in *Leishmania* acts as the redox partner for Δ12 fatty acid desaturases (FADs), which catalyse the production of linoleate from oleate [11]. However, the exact functions of parasite derived linoleate synthesis in host-parasite interaction are far from being elucidated.

Several experimental studies demonstrate that the expression of pro-inflammatory gene is induced by saturated fatty acids (lauric acid and palmitic acid) in macrophages (RAW264.7 cells) [12]. The saturated fatty acids activate macrophages via the activation of NF-

* Corresponding author.
E-mail address: adaks@iicb.res.in (S. Adak).

https://doi.org/10.1016/j.bbrc.2018.06.037
0006-291X/

κB as determined by the degradation of IκBα and the phosphorylation of p65. On the other hand, various unsaturated fatty acids including EPA (C20:5n-3), DHA (C22:6n-3) and linoleic acid (C18:2n-6) inhibit the expression of inflammatory genes such as COX-2, iNOS and IL-1α in macrophages [12]. Due to the anti-inflammatory properties of linoleic acid, our investigations have been aimed at understanding the connections between *Leishmania* derived linoleate synthesis and pathogenesis in this host-parasite interaction. In this study, for the first time we have established that *de novo* linoleate synthesis in *Leishmania* is required for parasite survival in both extracellular promastigote and intracellular amastigote stages. In addition, we have shown that infection with linoleate deficient mutant (Ncb5or deletion) results in dramatic increments in NF-κB activation and pro-inflammatory cytokine TNF-α as well as COX-2 and iNOS expression in RAW264.7 cells.

2. Materials and methods

2.1. Materials

Sodium palmitate and sodium stearate were purchased from Sigma. Ultra fatty acid free BSA was from Roche. Anti-COX-2, NF-κBp65, phospho NF-κBp65 [ser536], IκB alpha antibodies were from Santa Cruz Biotechnology. Anti-alpha-tubulin antibody and anti-iNOS/NOS II antibodies were from Millipore. Anti-IKKβ, Phospho-IKKα/β [Ser176/180] and Phospho- IκB alpha antibodies were purchased from Cell Signaling Technology. NBT/BCIP reagents were purchased from Roche. Both heat inactivated FBS and charcoal stripped FBS, as well as penicillin-streptomycin were from Invitrogen. All other reagents were purchased from Sigma (St Louis. MO) or sources previously reported [11,13–15].

2.2. Ethics statement

All BALB/c mice were obtained from and maintained in our Institutional animal facility (Kolkata, India). The studies were approved by IICB Animal Ethical Committee (Registration no. 147/1999, CPCSEA), registered with Committee for the purpose of Control and Supervision of experiments on Animals (CPCSEA), Govt. of India, and BALB/c mice were handled according to their guidelines.

2.3. Parasite culture

Leishmania major wild type parasites (strain 5ASKH) were routinely cultured at 22 °C in M199 medium (Invitrogen) supplemented with 40 mM HEPES (pH 7.4, Amresco), 1% penicillin-streptomycin (v/v), 200 μM adenine (Sigma), 50 μg/ml gentamycin (Abott), and 10% heat-inactivated fetal bovine serum (Invitrogen). The LmNcb5or knock-out strain was maintained in 60 μg/ml neomycin and 100 μg/ml hygromycin (Roche) drug.

2.4. Complementation of LmNcb5or in null mutants

Earlier we made the knockout cell lines by the gene replacement technique [11]. To restore LmNcb5or in the knock out parasites, cloned gene was transfected into the knockout promastigotes. A detailed description of complementation of LmNcb5or in null mutants is provided in SI Methods.

2.5. Macrophage cell culture

The murine macrophage cell line RAW 264.7 was maintained in RPMI-1640 medium (Invitrogen Life Technologies) containing 10% heat-inactivated fetal bovine serum (FBS), 100U/ml penicillin, and 100 μg/μl streptomycin at 37 °C in a humidified atmosphere containing 5% CO_2. After 24 h incubation with or without linoleate complexed with BSA (100 μM), the plates were washed with RPMI-1640 and re-incubated with LPS (1 μg/ml) or different type of *Leishmania* promastigotes (promastigote: macrophage ratio is 10:1) for indicated time periods.

2.6. Growth of parasites in lipid-depleted medium

To investigate the significance of linoleic acid in growth and survivability of *Leishmania*, different types of promastigotes (CT, CM and KO parasites) were cultured in M199 medium supplemented with either 10% fetal bovine serum (Gibco, #16000044) or charcoal stripped fetal bovine serum (Gibco life technologies, #12676-011) for different times of incubation period. Various fatty acids (either BSA-complexed oleate, palmitate and stearate along with linoleate [csFBS + FA] or oleate, palmitate and stearate without linoleate [csFBS-LA]) were added directly (40 μM) to the medium during the culture of the promastigotes in csFBS and comparative study was performed among different groups by counting the number of viable cells.

2.7. Assessment of viable cell by PI and Annexin-V staining

Apoptotic and necrotic cells can be seen by staining with FITC conjugated Annexin-V (ApoAlert™ Annexin V-FITC Apoptosis Kit, Clontech) and PI as they show both green and red fluorescence. A detailed description of PI and Annexin-V staining is provided in SI Methods. For microscopic examination, promastigotes were adhered on poly-L-lysine-coated slides (Sigma) and visualized under Olympus IX81 microscope at 100X magnification. For each sample 20 fields (200 macrophages per field) were observed.

2.8. In-vitro macrophage infection

CT, CM and KO promastigotes were used to infect cultures of the adherent murine macrophage cell line RAW 264.7 on glass cover slips (22 mm^2; 5×10^5 macrophages/cover slip) in 0.5 ml of RPMI 1640/10% FBS at a parasite to cell ratio of 10:1 (promastigote: macrophage) for a period of 2 h for determination of parasite entry and a period of >6 h for determination of intracellular parasite numbers. Cells were then fixed in methanol and stained with propidium iodide. Cells were visualized and quantified using Olympus IX81 microscope.

2.9. Infection in mice

For cutaneous infection, female BALB/c mice, 4–6 weeks old, were infected subcutaneously with 5×10^6 stationary-phase CT, CM and KO promastigotes in their left hind footpads [8 mice/group]. A detailed description of virulence studies in mice model and parasite burden is provided in SI Methods.

2.10. Real-time PCR for measuring mRNA expression

Real time PCR was performed to investigate the relative quantities of cytokine TNF-α as well as expression of COX-2 mRNA. A detailed description of real time PCR for measuring mRNA expression is provided in SI Methods.

2.11. Cytokine measurement by ELISA

The cell culture supernatant from the *L. major*/macrophage co-culture was collected and centrifuged to remove non-internalized

Please cite this article in press as: A. Mukherjee, et al., Loss of virulence in NAD(P)H cytochrome *b*5 oxidoreductase deficient *Leishmania major*, Biochemical and Biophysical Research Communications (2018), https://doi.org/10.1016/j.bbrc.2018.06.037

parasites and debris. The production of pro-inflammatory cytokine TNF-α was quantified using ELISA kit (R&D systems) according to the manufacturer's instructions.

2.12. Immunoblotting

Cells were collected following infection (24 h for COX-2 and NOS II and 30 min for signal-transduction proteins) and lysed in lysis buffer (Cell-Signaling Technology). A detailed description of immunoblotting is provided in SI Methods.

2.13. Preparation of nuclear extracts

Nuclear and cytoplasmic extracts were prepared after treatment of RAW264.7 cells with LPS or different type of log phase *Leishmania* cell lines. Briefly, following infection for 6 h, cells were washed with PBS (pH 7.4), gently scrapped and pelleted at 500 × g for 5 min at 4 °C. Nuclear and cytosolic fractions were extracted using the NE-PER nuclear and cytoplasmic extraction reagents (Pierce) according to the manufacturer's instructions. Protein concentration was determined by Bio-Rad protein estimation kit.

2.14. Electrophoretic mobility shift assay (EMSA)

Complementary NF-κB consensus oligonucleotides (5′-AGTTGAGGGGACTTTCCCAGGC-3′ and 5′-GCCTGGGAAAGTCCCCTCAACT-3′) were synthesized by GCC Biotech. The oligos were end-labeled with biotin separately using the biotin 3′-end DNA labeling kit (Thermo Scientific) and then annealed by heating to 95 °C for 2 min followed by slow cooling to room temperature. Probes were stored at −20 °C until use. EMSA was performed with the Light Shift chemiluminescent EMSA kit (Thermo Scientific) following the manufacturer's instructions.

2.15. Statistical analysis

All results were expressed as the mean ± SD from at least three independent experiments. Statistical difference between the different groups was calculated by one way analysis of variance (ANOVA) wherever applicable using Origin 6.0 software (Microcal software, Inc. Northampton, MA, USA). A p value of less than 0.05 was considered statistically significant.

3. Results and discussion

3.1. Linoleate is essential for growth and survival of L. major promastigotes

Earlier it was reported that linoleate deficient cells had higher percentage of dead cells compared to control under stationary phase promastigotes [11], but it is still unknown whether linoleate deficient cells can survive in fatty acid depleted media. To elucidate that, linoleate auxotroph *Leishmania* cells (null mutant) were grown in M199 media supplemented with 10% FBS or lipid depleted FBS (charcoal stripped). Culture of LmNcb5or KO (knock-out) cells in fatty acid deficient medium increased cell death (~22%) compared to CT (control) and CM (complement) cells within 4 days of incubation. When BSA-linoleate along with BSA-oleate, BSA-palmitate and BSA-stearate complexes were externally supplied in the fatty acid depleted FBS culture medium, there was significant decrease in cell death, but supplement of all fatty acids except linoleate caused more cell death (~46%) among the promastigotes (Fig. 1A and B). These results indicate that saturated or mono unsaturated fatty acids are more toxic to *Leishmania* promastigotes in absence of linoleate. Flow-cytometric data regarding cell death was further confirmed by fluorescence microscopy where similar result was observed in KO cell cultures compared to CT or CM cell lines. Culture of LmNcb5or KO cells in linoleate deficient medium caused ~100% cell death within 8 days of incubation period (data not shown) indicating that linoleate is an absolute requirement for *Leishmania* promastigote survival. Similar type of result is observed in other kinetoplastids like *T. brucei* and *T cruzi*, where the growth rate of parasite is inhibited by using inhibitors or RNA interference (RNAi) against Δ12 FAD (linoleate synthesis enzyme) [16].

3.2. Ncb5or gene is an essential for disease development

Leishmania are obligate intracellular pathogens, preferring phagocytes as host cells [17]. Because macrophages are the host cells for *L. major* promastigotes, we focused on promastigote infection in macrophages. We investigated to what extent CT, KO and CM cells were phagocytosed by macrophages. On the basis of 2 h–6 h of incubation time, the adhering rates of all promastigotes were same in all the cell lines (Fig. 2A). The internalization rates of KO promastigotes at 24 h of incubation were lesser than CT or CM cells. After phagocytosing CT or CM promastigotes, most of the infected macrophages still contained parasites up to 72 h of incubation, whereas the percentage of KO infected macrophages decreased significantly. In addition, the KO parasites resulted in negligible macrophage infection (Fig. 2B) compared to CT or CM cells. Upon addition of the BSA-linoleate complexes into macrophage culture media, the infection property of KO mutant was found higher than CT cells. These data strongly suggest that the linoleate deficient parasites were killed more easily inside the macrophages.

We investigated whether *Leishmania major* parasites lacking Ncb5or gene are able to develop infections in mice. For that, they were inoculated into the footpads of BALB/c mice, and we found that CT or CM cells induced a more severe disease with an earlier onset of footpad necrosis, as compared to KO cells (Fig. 2C). These data were confirmed by counting parasite burden 8 weeks post infection (Fig. 2D) in 1 mg of footpad tissue. Data showed ~60 and 50 fold increment in parasite burden in CT and CM parasites respectively compared to KO cells, indicating the pivotal role of linoleate in infection.

3.3. Linoleate deficient log phase parasite leads to increased expression of COX-2, TNF-α and nitric oxide synthase (iNOS) through the activation of NF-κB

Fatty acids have been shown to modulate macrophage function and thus to regulate inflammatory and immune responses [18]. COX-2 expression in CT, CM and KO infected macrophages were determined by both quantitative real time PCR assay (Fig. 3A) and Western blot analysis (Fig. 3B–C). KO cells caused huge induction of COX-2 (~16 fold) mRNA expression (Fig. 3A), whereas CT and CM cells had no significant effect. As expected, LPS (1 μg/ml) induced ~15 fold higher COX-2 mRNA expression in macrophages. Western blot analysis confirmed that KO cells are potent inducer of COX-2 expression (Fig. 3B and C). On the other hand, CT or CM cells were unable to induce COX-2 expression in RAW 264.7 cells. Another pro-inflammatory cytokine, TNF-α mRNA expression was determined by quantitative real time PCR assay. Like LPS treatment, KO infected macrophage showed huge induction of TNF-α (~3 fold) mRNA expression compared to CT or CM (Fig. 3A). To further confirm this data, ELISA was performed (Fig. 3D) and the results we got were almost similar to the quantitative real time PCR data. Inducible nitric oxide synthase (iNOS) is a key player in clearing *Leishmania* infection, whose expression in macrophages infected with CT, CM and KO cells were determined by Western blot analysis

Please cite this article in press as: A. Mukherjee, et al., Loss of virulence in NAD(P)H cytochrome *b*5 oxidoreductase deficient *Leishmania major*, Biochemical and Biophysical Research Communications (2018), https://doi.org/10.1016/j.bbrc.2018.06.037

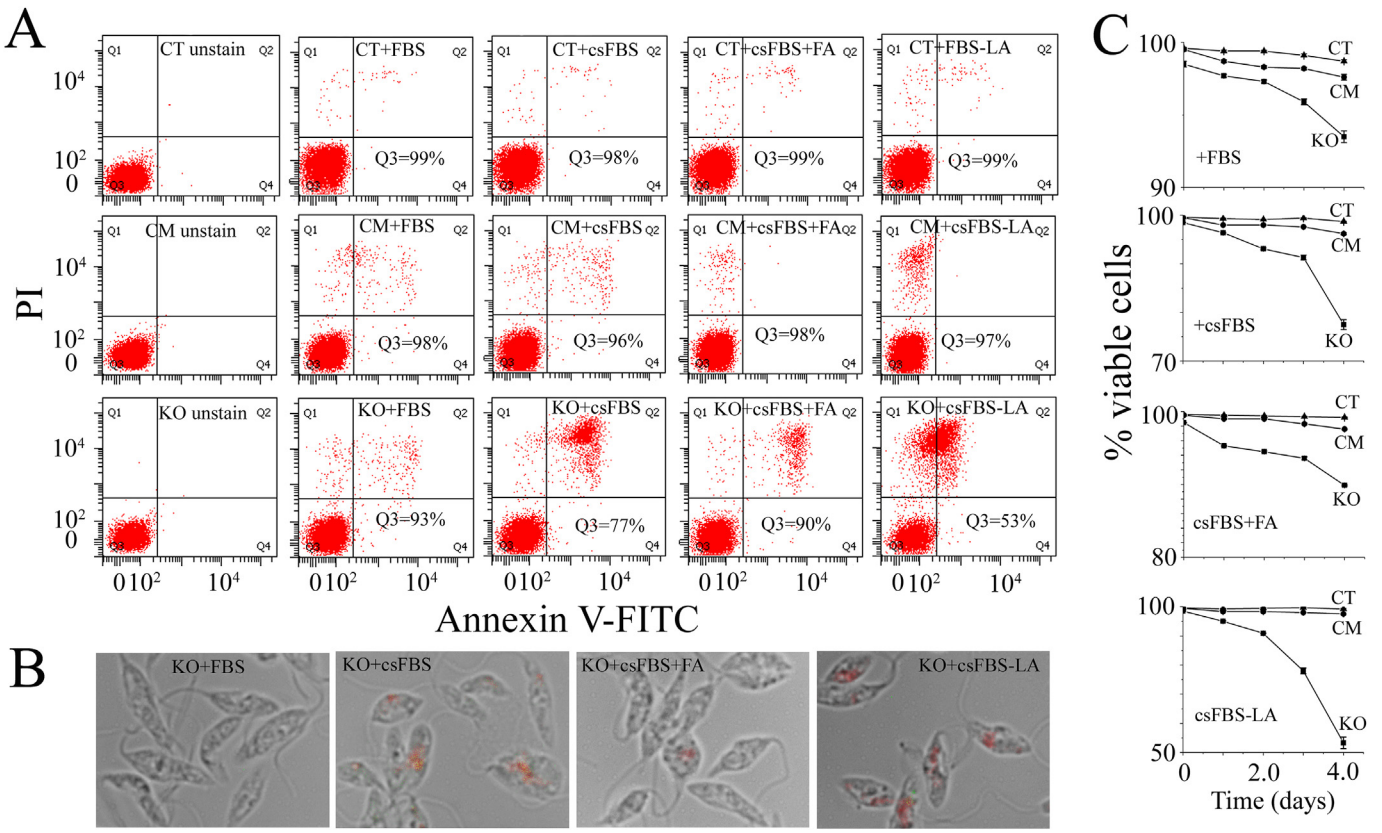

Fig. 1. Comparative studies of cell death among CT, CM and KO cell lines in lipid depleted medium. (A) Represents cells doubled-stained with AnnexinV-FITC and PI to access cell death. The lower left quadrant of each dot plot represents viable cells. (B) Merged microscopic images of the cells of panel A under bright field at 100X magnification. (C) The number of viable cells after incubation of CT, CM and KO cells in FBS, Charcoal stripped FBS (csFBS), csFBS with BSA-linoleate, BSA-oleate, BSA-palmitate and BSA-stearate (csFBS + FA) and csFBS with BSA-oleate, BSA-palmitate and BSA-stearate (csFBS-LA) were counted upto 4 days. Data are the means ± SD of three independent experiments.

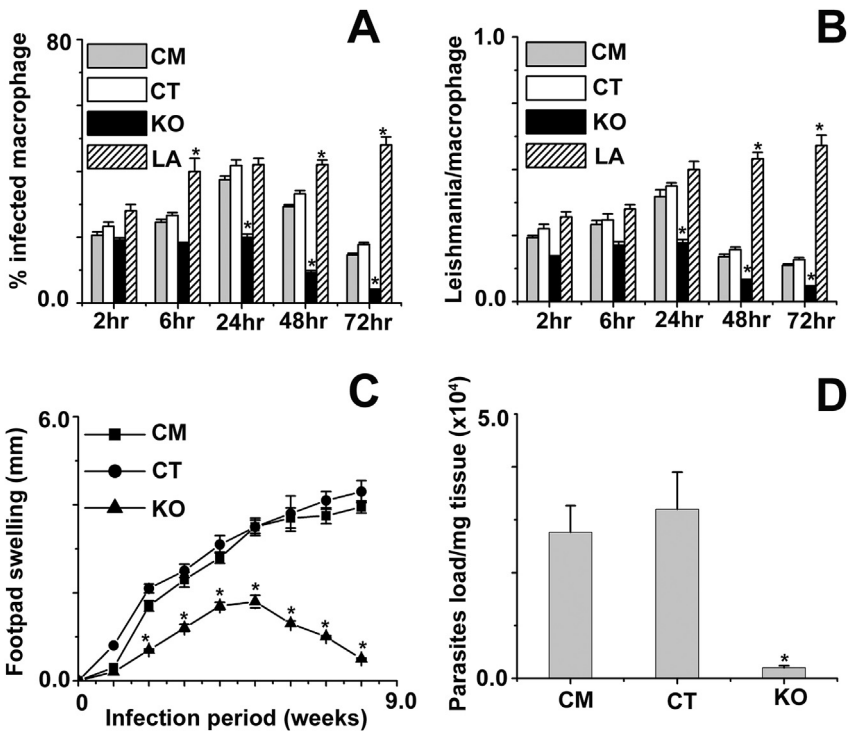

Fig. 2. *In vitro* mouse macrophages as well as *in vivo* BALB/c mice infection with stationary phase CT, CM and KO cells. (A) The percentage of macrophages infected with CT, CM and KO parasites. For each time point 200 macrophages were counted. (B) The number of *Leishmania* within each infected macrophage was counted. For each time point and cell type, 100 infected macrophages were analyzed. 'LA' denoted BSA-linoleate pre-incubated macrophage plus KO cells. (C) Infection in susceptible BALB/c mice. (D) Parasite burden in footpads 8 weeks post infection. Error bars represent the SD from three independent experiments. * Statistically significant value of less than 0.05.

Please cite this article in press as: A. Mukherjee, et al., Loss of virulence in NAD(P)H cytochrome *b*5 oxidoreductase deficient *Leishmania major*, Biochemical and Biophysical Research Communications (2018), https://doi.org/10.1016/j.bbrc.2018.06.037

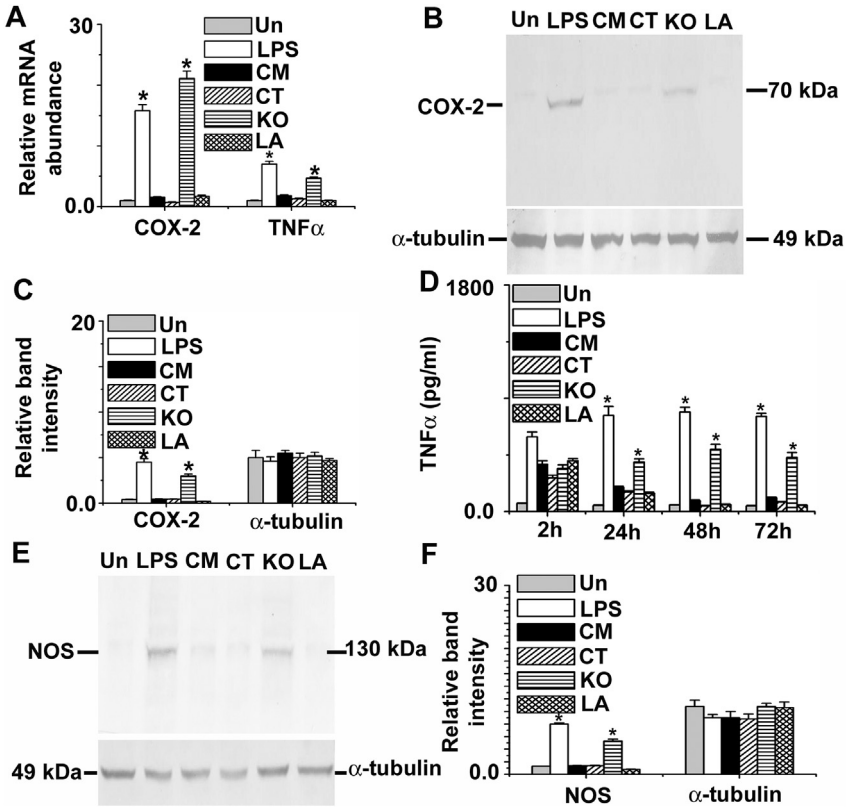

Fig. 3. The mRNA and protein expression of COX-2 and TNF α production in log phase *Leishmania* promastigote infected macrophage. (A) Measurement of gene transcript abundance was analyzed by using quantitative real-time PCR as described in materials and methods. All data were normalized using beta-actin as the endogenous control. (B) COX-2 protein levels were measured by Western blot analysis of protein lysates from RAW264.7 cells. Alpha tubulin was used as loading control. (C) Densitometric analysis of all bands was done using ImageJ software (from NIH). (D) Levels of TNF-α production were measured by ELISA in the cell culture supernatants after infection. (E) NOS protein levels were measured by Western blot analysis of protein lysates from RAW264.7 cells. Alpha tubulin was used as loading control. (F) Densitometric analysis of all bands of panel E was done using ImageJ software (from NIH). All the data are representative of three independent experiments. Error bars represent the SD from three independent experiments. 'Un' and 'LA' denoted uninfected macrophage (-*Leishmania*) and BSA-linoleate pre-incubated macrophage plus KO cells, respectively. * Statistically significant value of less than 0.05.

(Fig. 3E–F). The KO cells induced higher iNOS expression in macrophages compared to CT or CM. To check the effect of linoleate in the recovery of anti-inflammatory responses of the KO cells, we added the BSA-linoleate complex into macrophage culture media. On addition of BSA-linoleate complexes, the expression of COX-2, TNF-α and iNOS in KO infected macrophage cells become identical with CT or CM cells. Altogether these results suggest that *de novo* linoleate synthesis in *Leishmania* play anti-inflammatory role when they infect the host macrophage. It is well established that activation of NF-κB is required and sufficient to induce maximal expression of COX-2 [19] as well as TNF-α in RAW 264.7 cells. Therefore, we checked whether KO cell induced COX-2 and TNF-α expression were mediated through the activation of NF-κB. Translocation of NF-κBp65 to the nucleus and degradation of IκB alpha are the two major events involved in NF-κB activation. So we examined the phosphorylated form of NF-κB, Iκβ and IKKβ in RAW 264.7 cells with or without co-culture with different types of parasites. Western blot data suggested that increased level of NF-κBp65, Iκβ and IKKβ phosphorylation occurred in KO infected macrophage cells (Fig. 4A–C) compared to CT or CM cells. Macrophage treated with LPS was taken as positive control. To substantiate these observations, we used electrophoretic mobility shift assay (EMSA) to monitor the active form of NF-κB in nuclear extracts of *Leishmania*-infected RAW 264.7 cells. A labeled oligonucleotide duplex corresponding to the NF-κB binding site produced two retarded bands in LPS treated as well as KO-infected RAW 264.7 cells (Fig. 4D). Both of these retarded bands could be competed with a 200-fold molar excess of the unlabeled homologous oligonucleotide duplex. In comparison to CT or CM infected cell, the upper band was significantly increased for the KO-infected RAW 264.7 cell nuclear extract (Fig. 4D) that is known to contain an active form of NF-κB complexes [20]. These findings suggest that the transcriptional up-regulation of COX-2 as well as TNF-α in linoleate deficient *Leishmania* infected macrophage is carried out through the activation of NF-κB signaling pathway.

4. Conclusion

Leishmania acquire linoleate through a combination of salvage pathways or *de novo* synthesis, leading to a level of redundancy that complicate efforts to identify the exact role of this essential fatty acid. In our laboratory, we have grown linoleate deficient *Leishmania major* promastigotes (Ncb5or KO cell) in delipidated medium (charcoal stripped FBS) in presence or absence of BSA-linoleate complexes and measured the cell death with time. Comparison of cell death among CT, CM and KO cells indicate that linoleate is essential fatty acid for *Leishmania* promastigote. Similarly, *Leishmania* infected macrophages as well as mouse model studies shows that *de novo* linoleate synthesis in *Leishmania* is essential for parasite survival at intracellular amastigote stage. It is still unknown how parasite derived linoleate modulated the phosphorylation of IKKβ, IκB and NF-κB in host macrophages. Extensive lipidomic/fatty acid analysis in exosome and surface macromolecule of the promastigotes would be helpful in elucidating the complete signaling pathway of NF-κB activation by KO parasites in the near future.

Please cite this article in press as: A. Mukherjee, et al., Loss of virulence in NAD(P)H cytochrome *b*5 oxidoreductase deficient *Leishmania major*, Biochemical and Biophysical Research Communications (2018), https://doi.org/10.1016/j.bbrc.2018.06.037

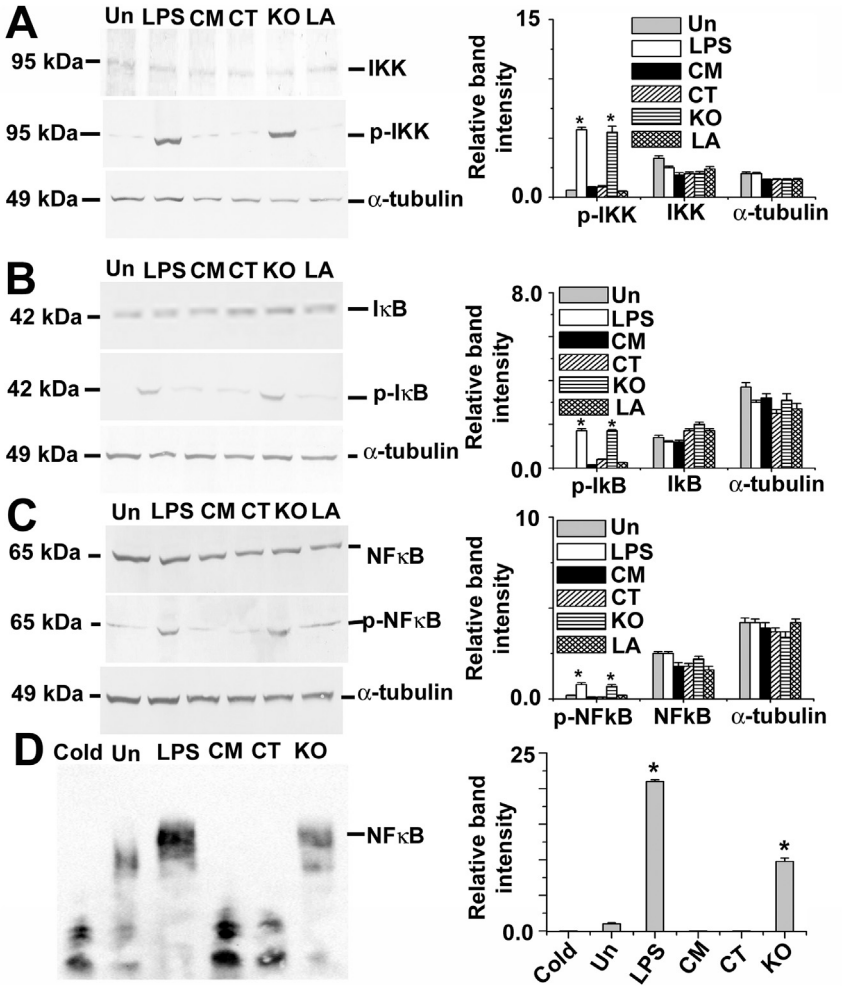

Fig. 4. Quantitation of phosphorylated form of NFκB p65, IκB, and IKKβ, and NF-κB binding to its DNA promoter region. Whole cell lysates were prepared to determine the levels of phosphorylated form of IKKβ (A), IκB (B) and NFκB p65 (C) by immunoblotting at 30 min post infection with log phase *L. major* cells. Alpha tubulin was used as the endogenous control. (D) The nuclear extracts were prepared after 6 h post infection and the EMSA measured NF-κB binding to its DNA promoter region in the extract. 'Cold' denoted 200 fold excess of unlabeled double-stranded NF-κB consensus oligonucleotides were added to the reaction mixture before addition of the labeled probes. 'Un' and 'LA' denoted uninfected macrophage (-*Leishmania*) and BSA-linoleate pre-incubated macrophage plus KO cells, respectively. Quantitation of all bands and densitometric analysis of all data were done using ImageJ software (from NIH). Error bars represent the SD from three independent experiments. * Statistically significant value of less than 0.05.

Competing interests

The authors declare that they have no Competing Interests with the contents of this article.

Acknowledgments

We thank Dr. S. M. Beverley (Washington University) for providing pXG-B2863, pXG-neo, pXG-hyg and pXG-phleo vectors. This work was supported by Department of Science and Technology (GAP 374), CSIR fellowships (to A.M., P.D. and S.B.), and University Grants Commission fellowship to A.A and S.M.

Transparency document

Transparency document related to this article can be found online at https://doi.org/10.1016/j.bbrc.2018.06.037.

Appendix A. Supplementary data

Supplementary data related to this article can be found at https://doi.org/10.1016/j.bbrc.2018.06.037.

Abbreviations list

FA	fatty acid
FAD	FA desaturase
Ncb5or	NAD(P)H cytochrome *b*5 oxidoreductase
LmNcb5or	Ncb5or from *L. major*
CT	control cell (wild type cell + pXG vector)
CM	LmNcb5or-complement cell
KO	LmNcb5or knockout cell
PUFA	polyunsaturated fatty acids
COX-2	cyclooxygenase 2
TNF-α	tumor necrosis factor alpha
IL-1α	Interleukin 1 alpha
IKK-β	inhibitor of nuclear factor kappa-B kinase subunit beta
NF-κB	nuclear factor kappa-light-chain-enhancer of activated B cells
LPS	lipopolysaccharides
IκB	inhibitor of κB

References

[1] J. Xie, H. Zhu, K. Larade, A. Ladoux, A. Seguritan, M. Chu, S. Ito, R.T. Bronson,

E.H. Leiter, C.Y. Zhang, E.D. Rosen, H.F. Bunn, Absence of a reductase, NCB5OR, causes insulin-deficient diabetes, Proc. Natl. Acad. Sci. U. S. A. 101 (2004) 10750–10755.
[2] M. Xu, W. Wang, J.R. Frontera, M.C. Neely, J. Lu, D. Aires, F.F. Hsu, J. Turk, R.H. Swerdlow, S.E. Carlson, H. Zhu, Ncb5or deficiency increases fatty acid catabolism and oxidative stress, J. Biol. Chem. 286 (2011) 11141–11154.
[3] Y. Zhang, K. Larade, Z.G. Jiang, S. Ito, W. Wang, H. Zhu, H.F. Bunn, The flavoheme reductase Ncb5or protects cells against endoplasmic reticulum stress-induced lipotoxicity, J. Lipid Res. 51 (2010) 53–62.
[4] K. Larade, Z. Jiang, Y. Zhang, W. Wang, S. Bonner-Weir, H. Zhu, H.F. Bunn, Loss of Ncb5or results in impaired fatty acid desaturation, lipoatrophy, and diabetes, J. Biol. Chem. 283 (2008) 29285–29291.
[5] N. Oshino, Hepatic Cytochrome P450 Monooxygenase Systems, Pergamon Press, New York, 1980.
[6] R.F. Steiger, E. Steiger, Cultivation of Leishmania donovani and Leishmania braziliensis in defined media: nutritional requirements, J. Protozool. 24 (1977) 437–441.
[7] A.D. Uttaro, Biosynthesis of polyunsaturated fatty acids in lower eukaryotes, IUBMB Life 58 (2006) 563–571.
[8] S.H. Lee, J.L. Stephens, P.T. Englund, A fatty-acid synthesis mechanism specialized for parasitism, Nat. Rev. Microbiol. 5 (2007) 287–297.
[9] S.H. Lee, J.L. Stephens, K.S. Paul, P.T. Englund, Fatty acid synthesis by elongases in trypanosomes, Cell 126 (2006) 691–699.
[10] A.G. Mitchell, C.E. Martin, A novel cytochrome b5-like domain is linked to the carboxyl terminus of the Saccharomyces cerevisiae delta-9 fatty acid desaturase, J. Biol. Chem. 270 (1995) 29766–29772.
[11] S. Mukherjee, S. Sen Santara, S. Das, M. Bose, J. Roy, S. Adak, NAD(P)H cytochrome b5 oxidoreductase deficiency in Leishmania major results in impaired linoleate synthesis followed by increased oxidative stress and cell death, J. Biol. Chem. 287 (2012) 34992–35003.
[12] J.Y. Lee, K.H. Sohn, S.H. Rhee, D. Hwang, Saturated fatty acids, but not unsaturated fatty acids, induce the expression of cyclooxygenase-2 mediated through Toll-like receptor 4, J. Biol. Chem. 276 (2001) 16683–16689.
[13] S. Dolai, S. Pal, R.K. Yadav, S. Adak, Endoplasmic reticulum stress-induced Apoptosis in Leishmania through Ca2+-dependent and caspase-independent mechanism, J. Biol. Chem. 286 (2011) 13638–13646.
[14] M. Bose, R. Saha, S. Sen Santara, S. Mukherjee, J. Roy, S. Adak, Protection against peroxynitrite by pseudoperoxidase from Leishmania major, Free Radic. Biol. Med. 53 (2012) 1819–1828.
[15] S. Sen Santara, J. Roy, S. Mukherjee, M. Bose, R. Saha, S. Adak, Globin-coupled heme containing oxygen sensor soluble adenylate cyclase in Leishmania prevents cell death during hypoxia, Proc. Natl. Acad. Sci. U. S. A. 110 (2013) 16790–16795.
[16] A. Alloatti, S. Gupta, M. Gualdron-Lopez, M. Igoillo-Esteve, P.A. Nguewa, G. Deumer, P. Wallemacq, S.G. Altabe, P.A. Michels, A.D. Uttaro, Genetic and chemical evaluation of Trypanosoma brucei oleate desaturase as a candidate drug target, PLoS One 5 (2010) e14239.
[17] G. van Zandbergen, A. Bollinger, A. Wenzel, S. Kamhawi, R. Voll, M. Klinger, A. Muller, C. Holscher, M. Herrmann, D. Sacks, W. Solbach, T. Laskay, Leishmania disease development depends on the presence of apoptotic promastigotes in the virulent inoculum, Proc. Natl. Acad. Sci. U. S. A. 103 (2006) 13837–13842.
[18] T. Martins de Lima, R. Gorjao, E. Hatanaka, M.F. Cury-Boaventura, E.P. Portioli Silva, J. Procopio, R. Curi, Mechanisms by which fatty acids regulate leucocyte function, Clin. Sci. 113 (2007) 65–77.
[19] S.H. Lee, E. Soyoola, P. Chanmugam, S. Hart, W. Sun, H. Zhong, S. Liou, D. Simmons, D. Hwang, Selective expression of mitogen-inducible cyclooxygenase in macrophages stimulated with lipopolysaccharide, J. Biol. Chem. 267 (1992) 25934–25938.
[20] P.C. Supakar, M.H. Jung, C.S. Song, B. Chatterjee, A.K. Roy, Nuclear factor kappa B functions as a negative regulator for the rat androgen receptor gene and NF-kappa B activity increases during the age-dependent desensitization of the liver, J. Biol. Chem. 270 (1995) 837–842.

Please cite this article in press as: A. Mukherjee, et al., Loss of virulence in NAD(P)H cytochrome *b*5 oxidoreductase deficient *Leishmania major*, Biochemical and Biophysical Research Communications (2018), https://doi.org/10.1016/j.bbrc.2018.06.037

Conference presentations

- **The role of proximal His 161 in the ferrous-dioxy complex of Leishmania major heme containing adenylate cyclase**. Poster presentation delivered at the Indo-Brazil symposium on Biochemistry of kinetoplastid parasites, organized by CSIR- Indian Institute of Chemical Biology, Kolkata-700032, September, 2016

- **Glyceraldehyde-3-phosphate present in the extracellular vesicles from Leishmania major suppresses host TNF-alpha expression**. Poster presentation in the 90th Annual Meeting of SBC(I) "Metabolism to Drug Discovery: Where Cemistry and Biology Unite" organized in virtual mode by Amity Institute of Biotechnology & Amity Institute of Integrative Sciences and Health, Amity University Haryana (AUH), Gurugram, India during 16th to 19th December 2021.

- **Role of moonlighting protein in host pathogen interaction and disease progression.** Poster presentation in the International Webinar, Modern Trends in Microbiology Chapter XVIII, organized by St. Xavier's College (Autonomous), Kolkata, held on 8th to 10th October, 2021.

INDO-BRAZIL SYMPOSIUM
ON
BIOCHEMISTRY OF KINETOPLASTID PARASITES

SEPTEMBER 19-20, 2016

Organized by

CSIR-Indian Institute of Chemical Biology

4, Raja S. C. Mullick Road, Jadavpur, Kolkata-700 032

Certificate

This is to certify that Prof. / Dr. / Mr. / Ms. PRIYA DAS

participated / ~~delivered an invited lecture~~ / presented a poster in the ***Indo-Brazil Symposium on Biochemistry of Kinetoplastid Parasites*** *organized by CSIR-Indian Institute of Chemical Biology, Kolkata - 700 032.*

Prof. Samit Chattopadhyay, Director
Chairman, Organizing Committee
CSIR-IICB, Kolkata-700 032

Dr. Rupak K. Bhadra
Secretary, Organizing Committee
CSIR-IICB, Kolkata-700 032

AMITY UNIVERSITY HARYANA

Society of Biological Chemists INDIA 1930

CERTIFICATE OF RECOGNITION

The Scientific Organizing Committee certifies that

Priya Das

CSIR-IICB, Kolkata

has presented a poster, which was selected as one of the **Top 10% posters** in the 90th Annual Meeting of SBC(I) *"Metabolism to Drug Discovery: Where Chemistry and Biology Unite"* organized in virtual mode by Amity Institute of Biotechnology & Amity Institute of Integrative Sciences and Health, Amity University Haryana (AUH), Gurugram, India during 16th to 19th, December 2021.

For Scientific Organizing Committee

Dr. Machiavelli Singh
Organizing Secretary

Prof. Rajendra Prasad
President, SBC(I)

St. Xavier's College (Autonomous), Kolkata

DEPARTMENT OF MICROBIOLOGY

presents

MODERN TRENDS IN MICROBIOLOGY

CHAPTER XVIII

supported by

DEPARTMENT OF BIOTECHNOLOGY, GOVT. OF INDIA

(under DBT Star College Scheme)

Certificate of Achievement

This is to certify that Dr./Mr./Ms. Priya Das *of* CSIR-IICB *has presented a poster/ delivered an oral presentation titled* Role of the moonlighting protein in host pathogen interaction and disease progression *in the three-day International webinar, Modern Trends in Microbiology Chapter XVIII, organised by the Department of Microbiology, St. Xavier's College (Autonomous), Kolkata held on 8th, 9th and 10th October, 2021.*

Rev. Dr. Dominic Savio, S.J. Principal St. Xavier's College, Kolkata	Dr. Sudeshna Shyam Chowdhury H.O.D. P.G. Department of Microbiology	Dr. Arup Kumar Mitra Convener MTIM 2021

Enrolment No. : PhD CW / 2016/44

CSIR-Indian Institute of Chemical Biology

(An autonomous body, under the Ministry of Science & Technology, Government of India)

Certificate

(Courses offered as per UGC guidelines, July 2009)

This is to certify that Mr./Ms. **Priya Das**

has successfully completed the Ph.D Course Work conducted by CSIR-IICB for the session **2016**

Uday Bandyopadhyay
Chairperson, Academic Affairs Committee

Samit Chattopadhyay
Director

Certificate

Presented to

PRIYA DAS

for participation in the

Training Programme On Laboratory Safety : Biosafety, Chemical Safety, Radiation Safety & Fire Safety.

Organized by

CSIR-Indian Institute of Chemical Biology, Kolkata

1st February 2016

D. Bhattacharyya
Dr. D. Bhattacharyya
Chairman

Dr. R. K. Bhadra
Chairman

Dr. A. Bandyopadhyay
Chairman

M. C. Debnath
Dr. M. C. Debnath
Organizing Secretary

Prof. Samit Chattopadhyay
Director

JADAVPUR UNIVERSITY

KOLKATA-700 032

MARK SHEET

NO.: CW/16052/ 000237

(For Ph.D/M. Phil. Course Work)

Results of the PH.D. COURSE WORK EXAMINATION, 2017

In SCIENCE held in DECEMBER, 2017

Name PRIYA DAS Class Roll No. 201720502002

Examination Roll No. PHDLSBT17202 Registration No. 30/17/Life Sc/25 of 17-18

Subject Code / Name	Credit Hr.(c_i)	Marks
COMPULSORY UNITS:: EX/LSBT/PHD/A & B RESEARCH METHODOLOGY & REVIEW OF LITERATURE	4	71
ELECTIVE UNITS ::	4	70
EX/LSBT/PHD/1.2A :: TISSUE CULTURE TECHNIQUES EX/LSBT/PHD/1.2B :: MICROBIOLOGY EX/LSBT/PHD/1.2C :: INTRODUCTION TO MOLECULAR BIOLOGY TECHNIQUES		

Total Marks : 141 (out of 200) **Remarks:** P

Prepared by : Checked by :

Date of issue : 10-05-2018

Controller of Examinations

No. Sc. 0225

Jadavpur University

Registration Certificate

~~Shri~~/Sm Priya Das

has been registered as a student of Ph.D. programme of this university

~~His~~/her Registration Number is SLSBT1103017

Kolkata 11th May, 2017

Registrar 5/9/18